Academic Dissertation

Helsinki 2004

INTRODUCING WILSON DISEASE MUTATIONS INTO ZNTA

Studies on the nucleotide and metal-binding sites of a bacterial zinc-translocating P-type ATPase

Juha Okkeri

Institute of Biomedicine
Department of Biochemistry
Faculty of Medicine

and

Viikki Graduate School of Biosciences

and

Department of Biological and Environmental Sciences
Division of Biochemistry
Faculty of Biosciences

University of Helsinki
Finland

To be presented for public criticism, with the permission of the Faculty of Science of the University of Helsinki, in the lecture hall 2, at Biomedicum Helsinki, on June 30th, 2004, at 12 o'clock

Supervisor

Docent Tuomas Haltia
Institute of Biomedicine
Department of Biochemistry
University of Helsinki

Reviewers

Professor Kari Keinänen
Viikki Biocenter
Department of Biological and Environmental Sciences
University of Helsinki

Professor Mauno Vihinen
Institute of Medical Technology
University of Tampere

Opponent

Professor Marc Solioz
Department of Clinical Pharmacology
University of Berne
Switzerland

ISBN 952-10-1906-9 (PDF)
http://ethesis.helsinki.fi
ISBN 952-91-7437-3 (paperback)
Yliopistopaino
Helsinki 2004

Table of contents

Original publications

I) Okkeri, J. ja Haltia, T. (1999) Expression and mutagenesis of ZntA, a zinc-transporting P-type ATPase from *Escherichia coli*. Biochemistry 38: 14109-14116

II) Okkeri, J.*, Bencomo, E.*, Pietilä, M., and Haltia, T. (2002) Introducing Wilson disease mutations into the zinc-transporting P-type ATPase of *Escherichia coli*. The mutation P634L in the "hinge" motif (GDGXNDXP) perturbs the formation of the E_2-P state. Eur. J. Biochem. 269: 1579-1586

III) Okkeri, J., Laakkonen, L., and Haltia, T. (2003) The nucleotide-binding domain of the Zn^{2+}-transporting P-type ATPase from *Escherichia coli* carries a glycine motif that may be involved in binding of ATP. Biochem. J. 377: 95-105

In addition, some unpublished data is included

*) Equal contribution

Abbreviations

A domain	actuator domain
ATPase	adenosine triphosphatase
cAPK	cAMP-dependent protein kinase
Cox	cytochrome c oxidase
GSH	glutathione
HAD	haloacid dehalogenase
IPTG	isopropyl-β-D-thiogalactoside
M domain	membrane domain
MBD	metal-binding domain
MNK	Menkes disease protein
N domain	nucleotide-binding domain
P domain	phosphorylation domain
P_i	inorganic phosphate
PMSF	phenylmethyl sulfonyl fluoride
SDS	sodium dodechyl sulphate
SDS-PAGE	sodium dodechyl sulphate polyacryl amide gel electrophoresis
SOD	superoxide dismutase
TGN	trans-Golgi network
TM-helix	transmembrane helix
TNP-AMP	trinitrophenyl adenosine monophosphate
WND	Wilson disease protein
Wt	wild-type

Introduction

P-type ATPases are membrane proteins typically involved in ion transport. Even though the two best known members of this protein family, Ca^{2+}-ATPase and Na^+/K^+-ATPase, have been studied for decades, the functional mechanism has not been described in detail. Recently, there has been significant progress in the field, as the crystal structure of Ca^{2+}-ATPase has been determined in two different states (Toyoshima et al., 2000; Toyoshima & Nomura, 2002).

According to the basic scheme (De Meis & Vianna, 1979) the transport cycle consists of four main steps. In the first step cations bind to the ATPase from the cytoplasmic side, activating the protein. The ATPase phosphorylates itself by ATP, creating an E_1~P species. This high-energy form converts rapidly to the E_2-P state. Cation transport is linked to this step. In the third phase, the enzyme is dephosphorylated after which it returns to the E_1 state in the last step. The key question is how the phosphorylation/dephosphorylation reactions in the catalytic binding site drive the translocation of cations bound to a site located some 50 Å from the former (Toyoshima et al., 2000).

Recent studies have concentrated on the ATP binding site. ATP not only acts as a substrate in the phosphorylation reaction, but the energy of ATP binding is also used to drive the E_2-E_1 state conversion. While the orientation of the nucleotide bound to Ca^{2+}- and Na^+/K^+-ATPase is emerging, it is interesting that none of the ATP-binding residues are conserved in heavy-metal-transporting P-type ATPases, known as P_{1B}-ATPases.

Heavy metals, such as copper and zinc, are vital elements in metalloenzymes, but they are also potentially toxic, if existing in too high concentrations. Hence, an elaborate machinery has been evolved to transport heavy metals both into and out of the cytoplasm. P_{1B}-ATPases are mainly used to export heavy metals in prokaryotes, but in eukaryotes they are also involved in intracellular metal transport, playing a role in metalloprotein biogenesis.

Humans have two P_{1B}-ATPases, which function in copper homeostasis. Mutations in their genes bring about copper disorders called Wilson and Menkes diseases. Menkes disease is a copper deprivation state caused usually by large deletions in a gene of the copper ATPase

responsible for copper delivery to the circulation. In contrast, Wilson disease is a copper accumulation disorder which is caused by a blocked copper excretion route via bile. Most of the mutations causing Wilson disease are point mutations and they are likely to preserve partial activity.

P_{1B}-ATPases possess several characteristic features which distinguish them from other P-type ATPases. They lack all the residues forming the ATP-binding site in Ca^{2+}- and Na^{+}/K^{+}-ATPases, but instead they have two sequence motifs in their N domain; an HP dipeptide and a GxGxxG/A motif. Mutation of the histidine to glutamine in the first motif is the most common Wilson disease mutation in the Western population.
In addition to these motifs, two metal-binding sites are found. An N-terminal CxxC motif is the site where the transported metal ion is first delivered by copper chaperones. The second site is a CPx motif found in the putative sixth TM-helix. This is likely to form the actual translocation site. The motif exists in several variants, the most common of them being CPC. However, the same motif is found both in copper and zinc-translocating ATPases, indicating that the variation of this motif alone does not determine the metal selectivity.

The primary focus of this work is to characterize nucleotide and metal-binding sites in P_{1B}-ATPases. The main strategy is to introduce Wilson disease mutation analogs into a bacterial zinc-translocating P-type ATPase, ZntA. The mutagenesis was extended to cover the metal-binding motifs CxxC and CPC. In addition, molecular modeling of the ZntA N domain was carried out. The model is based on the crystal structures sarcoplasmic of Ca^{2+}-ATPase.

Review of the literature

1 P-type ATPases

1.1 General aspects of P-type ATPases

Biological membranes separate subcellular compartments and entire cells from their surroundings. Basically they are composed of a lipid bilayer, which acts as a barrier that prevents uncontrolled passage of water soluble molecules, and of proteins that transport various solutes in an organized way. Molecular transport across a membrane occurs either passively down to the concentration gradient, or actively by using the energy of ion gradients or ATP hydrolysis. P-type ATPases form a large family of transporters utilizing the latter strategy. They are distinct from all the other ATPases in that they are transiently phosphorylated during the catalytic cycle.

Canonical P-type ATPases: Ca^{2+}-ATPase and Na^+/K^+-ATPase

The two best known P-type ATPases, Na^+/K^+-ATPase and sarcoplasmic Ca^{2+}-ATPase were first reported in 1957 and 1961, respectively, and they remain the best characterized members of the P-type ATPase protein family (Skou, 1957; Hasselbach & Makinose, 1961). Sarcoplasmic Ca^{2+}-ATPase is responsible for keeping the concentration of cytoplasmic Ca^{2+} ions at a low level. Ca^{2+} is a well-known secondary messenger that, when released from the sarcoplasmic reticulum, triggers a muscle contraction. To allow the muscle to relax again, the ATPase pumps the Ca^{2+} ions back to the sarcoplasmic reticulum (for more information on the specific Ca^{2+}-ATPase types and their functions, see Shull et al., 2003).

Na^+/K^+-ATPase exchanges three cytoplasmic Na^+ ions for two extracellular K^+ ions (recently reviewed in Kaplan, 2002). The accumulation of positive charge on the extracellular side brings about an electric potential across the membrane. This potential energy is used by all animal cells by coupling the backflow of Na^+ ions to the uptake of a variety of solutes. Na^+/K^+-ATPase spends more than 25% of the cellular ATP to maintain the electrochemical gradient of Na^+ and K^+. This potential plays a special role in nerve cells, which transmit nerve signals. The signals are created by transient depolarization, i.e. disappearance of the membrane potential. This occurs when Na^+ and K^+ channels open

allowing these cations to flow down their concentration gradient. To be able to transmit a signal again, the membrane potential must be recreated by Na^+/K^+-ATPase.

1.2 Subfamilies of P-type ATPases

Na^+/K^+- and Ca^{2+}-ATPases have been studied for decades and the whole family of P-type ATPases was first known as transporters of bulk solutes like Na^+, K^+, Ca^{2+} and H^+. During the last ten years, the functional field of P-type ATPases has broadened significantly and now includes also activities such as heavy metal detoxification and flipping of lipid molecules from outer to inner leaflet of a bilayer.

Phylogenetic analysis reveals five main branches in the P-type ATPase family (Axelsen & Palmgren, 1998; Palmgren & Axelsen, 1998) (see Figure 1). The first group, the P_1-ATPases, contain heavy metal transporting ATPases, denoted P_{1B}-ATPases, and a unique K^+-ATPase, Kdp, that forms its own sub-group of P_{1A}-ATPases. In literature heavy metal-transporting P-type ATPases have also been called soft-metal ATPases, P_1-type ATPases and CPx-ATPases. Ca^{2+}- and Na^+/K^+-ATPases both belong to P_2-ATPases, although in different sub-branches of P_{2A}- and P_{2C}-ATPases respectively. H^+-ATPases are classified as P_3-ATPases. P_4-ATPases are not involved in cation transport, but experimental evidence indicates them to be lipid flippases (Auland et al., 1994; Tang et al., 1996). Finally, there is the last main branch of P_5-ATPases, the function of which remains to be identified.

Notably, the phylogenetic tree is organized into subfamilies according to the substrates of ATPases regardless of whether they originate from eukaryotes or prokaryotes.

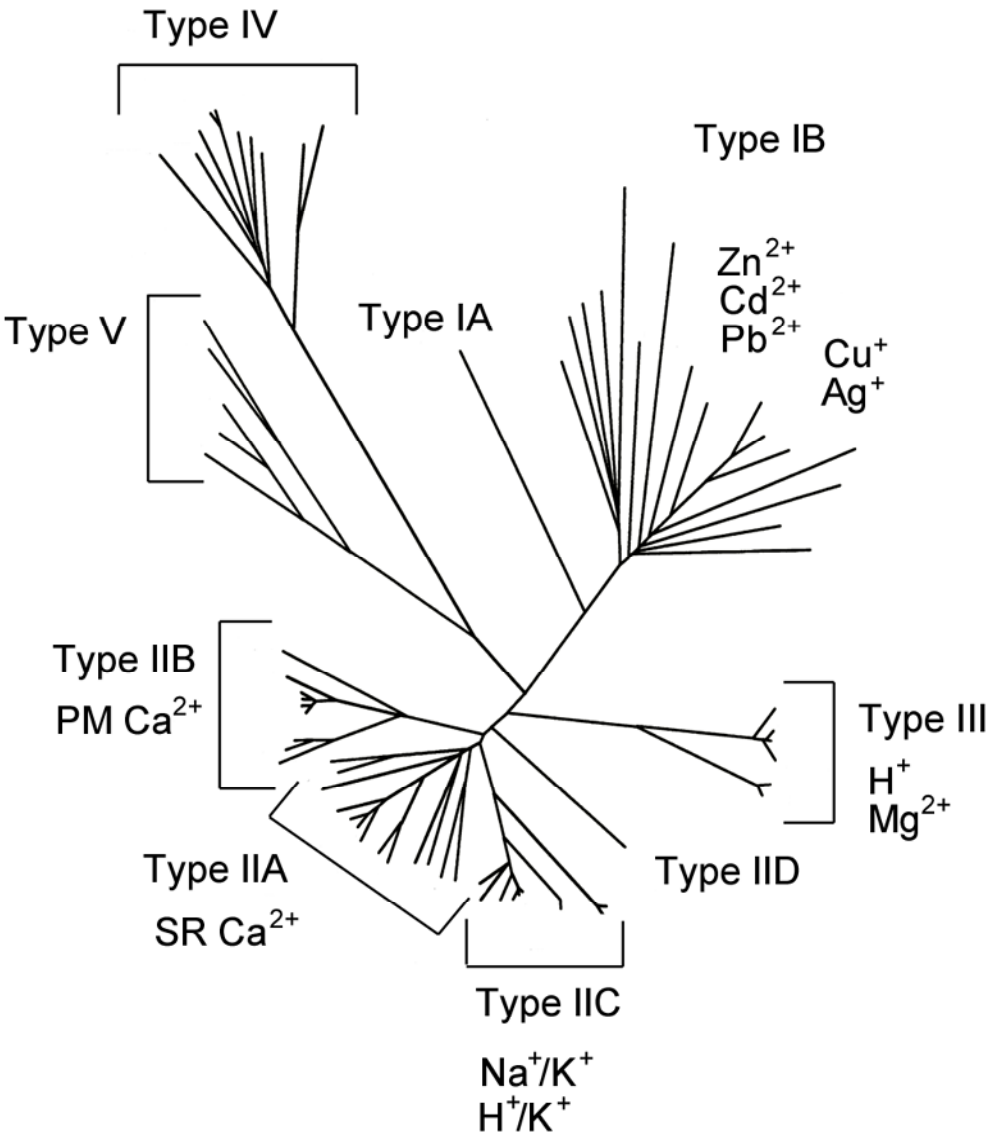

Figure 1. The phylogenetic tree of P-type ATPases. Substrate specificity of ATPases is listed for the most common ATPase sub-groups. PM and SR denote for plasmamembrane and sarcoplasmic forms of the Ca^{2+}-ATPases respectively. The figure is a simplified modification from Palmgren & Axelsen, 1998.

2 Catalytic cycle of P-type ATPases

2.1 The E_1-E_2 model of the catalytic cycle

Allosteric model of two conformational states

Early studies conducted on Na^+/K^+- and Ca^{2+}-ATPases form the basis of the classical model of the catalytic cycle (Post et al., 1965; Post et al., 1972; Makinose, 1971; Makinose &

Hasselbach, 1971; Shigekawa & Dougherty, 1978). The key findings that led to the formulation of the functional model were that the enzyme can exist in two principal states, one of which can be phosphorylated by ATP (Post et al., 1965; Martonosi, 1967; Yamamoto & Tonomura, 1967; Yamamoto & Tonomura, 1968; Makinose, 1969), and the other which reacts with inorganic phosphate (P_i) (Masuda & de Meis, 1973; Glynn & Karlish 1975; Robinson & Flashner, 1979). Later these states were realized to represent intermediates of the catalytic cycle.

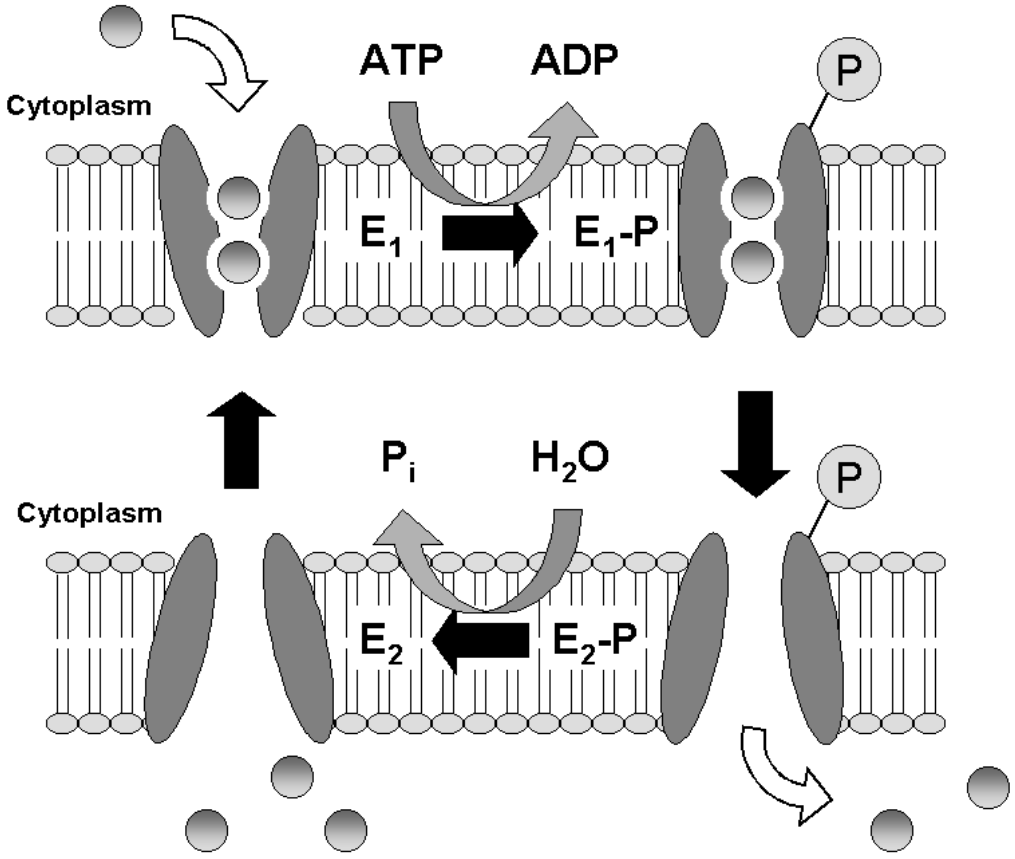

Figure 2. The classical model of the catalytic cycle of Ca^{2+}-ATPase. Ca^{2+} ions are represented as grey balls. In E_1 state the cation-binding sites face the cytoplasm, whereas in the E_2 state they are open to the lumenal side of the membrane. This side has a higher concentration of Ca^{2+}, but these cations do not bind to the ATPase because of the low-affinity of the metal-binding sites in the E_2 state. In the E_1-P state the cations are occluded and have no access to either side of the membrane. Ca^{2+}-ATPase transports two ions per cycle, but the stoichiometry depends on the specific type of the ATPase. Na^+/K^+-ATPase, for instance, transports three Na^+ ions outside a cell. In addition, the final step of $E_2 \rightarrow E_1$ state conversion is also connected to a transport event in some P-type ATPases. Two K^+ ions are imported by Na^+/K^+-ATPase, whereas sarcoplasmic Ca^{2+}-ATPase is likely to transport two H^+.

Long before any actual evidence of structural changes occurring during the catalytic cycle, a transport model of two alternating conformational states was formulated (Jardetzky, 1966). Initial findings supporting this idea included the protease cleavage studies, which displayed a different pattern of Na^+/K^+-ATPase fragments depending on whether the experiment was carried out in the presence of Na^+ or K^+ salt (Jørgensen, 1975; Jørgensen, 1977). A lot of evidence has been accumulated to support these results, but the final proof was gained only a few years ago from the crystal structures of the Ca^{2+}-ATPase in the E_1 and E_2 states (Toyoshima et al., 2000; Toyoshima & Nomura, 2002).

As Ca^{2+}-ATPase is the best characterized P-type ATPase up to date, it is used as an representative example for a P-type ATPase in the following discussion. The foundation of this model is the assumption that the enzyme can adopt two principal conformational states, which are called E_1 and E_2. The ATPase in the E_1 state has a high affinity for Ca^{2+} and the Ca^{2+} binding sites are accessible only from the cytoplasmic side. In contrast, an enzyme in the E_2 state has a low affinity for Ca^{2+} and in this conformation, the binding sites face the opposite side of the membrane. The principles of the catalytic cycle can be illustrated by a minimal functional model consisting of four steps (Albers, 1967; Post et al., 1972; Makinose, 1973; de Meis & Vianna, 1979) (Figure 2).

Catalytic cycle – the sequence of events

The cycle begins with the binding of the cytoplasmic cations to their binding sites with the enzyme being in the E_1 state. The ATP binding site must be occupied also for the reaction to start. However, unlike the substrate cations, ATP can bind during almost any phase of the catalytic cycle (Kanazawa et al., 1971; Skou, 1979), and therefore metal binding can be considered as the critical event that triggers ATPase activity.

In the first step of the cycle, the activated enzyme transfers the γ-phosphate of ATP to a certain aspartate in the catalytic site. This results in occlusion of the cations in their binding site, meaning that they become trapped inside the enzyme with no access to either side of the membrane. The state formed by the autophosphorylation, E_1~P, is unstable and converts rapidly to the E_2-P state. This is the second step of the cycle, opening up the cation binding sites to the other side of the membrane (Makinose, 1973; Ikemoto, 1975; Ikemoto, 1976). Because at the E_2/E_2-P state these sites have a low affinity, the cations are released to the lumenal/extracellular side of the membrane. The dephosphorylation of the enzyme, which follows the vacating of the cation binding sites, makes up the third step of the catalytic

cycle. The final step is the conformational change that returns the enzyme back to the E_1 state.

2.2 Energetics and stoichiometry of the cycle

E_1~P and E_2-P phosphoenzyme species

The catalytic cycle of P-type ATPases is reversible. In nature these pumps use the chemical energy stored in the form of ATP to create ion gradients across a membrane, but *in vitro* they can be used to synthesize ATP from ADP and P_i by utilizing the potential energy of the artificially made ion gradient (Makinose, 1971; Makinose & Hasselbach, 1971).

In the presence of substrate cations the enzyme is mainly in the E_1 state. Instead, in the absence of cations the enzyme prefers the E_2 conformation (Skou & Esmann, 1983). In this state, an ATPase can be phosphorylated by P_i to form the E_2-P state (Carvalho et al., 1976; Masuda & de Meis, 1973; Glynn & Karlish, 1975; Robinson & Flashner, 1979). This phosphoenzyme species is in a low-energy state. In contrast, the phosphoenzyme formed by ATP, the E_1~P state, is a high-energy form. The energy level of the phosphointermediates is reflected in their ability to donate the phosphoryl group: the E_1~P form is able to phosphorylate ADP back to ATP, whereas the E_2-P is not dephosphorylated by ADP (Martonosi, 1967; Shigekawa & Dougherty, 1978). Hence, the two phosphoenzyme species are called ADP sensitive and ADP insensitive forms, respectively.

Characterization of the phosphorylation and dephosphorylation properties of mutant proteins gives detailed information about the specific effect the mutations have during a particular step of the catalytic cycle.

$E_2 \rightarrow E_1$ state transition

Na^+/K^+-ATPase pumps three Na^+ ions out of a cell during the $E_1 \rightarrow E_2$ state conversion. In addition the last step of the catalytic cycle, the $E_2 \rightarrow E_1$ state transition, is linked to the countertransport of two K^+ ions into the cell. In the absence of the substrate cations an equilibrium exists between the two conformational states (de Pont et al., 2003). In the presence of Na^+ ions the E_1 state is stabilized, whereas the E_2 state is dominant in the presence of K^+ ions (Post et al., 1975; Jørgensen, 1975; Jørgensen, 1977; Jørgensen, 2003). ATP hydrolysis drives the $E_1 \rightarrow E_2$ transition, but this leaves the question about the driving force of the final step, the $E_2 \rightarrow E_1$ state transition. It turns out that it is the binding energy

of ATP. ATP has been shown to bind with a high affinity to an ATPase in the E_1 state, with a K_d of micromolar range, compaired to a K_d of a millimolar range measured for an enzyme in the E_2 state (Cornelius & Skou, 1987; Goldshleger & Karlish, 1999; Teramachi et al., 2002). Similar results have been obtained with sarcoplasmic Ca^{2+}-ATPase, which has been demonstrated to transport two H^+ as counter-ions during the fourth step (Levy et al., 1990; Yu et al., 1993).

Hence, ATP has a dual role in the catalytic cycle. On the one hand it is the substrate of the phosphorylation reaction, which drives the $E_1 \rightarrow E_2$ state conversion at submicromolar concentrations. On the other hand, at millimolar concentrations it shifts the conformational equilibrium to favor the E_1 state, effectively enhancing the $E_2 \rightarrow E_1$ transition. This is reflected in ATPase activity, which shows a biphasic dependance on the ATP concentration (Hua et al., 2002a; Inesi et al., 1967). While significant ATPase activity is observed at submillimolar ATP concentrations, the maximal activity is reached only at millimolar ATP concentrations, which corresponds to the intracellular ATP levels. The molecular basis for the different ATP affinities in E_1 and E_2 states is not known.

3 Structural aspects of P-type ATPases

3.1 Functional motifs and domain structure

P-type ATPases in general share a relatively low sequence similarity. Also the number of transmembrane helices (TM-helices) varies (see chapter 3.6). Yet, all of them have a common core structure with two large cytoplasmic loops sandwiched between three pairs of TM-helices (Figure 3). Most P-type ATPases (P_2 - P_5-ATPases) are likely to share a topology of ten TM-helices, four of which reside on the C-terminal side of the core unit (Axelsen & Palmgren, 1998; Palmgren & Axelsen, 1998).

While some of the P-type ATPases are composed of more than one subunit, the catalytic activity is always carried by a single polypeptide and the other chains serve as regulators or stabilizers.

The smaller of the two large cytoplasmic loops contains a T^{214}GES motif (the sequence numbering refers to sarcoplasmic Ca^{2+}-ATPase). Mutation in this motif results in accumulation of the phosphointermediates (Portillo & Serrano, 1988; Clarke et al., 1990; Kato et al., 2003). Accordingly, it has been known formerly as the dephosphorylation domain. In the 3-D structure of Ca^{2+}-ATPase this loop folds together with the N-terminus,

and this structural unit has been renamed an actuator domain (A domain) (Toyoshima et al., 2000).

ATPase activity resides in the larger cytoplasmic loop. This loop contains several conserved sequence motifs including the phosphorylation motif D^{351}KTG. The aspartate-351 is transiently phosphorylated during the catalytic cycle. Biochemical studies have not assigned a similarly clear function for the three other motifs, D^{601}xxR, T^{625}GDN and G^{702}DGxNDxP. The two last motifs have been proposed to be involved in nucleotide binding and the latter also to function as a structural hinge (Taylor & Green, 1989; MacLennan et al., 1985). However, the crystal structures of Ca^{2+}-ATPase argue against both of these ideas.

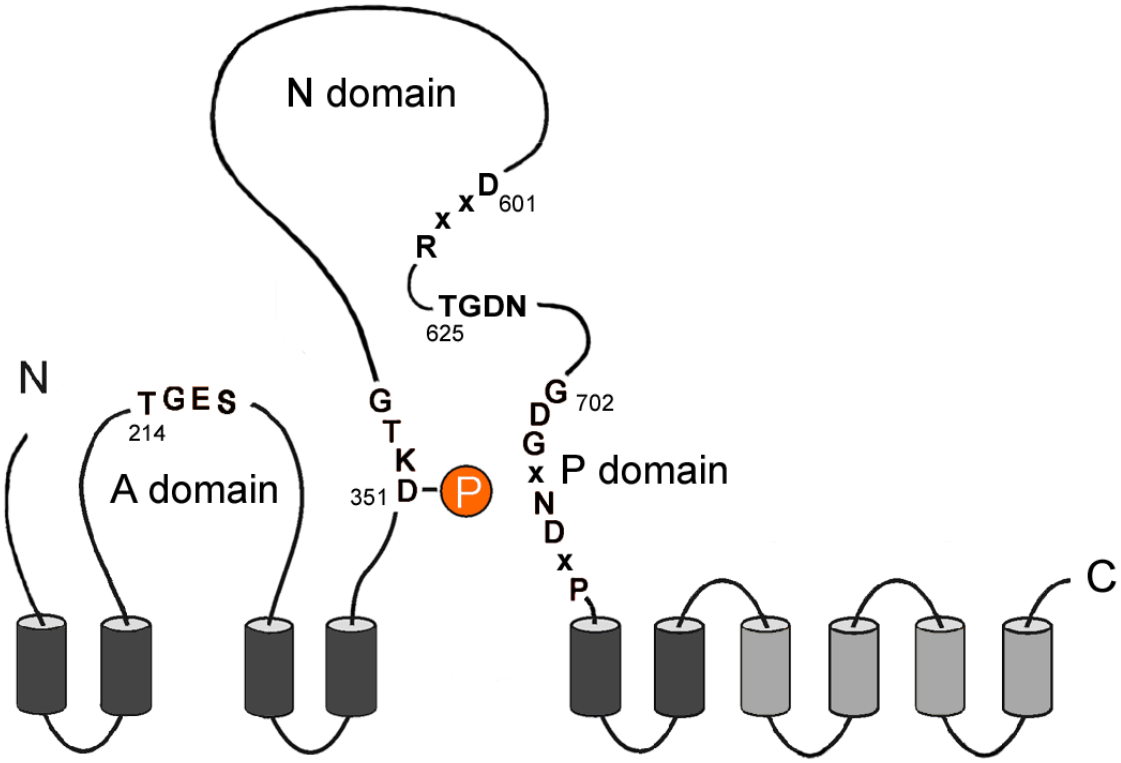

Figure 3. Topological model of a P_2-type ATPase showing the domain organization and the conserved sequence motifs. The helices which belong to the common core structure of the P-type ATPases are highlighted with dark grey. The loop that contains the T^{214}GES motif is folded together with the N-terminus to form the A domain. This domain plays a role in the dephosphorylation step. The P domain is composed of the N- and C-terminal parts of the larger cytoplasmic loop. The D^{351}KTG and G^{702}DGxNDxP motifs are structural parts of the catalytic site. Aspartate-351 in the former motif is phosphorylated during the catalytic cycle. The N domain is situated in the middle of the P domain and does not contain motifs that would be conserved in all P-type ATPases. D^{601}xxR motif resides at the interface of the P and N domains. The numbering corresponds to sarcoplasmic Ca^{2+}-ATPase

Already before the first high-resolution P-type ATPase structure was determined, the P-type ATPase family was shown to belong to a halo acid dehalogenase (HAD) protein superfamily (Aravind, 1998). The structure of one HAD protein, DhlB, has been solved, which allowed the catalytic site of a P-type ATPase to be predicted by homology modelling. This model predicted the TGDN and GDGxNDxP motifs to be integral parts of the phosphorylation site (Ridder & Dijkstra, 1999).

Additionally, comparison of the P-type ATPases with other HAD proteins revealed the domain organization of the larger cytoplasmic loop (Aravind, 1998). It turned out to be composed of a phosphorylation domain (P-domain) formed by the N- and C-terminal ends of the loop and of a nucleotide binding domain (N-domain) flanked by these sequences. The N-domain has propably been inserted into the P-domain during the evolution.

3.2 Structure of the Ca^{2+}-ATPase in the E_1 state

Sarcoplasmic Ca^{2+}-ATPase was first crystallized in the presence of Ca^{2+} ions and the structure was solved at a resolution of 2.6 Å (Toyoshima et al., 2000). Soon after, crystals were obtained also in the absence of metal ions but in the presence of an ATPase inhibitor, thapsigargin, which was acting as a stabilizing ligand (Toyoshima & Nomura, 2002). The latter structure has been solved at a resolution of 3.1 Å. The first structure is believed to represent the E_1 state and the latter the E_2 state.

Functional sites in the E_1 structure

Ca^{2+}-ATPase crystallized in the presence of Ca^{2+} ions shows the enzyme in an orientation with the cytoplasmic domains spread wide apart from each other (Figure 4). Two Ca^{2+} ions are bound in the intramembraneous binding sites formed between helices M4, M5, M6 and M8. The nucleotide binding site in the N domain could be visualized by determining the structure from the crystals soaked with the nucleotide analog trinitrophenyl adenosine monophosphate (TNP-AMP). In the structure the distance between the Ca^{2+} binding sites and the phosphorylation site is about 50 Å, whereas the key aspartate is ~ 25 Å apart from the nucleotide binding site. To understand the mechanism of ion translocation driven by ATP hydrolysis, the interplay of all these sites has to be described in molecular terms.

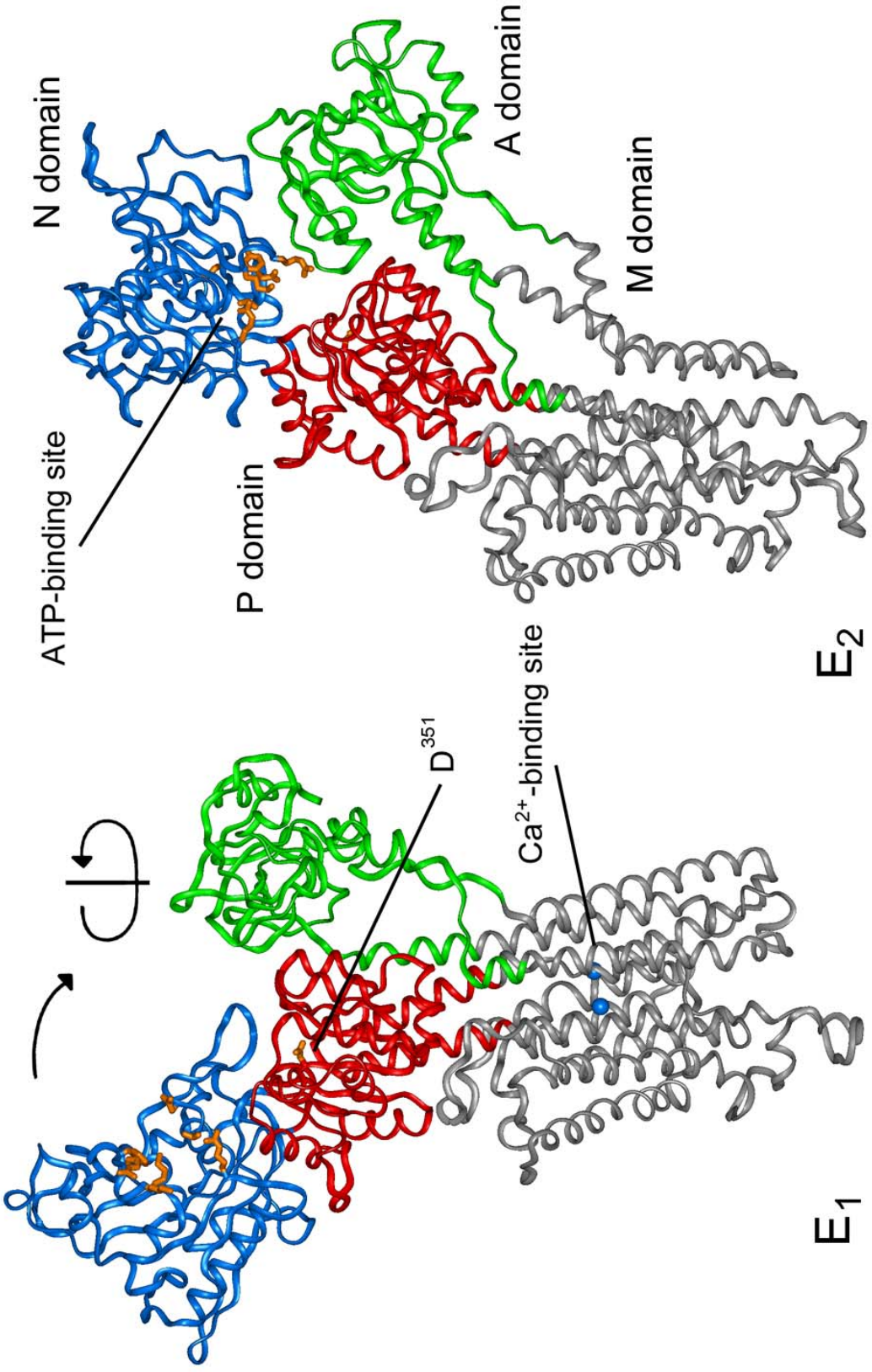
N domain
A domain
ATP-binding site
P domain
M domain
D^{351}
Ca^{2+}-binding site
E_2
E_1

Figure 4. (Previous page) The structure of Ca^{2+}-ATPase in the E_1 (left) and E_2 state (right). Domains are indicated with different colours: N domain with blue, P domain with red, A domain with green and M domain with grey. The key aspartate and nucleotide-binding residues are shown in yellow. The bound Ca^{2+} ions are shown as blue spheres. The domain movements, which take place during the state conversion, are also illustrated with arrows. The N domain and P domain incline towards the A domain, which does not move, but rotates around itself by a vertical axis. Domains themselves retain their structure practically unchanged, except the M domain, in which significant intradomain movements take place.

Conserved sequence motifs of the P domain in the structure

The E_1 structure shows that the aspartate of the T^{625}GDN motif interacts with the lysine of the D^{351}KTG motif. The G^{702}DGxNDxP motif, formerly known as the hinge motif, has the first aspartate in a position in which it could participate in the binding of the Mg^{2+} together with the threonine-353 of the D^{351}KTG motif (Pedersen et al., 2000; Clausen et al., 2001). The structure does not support the idea that the G^{702}DGxNDxP motif would function as a hinge. However, the D^{601}xxR motif seems to be a true structural hinge. It is found in a stretch connecting the N and P domains and this area is known to be flexible to allow the N domain movements (see the next chapter).

3.3 Ca^{2+}-ATPase structure in the E_2 state – the state conversion

Comparison of structures of the E_1 and E_2 states

The crystal structure of Ca^{2+}-ATPase in the absence of Ca^{2+} ions has a rather different overall appearance. In contrast to the E_1 structure, the head piece of Ca^{2+}-ATPase in the E_2 state has a much more compact shape in which all three cytoplasmic domains are in contact with each other. Compared to the E_1 state, the N domain in the E_2 state is inclined roughly by 50º in respect to the P domain, which in turn rotates itself ~ 30º towards the A domain. The whole loop containing both domains moves laterally closer to the A domain, which rotates 110º around the axis perpendicular to the membrane level. All the previous transitions can be modelled as rigid body movements of the three domains without any significant changes taking place in the structure of the domains themselves, excluding the residues in the region connecting the N and P domains (T^{358}NQMS and D^{601}PPR). As a striking contrast, the M domain undergoes major structural changes during the state conversion, as evident by the significantly different arrangement of the membraneous part in the E_1 and E_2 structures (Toyoshima & Nomura, 2002; Toyoshima et al., 2003). In

relation to the E_1 structure, in the E_2 state the helices M1 and M2 are shifted upwards toward the cytoplasm, whereas the helices M3 and M4 are shifted downwards, both by about 5 Å. The M1 helix is the only one to move also laterally. In addition, the helices M3 and M5 are strongly curved in opposite directions. The helices M7-M10 remain relatively unchanged. The helix M8 carries Glu^{908} that has been identified to be a metal ligand of the Ca^{2+} binding site I (Clarke et al., 1989; Toyoshima et al., 2000). The C-terminal helices M7-M10 are not known to be involved in any other function in the translocation process. Thus, it is not surprising that their equivalents are missing in P_{1B}-ATPases.

Interaction of the N and P domains

In the E_1 structure the nucleotide binding site is ~ 25 Å away from the phosphorylation site. In the E_2 conformation the domain movements reduce this distance to about 15 Å, but it is still too much for the γ-phosphate of ATP bound to the nucleotide binding site to reach the key aspartate. It seems that a conformation must exist, in which the N domain is in an orientation that brings the two sites closer to each other. Interestingly, when the N domain is modelled into a low-resolution structure of H^+-ATPase from *Neurospora crassa*, it is orientated in a way clearly different compared with the N domain in the E_1 structure of Ca^{2+}-ATPase (Kühlbrandt et al., 2002). In the H^+-ATPase structure the N domain is in an almost vertical position in respect to the P domain (Auer et al., 1998). Still, both these structures are assumed to represent the E_1 state. The apparent contradiction of the two dissimilar structures of the same state has been explained by proposing that the N domain in the E_1 state would not be fixed, but it could move by Brownian motion (Xu et al., 2002; Kühlbrandt et al., 2002; Stokes & Green, 2003). Accordingly, the Ca^{2+}-ATPase and H^+-ATPase structures can be considered as snapshots of conformations that the enzyme can adopt in the E_1 state. It has been demonstrated by molecular modelling that the N domain can be rotated using rigid body movements to bring K^{492} to a distance of 4 Å from R^{678} in the E_1 structure of Ca^{2+}-ATPase (Xu et al., 2002). These two residues have been shown to be crosslinked by glutaraldehyde while the enzyme resides in the E_1 state proving that the N domain is able to adopt an orientation similar to that in the model (McIntosh, 1992).

The role of the A domain

The catalytic site performs two different tasks during the catalytic cycle depending on whether the enzyme is in the E_1 or in the E_2 state. In the former case it facilitates the formation of the aspartyl phosphate bond, whereas in the latter case it catalyzes a

nucleophilic attack by a water molecule on the very same bond. Both of these reactions require Mg^{2+} to be present as a cofactor. However, experimental evidence indicates that the coordination sphere of Mg^{2+} is significantly different in the two conformations. There is no Mg^{2+} ion present in either the E_1 or E_2 crystal structures, but the surroundings of the Mg^{2+} binding site have been probed by using an Fe^{2+}-catalyzed cleavage technique (Goldshleger & Karlish, 1997). Several divalent cations can be used to replace Mg^{2+} as a cofactor. If Mg^{2+} is substituted by Fe^{2+}, ~ 25% ATPase activity can be achieved with Ca^{2+}-ATPase (Fukushima & Post 1978, Hua et al., 2002b). Unlike Mg^{2+}, in the presence of H_2O_2 and ascorbate Fe^{2+} catalyzes oxygen radical production by Fenton chemistry. Highly reactive radical species cleave the peptide bonds in the vicinity of Fe^{2+}. Na^+/K^+-ATPase cleaved by ATP-Fe^{2+} in the E_1 state is cleaved at the sites ^{440}VAGDA (N domain) and ^{712}VNDS (P domain), which is consistent with the prediction that the ATP binding site comes close to the phosphorylation site (Patchornik et al., 2000). When the enzyme is cleaved while in the E_2 state, the first cleavage is not observed, but instead a new fragment appears showing a cleavage site at ^{214}ESE (Patchornik et al., 2000; Goldshleger & Karlish, 1999). This is part of the TGES motif located in the A domain. In the E_2 structure the TGES loop comes close to the catalytic site while the nucleotide binding site is no longer associated with the phosphorylation site. Thus, in the E_1~P $\rightarrow$ E_2-P state conversion A domain replaces the N domain from the active surface of the P domain and effectively turns the enzyme to catalyze the hydrolysis of the aspartyl phosphate. In contrast, when the enzyme reverts back to the E_1 state, the A domain moves away from the active site. The structural model is supported by the mutagenesis data showing mutations in the A domain increase the stability of phosphointermediates, without affecting the ATP phosphorylation step itself (Kato et al., 2003; Clarke et al., 1990; Toustrup-Jensen et al., 2003).

3.4 Cation-binding sites and the ion translocation pathway

According to the standard model, the Ca^{2+}-binding sites should be accessible from the cytoplasm in the E_1 state. The channel should stay open even when the cations are bound, until the enzyme is phosphorylated by ATP. This has also been observed experimentally; bound $^{45}Ca^{2+}$ ions are exchangeable with soluble $^{40}Ca^{2+}$ ions in the absence of ATP (Dupont, 1982; Inesi, 1987), but become occluded following ATP phosphorylation (Sumida & Tonomura, 1974; Dupont, 1980). In the E_1 structure two Ca^{2+} ions are bound to the sites

in the middle of the helices M4-M6 and M8. The binding sites are formed by several acidic residues, which neutralize the strong positive charge of the Ca^{2+} ions. A clear path from the cytoplasm to the cation binding sites has not been identified, but a channel surrounded by the helices M2, M4 and M6 has been proposed (Toyoshima et al., 2000).

On the other hand, the E_1-E_2 model suggests that in the E_2 conformation the metal binding sites should be accessible from the lumenal side of the membrane. Surprisingly, there is no such path in the E_2 structure, but a clear path is seen to the Ca^{2+}-binding sites from the cytoplasmic side. The pathway starts between the M1 and M3 helices and ends up to the E^{309} in the M domain. Mutations in a stretch K^{252}LDE and G^{257}EQL in the M3 affect strongly the release rate of bound Ca^{2+} ions supporting this area to be involved in the ion translocation (Andersen et al., 2003). Glu-309 is one of the residues forming the Ca^{2+}-binding site II in the E_1 structure, whereas in the E_2 structure it is actually pointing away from the binding site. Rearrangements of this residue might be part of the gating mechanism that regulates the access to the metal binding sites from the cytoplasmic side. This still leaves the question about how the cations are eventually released to the lumenal side. A likely explanation is that the lumenal gate of the metal-binding sites is only transiently open during the E_1P-E_2P state conversion, or in the E_2P state.

3.5 Nucleotide-binding site and orientation of the ATP molecule

Structure of the ATP-binding site

Many nucleotide-utilizing proteins have special nucleotide-binding motifs which are rich in glycines. These include the GxxGxGK motif, known as the P-loop, and GxGxxG, a motif found in protein kinases (Saraste et al., 1990; Bossemeyer, 1994; Kinoshita et al., 1999; Vetter & Wittinghofer, 1999). Glycine-rich motifs were likely formed by convergent evolution, as they are found in otherwise completely unrelated proteins (Via et al., 2000). In P-loop structures the dihedral angles of the glycines are not allowed for residues with side chains, whereas in protein kinases the lack of a side chain is utilized to provide a space for phosphate groups of a nucleotide to fit in a binding site (Bossemeyer, 1994). In both cases the glycine motifs fold into a loop, which interacts with the phosphate groups by the mainchain amide groups (Kinoshita et al., 1999). However, P-type ATPases are considered to be an example of a nucleotide-hydrolyzing protein family that does not have glycine-rich motifs (Vetter & Wittinghofer, 1999).

The N domain does not possess any sequence motifs which would be common to all P-type ATPases. Still, there are several individual residues highly conserved within the P_2-P_5 subfamilies. Mutagenesis (McIntosh et al., 1996; Kubala et al., 2002; Kubala et al., 2003; Jacobsen et al., 2002; Clausen et al., 2003), NMR (Abu-Abed et al., 2002), FeATP-catalyzed cleavage (Hua et al., 2002b; Patchornik et al., 2002; Patchornik et al., 2000), labelling (Mitchinson et al., 1982; Hua et al., 2002a) and crosslinking experiments have shown three basic residues (K^{492}, K^{515}, R^{560}) and a phenyl alanine F^{487} to be the key residues forming the ATP-binding site of Ca^{2+}- and Na^+/K^+-ATPases (Ca^{2+}-ATPase numbering, see alignment in Figure 8). Consistent with this data, the structure of Ca^{2+}-ATPase determined from the E_1 crystals soaked with TNP-AMP solution shows the nucleotide analog bound in a site formed by these residues (Figure 5A).

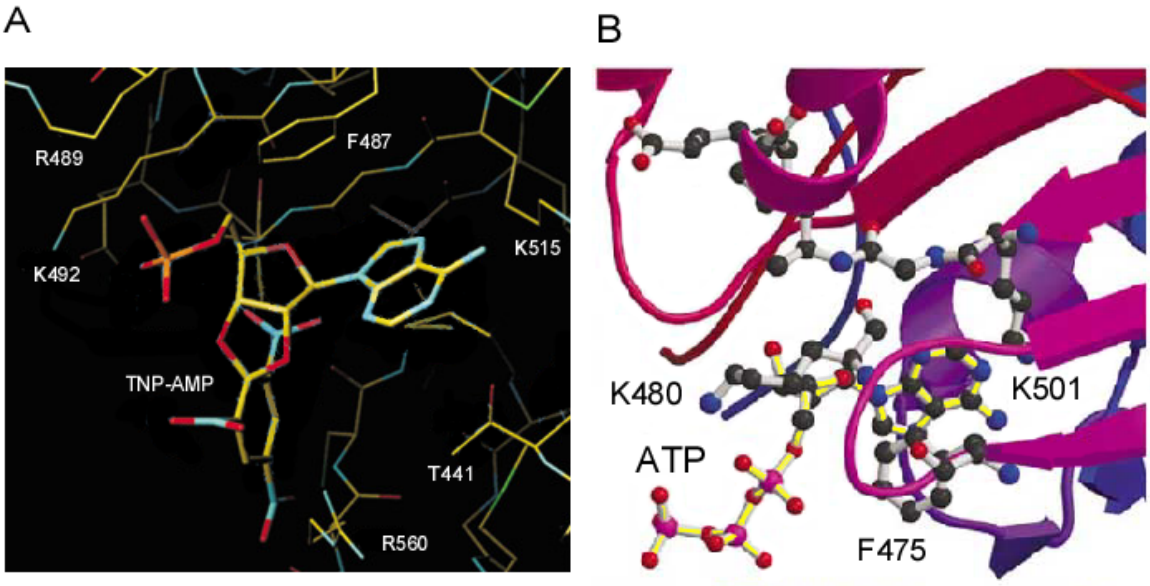

Figure 5. A) TNP-AMP bound in the Ca^{2+}-ATPase in the E_1 state (Toyoshima et al., 2000). The structure was gained by soaking the protein crystals in TNP-AMP solution. The figure is modified from Toyoshima et al., 2000. **B)** ATP bound in the N domain of Na^+/K^+-ATPase. The ATP molecule is highlighted in yellow. The structure of the domain with the nucleotide bound was solved by NMR (Hilge et al., 2003). The figure is modified from Hilge et al., 2003.

Orientation of the bound nucleotide

When considering the orientation of the nucleotide in the binding pocket, the picture gained using TNP-AMP should be viewed cautiously. The bulky and hydrophobic TNP moiety is known to affect the binding affinity of a nucleotide analog (Watanabe & Inesi, 1982) and it

might cause the adenine ring to bind in non-native way. Also, the analog does not provide information about the alignment of the β- and γ-phosphates, which are missing in this compound. Several proposals of the binding of an ATP molecule have been put forth by using molecular modelling (Ma et al., 2003; Munson et al., 2003; Patchornik et al., 2002; Ettrich et al., 2001), but until recently there was little experimental data about the exact orientation of the nucleotide in the binding site.

An NMR structure of the N-domain (containing residues Q^{376}-P^{588}) of Na^+/K^+-ATPase with an ATP molecule bound has been described in Hilge et al., 2003 (Figure 5B). The structure shows the nucleotide to form the binding interactions mainly with its purine and sugar rings, leaving the phosphate groups exposed to the solvent. F^{475} (F^{487} in Ca^{2+}-ATPase), a critical residue for the ATP binding, provides an aromatic ring that binds the purine ring of the ATP with a hydrophobic stacking interaction. The strictly conserved K^{480} (which corresponds to K^{492} in Ca^{2+}-ATPase) stabilizes the negatively charged α-phosphate of ATP with its positive charge. Instead, the β- and γ-phosphates seem to be relatively free to move. In the structure they point away from D^{443}. This residue is proposed to be coordinating the Mg^{2+} ion, because Fe^{2+}-ATP causes a cleavage at this site (Patchornik et al., 2002). However, D^{443} is not conserved and no analogous cleavage is observed, when the experiment is conducted with Ca^{2+}-ATPase. Instead, in this case Fe^{2+}-ATP causes oxidation of a residue nearby, T^{441}, suggesting that the region could be involved in the Mg^{2+} binding also in Ca^{2+}-ATPase (Hua et al., 2002b).

The structural and biochemical findings discussed above are consistent with the observation that even though the true substrate in biological conditions is MgATP, both Mg^{2+} and ATP can bind independently and in a random order (Reinstein & Jencks, 1993). The structure explains how ATP binds effectively without Mg^{2+} and also how the latter can bind without the need for the nucleotide to dissociate first.

3.6 Structural organization of P_{1B}-type ATPases

Special structural features of P_{1B}-ATPase

Sequence analysis suggests that P_{1B}-ATPases do not share the topology of the ten TM-helices with the rest of the P-type ATPases. Instead, they are predicted to contain six or eight TM-helices (Møller et al., 1996; Lutsenko & Kaplan, 1995; Solioz & Vulpe, 1996). Moreover, when compared to other P-type ATPases, the helices are organized in a different

way (Figure 6, compare with Figure 3). An extra pair of TM-helices resides N-terminally to the common core of the P-type ATPases, while four helices are missing from the C-terminus. This topology is supported by experiments conducted with CadA and CopA from *Staphylococcus aureus* (Tsai et al., 2002) and *Helicobacter pylori* (Melchers et al., 1996; Bayle et al., 1998).

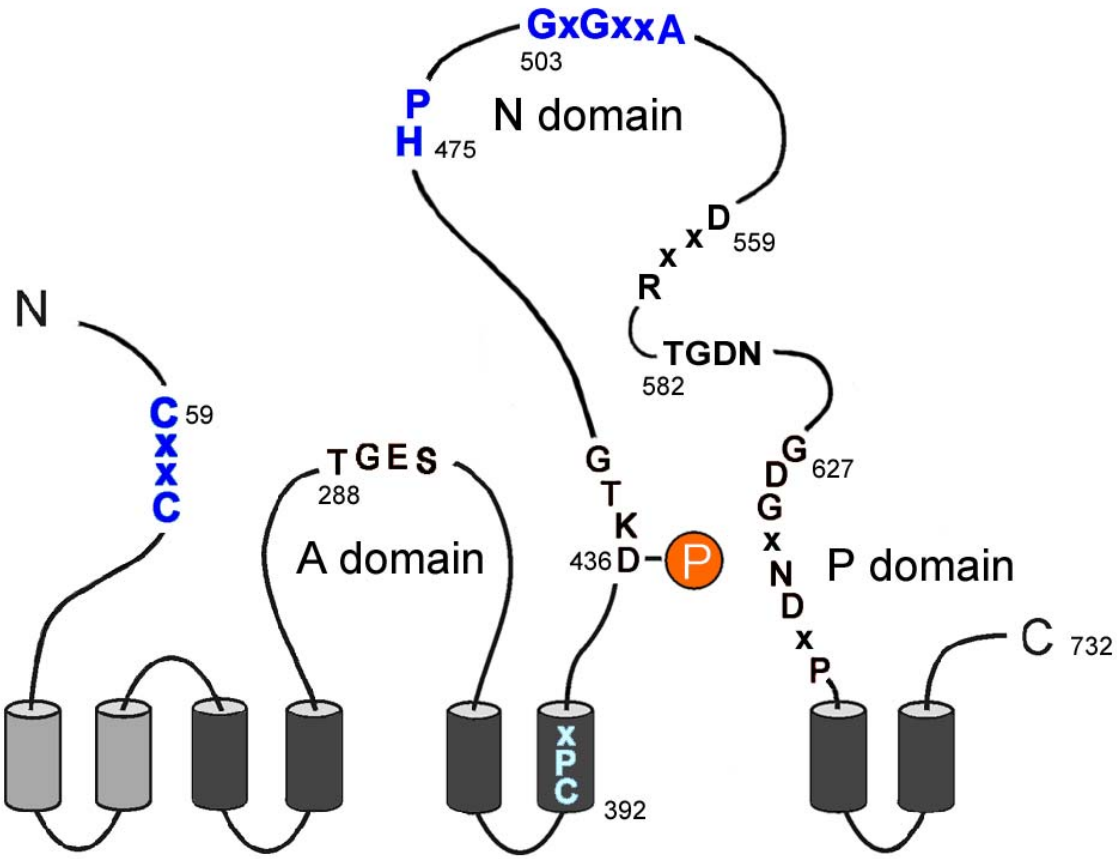

Figure 6. Topological model of a P_{1B}-ATPase. Note that both the number and the order of TM-helices differs from the topology of a non-heavy-metal-transporting P-type ATPase (compare with the figure 3). TM-helices with darker color belong to the core unit common to all P-type ATPases. In addition to motifs conserved in all P-type ATPases, also P_{1B}-ATPase specific motifs are shown. The CxxC and the CPx motifs are putative metal-binding sites. In the former motif x is any residue, whereas in the latter it is a Cys, His or Ser. An HP motif is always found in the N domain and mutation of the His to Gln is the most common WD mutation in the Western population. The GxGxxA is a motif also located in the N domain. The last residue can be also a Gly, Ser or Cys. The numbering corresponds to ZntA sequence.

In addition to the differences in the TM part, there are a number of sequence motifs which are unique for heavy-metal-transporting ATPases. A putative intramembraneous metal-binding site, the CPx motif, is invariantly found at the sixth TM-helix (Solioz & Vulpe, 1996; Lutsenko & Kaplan, 1995). Two motifs are found in the N domain, an HP motif (Solioz & Vulpe, 1996; Lutsenko & Kaplan, 1995) and a protein kinase-like motif GxGxxG/A (**III**). Most of P_{1B}-type ATPases also contain one to six copies of metal-binding sites in their N-terminus, carrying either a CxxC motif, or a sequence rich in histidines (Argüello, 2003). These domains are discussed more in detail in the chapter 5.2.

4 P-type ATPases in heavy metal transport – Wilson disease

4.1 Overview of the biology of heavy metals

Heavy metals play a dual role in biology. On the one hand, metal ions like Cu^{+}/Cu^{2+}, Zn^{2+} and Fe^{2+}/Fe^{3+} serve as important co-factors of enzymes, being able to catalyze a variety of reactions, and stabilize protein structures. On the other hand, other metal ions like Pb^{2+}, Cd^{2+} and Hg^{2+} are purely toxic. Essential metal ions can also become poisonous when present in excess. Exceeding the capacity of the metal handling machinery results in mainly misincorporation of metal ions into vital proteins and oxygen radical production (Maret et al., 1999; Gazaryan et al., 2002; Videla et al., 2003). The nature of heavy metals makes it imperative that cells must be able to keep the intracellular concentrations of heavy metal ions within a narrow range.

Cytosolic control of heavy metals

According to the current view, heavy metal ions, unlike alkaline and earth-alkaline metal ions, do not exist as free ions in the cytosol, but are always bound to carrier molecules such as glutathione (GSH), metallothioneins, and metal chaperones (Finney & O'Halloran, 2003). In addition to these primary carriers, many other small molecules, including amino acids and nucleotides can bind metal ions non-specifically. According the current estimates the concentration of the free cytosolic Zn^{2+} and Cu^{+} ions is in a femtomolar range, even though the total intracellular concentrations of these ions are about 100 μM and 10 μM respectively (Changela et al., 2003; Outten & O'Halloran, 2001; Rae et al., 1999). There is

little experimental data on how other metal ions are handled inside a cell, but it is assumed that the same principles apply also to other vital heavy metal ions, such as Fe^{2+} and Co^{2+}.

Metal chaperones

Metal chaperones provide a coordinated way to incorporate metal ions into proteins (Field et al., 2002; Lu et al., 2003). They are small intracellular proteins that bind metal ions and deliver them specifically to their target protein. In prokaryotes there is only one protein, which is known to function as a metal chaperone. CopZ has been shown to interact with CopA copper importer and to deliver copper to CopY repressor protein in *Enterococcus hirea* (Multhaup et al., 2001; Cobine et al., 1999). Instead, in *Bacillus subtilis* the homologous protein by the same name provides copper to a copper exporting protein (Banci et al., 2003). In eukaryotes three chaperones, Cco, Cox17 and Atx1 are known, which were first found in *Saccharomyces cerevisiase*. They transfer copper to Zn,Cu - superoxide dismutase, cytochrome c oxidase and for a Cu^{+}-ATPase Ccc2 respectively (Glerum et al., 1996; Lin et al., 1997; Pufahl et al., 1997). Atx1 has a human counterpart, called HAH1, or Atox1. It carries copper to two human Cu^{+}-ATPases called Wilson and Menkes disease proteins (Hamza et al., 1999), which are discussed in the next chapter.

Up to date, no other metallochaperones are known in addition to the three listed above. It remains to be seen if there are chaperones also for other copper enzymes and if any chaperone capable of transferring a metal ion other than copper exists.

Import and export of heavy metals

All organisms have a variety of metal uptake systems, which differ in their specificity and affinity. Specific metal importers are usually tightly regulated, but metal ions can accumulate in a cell via transporters with a broad specificity. For example, the human iron transporter DMT1 has been shown to be able to transport almost any divalent cation (Gunshin et al., 1997; Garrick et al., 2003). Metal ions can also infiltrate into a cell by using molecular mimicry, which means that they are translocated by a transporter destined for an entirely different purpose (Rosen, 2002; Beard et al., 2000). Example of the latter case is the accumulation of Mn^{2+}, Co^{2+} and Zn^{2+} ions via the phosphate transporter (Jensen et al., 2003; Beard et al., 2000; Van Veen et al., 1994). Excess metal ions are detoxified either by capturing them with metallothioneins, or by storing them in vacuoles or other vesicles. These metal ions are finally removed when the cells are sloughed off from the epithelial layer. The role of the metal storage system is well established in metal detoxification

(Thiele et al., 1986; Hamer et al.,1985), but whether this pool of metal ions can be used in the biosynthesis of metalloproteins has not been clearly demonstrated. However, the experimental evidence supports the idea that metals bound to glutathione (GSH) can be utilized this way (da Costa Ferreira et al., 1993; Freedman et al., 1989; Ciriolo et al., 1990; Brouwer & Brouwer-Hoexum, 1992; Musci et al., 1996).

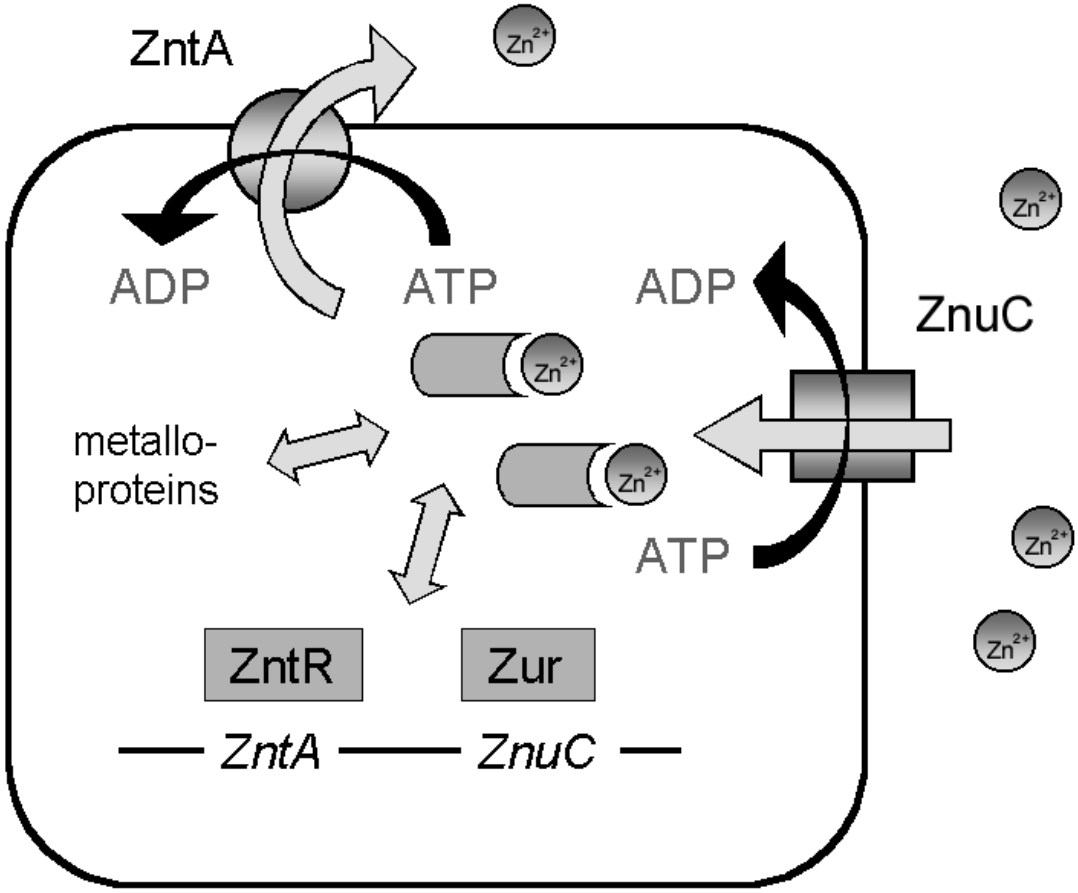

Figure 7. Simplistic scheme of zinc metabolism in *E. coli*. Zinc is imported via ZnuC transporter (Patzer & Hantke, 1998) and inside the cell it is likely to exist bound to some carrier molecule. No metallochaperones are known to exist in *E. coli*, but GSH might play a similar role (see the text). Zinc in this pool can be delivered to zinc proteins including many enzymes and the ZntR and Zur proteins that regulate the *ZntA* and *ZnuC* genes respectively (Brocklehurst et al., 1999; Silke & Hantke, 1998). Excess zinc is removed by ZntA P-type ATPase. In reality, ZntA and ZnuC do not exist in the cell at the same time because one gene is always repressed when the other is active (Outten & O'Halloran, 2001).

Not all cells have vacuoli or metallothioneins. In such cases, effective protection against metal poisoning can be gained by pumping excess ions out of the cells. The majority of the prokaryotic P_{1B}-ATPases are used for this purpose (Nies, 2003). Consequently, they are expressed only in the presence of high concentrations of metal ions in the environment (Brocklehurst, et al., 1999; Petersen & Møller, 2000). A few cases have been reported in which P_{1B}-type ATPases are likely to function as copper importers (Francis et al., 1997; Odermatt et al., 1993; Solioz & Odermatt, 1995). In contrast, eukaryotes utilize these ATPases to deliver copper to intracellular compartments, like the Golgi complex (Shim & Harris, 2003). The same transporters can be used also to maintain the metal homeostasis in higher organisms by means of copper-dependent trafficking (see chapter 4.4).

The subject of this work is ZntA, a zinc exporting ATPase that protects *Escherichia coli* from high levels of zinc (Beard et al., 1997). Key components of a bacterial heavy metal homeostasis system is summarized in Figure 7, by using *E. coli*'s zinc metabolism as an example.

4.2 ZntA – a zinc-translocating P_{1B}-ATPase from Escherichia coli

ZntA is a heavy-metal-transporting P-type ATPase from *Escherichia coli*. It has been demonstrated to drive extrusion of Zn^{2+} and Cd^{2+} ions across the cell membrane (Rensing et al., 1997). Pb^{2+} is also a potent stimulator of the ATPase activity like Zn^{2+} and Cd^{2+} ions (Rensing et al., 1998), but there is no radioactive isotope for Pb^{2+} which could be used to show the actual ion transport to occur. However, disruption of the *ZntA* gene abolishes the ability of the bacterium to grow in the presence of high concentrations of lead, zinc and cadmium salts, which essentially proves that the ATPase functions to export all the three cations (Beard et al., 1997; Rensing et al., 1997; Rensing et al., 1998). The growth of the ΔZntA strain is not disturbed by the presence of metals other than Zn^{2+}, Cd^{2+} and Pb^{2+}. However, this does not exclude the possibility that ZntA has additional substrate cations, because there might exist other systems that could compensate the lack of ZntA by detoxifying these metals. Cu^{2+}, Ni^{2+} and Co^{2+} have been shown to partially activate ZntA (See chapter 3.1 in the results section), but it is unclear whether these cations are actually translocated across the membrane (**I**; Hou et Mitra 2003).

ZntA is not a housekeeping gene; it is expressed only when there is Zn^{2+}, Cd^{2+}, or Pb^{2+} present in the environment of the cell (Brocklehurst et al., 1999). *ZntA* gene is regulated by

ZntR, a zinc-binding protein that activates the expression (Brocklehurst et al., 1999). ZntR is extremely sensitive to the presence of zinc; the expression level starts to rise already at femtomolar (10^{-15}) intracellular zinc concentration (Outten & O'Halloran, 2001).

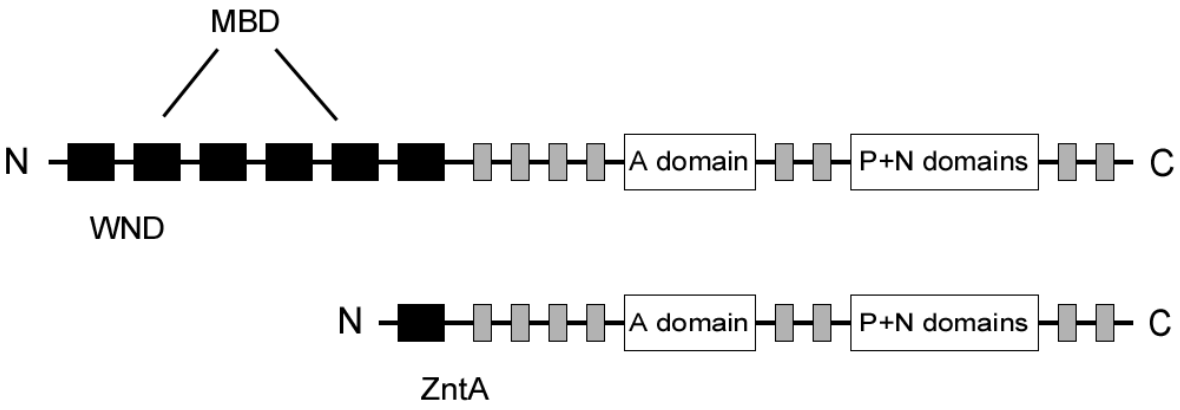

Figure 8. Comparison of the ZntA and Wilson disease protein (WND). The black boxes represent metal-binding domains (MBD), whereas TM-helices are represented with grey. Other cytoplasmic domains are indicated with labels.

The operon contains also another gene, predicted to code for a membrane protein with an unknown function (Sofia et al., 1994). However, ZntA can be expressed and purified in an active form without this protein (expression and activity reported in **I**, purification results not shown. Activity of the purified protein reported in Sharma et al., 2000).

Up to date ZntA remains the best characterized P_{1B}-ATPase. It is used in this work to study the consequences of Wilson disease mutations by introducing disease mutations into ZntA. The metal specificity of the two proteins is different, WND is a Cu^{+}-ATPase and ZntA is transporting divalent cations like Zn^{2+} and Cd^{2+}. Still, the overall identity of the two proteins is ~30%. The size of WND is almost twice as large as that of ZntA, mainly because there are six MBDs in WND, while only one is found in ZntA (Figure 8). WND and Wilson disease are discussed in the next chapters.

4.3 Human copper metabolism disorders – Wilson and Menkes diseases

There are two diseases, known as Wilson and Menkes diseases, which manifest severe consequences of an imbalance of heavy metal homeostasis. The former is a copper accumulation disorder, while the latter is a copper deprivation state (for a recent review, see Shim & Harris, 2003).

Menkes disease

Several Cu-enzymes are known to be vital for the human beings, such as cytochrome c oxidase (Cox), superoxide dismutase (SOD1) and lysyl oxidase (Shim &Harris, 2003). Cox is a terminal oxidase of the respiratory chain (Richter & Ludwig, 2003) and SOD1 is involved in radical scavenging by metabolizing superoxide radicals into hydrogen peroxide (Fridovich, 1997). Lysyl oxidase is required for the formation of connective tissue making the collagen crosslinks (Rucker et al., 1998). A failure to meet the body's copper requirement has therefore serious consequences. Nutritional lack of copper is very rare, but a copper depletion state may develop as a result of a genetic disorder, called Menkes disease (Menkes et al., 1962). In this disease copper transport from intestinal cells to the circulation is blocked (Danks et al., 1972). Hence, copper accumulates in the cells of the intestinal wall, whilst all other tissues are suffering from copper deficiency. The symptoms include impaired growth, defects of connective tissue, kinky hair, hypothermia and neurological degeneration (Menkes et al., 1962; Danks et al., 1972). This difficult condition is treated by administrating copper to the circulation as a Cu-His compound (Sarkar, 1999), but even when treated, the patients often die during the early stages of life.

Wilson disease

Lack of copper has devastating results, but also too high an amount of copper leads to a pathological condition. Copper toxicosis, like copper deficiency, is rarely encountered, but it too can be caused by a hereditary disease, which is called Wilson disease. The first cases were described by a Finnish physician E.A. Homén, who reported a development of neurological symptoms like muscle stiffness and tremor (Homén, 1890a; Homén, 1890b). He also reported the most important post-mortem findings of the patients: badly degenerated lenticular nuclei in the brain and liver chirrosis (Homén, 1892). More than 20 years later, S.A. Kinnier Wilson wrote an extensive article about the disease, reviewing

Homén's patients together with other cases with similar symptoms and post-mortem findings (Wilson, 1912). He called the disease "progressive lenticular degeneration", but it soon got named after him. The disease is also known as hepato-lenticular degeneration. It took several decades before the symptoms were connected to the accumulation of copper in affected organs (Cumings, 1948). Finally, the fundamental basis of the disease was discovered when the Wilson disease gene was cloned simultaneously by three research groups. It turned out to be a copper-transporting P-type ATPase similar to Menkes disease gene cloned earlier in the same year (Tanzi et al., 1993; Bull et al., 1993; Yamaguchi et al., 1993; Vulpe et al., 1993; Chelly et al., 1993; Mercer et al., 1993).

Originally Wilson disease was described as a neurological disorder associated with liver chirrosis (Homén, 1890a; Homén, 1890b; Homén, 1892; Wilson, 1912), but later it was found to manifest also as an acute, or chronic liver disease in children and adolescents. While the severity and onset age of the disease are highly variable, the patients can be divided into two groups on the basis of whether they display mainly neurological or hepatic symptoms (Ferenci, 2003).

There are two principal means to treat the disease (Sarkar, 1999; Subramanian et al., 2002). The first one is to use a copper chelator, such as penicillamine. The metal ions in the plasma are harvested by the drug and the metal-chelator complex is finally removed via urinal excretion. The other strategy is the administration of zinc, which is a potent inducer of metallothionein expression. The metallothionein in the intestinal cells binds copper with much higher affinity than zinc, thus reducing the copper delivery to the circulation. The body gets rid of this copper when the cells are eventually sloughed off from the intestinal wall.

Genetic basis of the diseases

The majority of Menkes disease mutations are small insertions, deletions or splice site mutations, which result in a severe condition (Hsi and Cox, 2004; Chelly et al., 1993; Mercer et al., 1993). Point mutations are also found, but most of them are nonsense mutations and only 17% of all MNK mutations are missense mutations (Hsi and Cox, 2004). Thus, the classical form of Menkes disease develops because of a non-functional or an absent ATPase. Milder forms of Menkes disease have been also been described, including the occipital horn syndrome (Kaler et al., 1994; Møller et al., 2000), that comprise roughly 5-10% of the cases. In contrast, Wilson disease occurs largely due to missense mutations, over a hundred of which have been described so far (Hsi and Cox,

2004; Cox, 2002). Unlike in Menkes disease, it seems that in most cases the mutation do not lead to complete loss of Cu-ATPase activity (Thomas et al., 1995; Shah et al., 1997).

4.4 Multiple roles of MNK and WND copper pumps

Menkes disease and Wilson disease ATPases share about 60% identity and they are functionally interchangeable (La Fontaine et al., 1998). Still, the outcomes of the two diseases are completely the opposite. This is due to the different expression patterns of the genes: Menkes disease protein (MNK) is expressed in almost every tissue excluding the liver (Vulpe et al., 1993; Chelly et al., 1993), while Wilson disease protein (WND) is expressed mainly in the liver (Tanzi et al., 1993; Bull et al., 1993).

MNK and WND in copper homeostasis

MNK is the pump that delivers copper to the circulation from the intestinal cells during copper uptake (Linder & Hazegh-Azam, 1996; Shim & Harris, 2003). In Menkes disease this step is abolished, which explains the accumulation of copper in intestinal cells and the systemic lack of this metal in all other tissues. In contrast, WND functions in the liver in the excretory route of copper (Linder & Hazegh-Azam, 1996; Shim & Harris, 2003). The only way for human beings to secrete copper in significant amounts is via bile, synthesized in the liver. In order to get into bile canaliculae, the cytoplasmic copper ions in a hepatocyte have to be pumped out by WND. It is straightforward to connect the hepatic accumulation of copper with ATPase impaired by a Wilson disease mutation. The basis of the copper-induced neurological degeneration, however, is poorly understood. WND is not expressed exclusively in the liver, as significant WND expression is seen in the kidney and the placenta and minor levels are detected also in other tissues, including the brain (Bull et al., 1993; Tanzi et al., 1993). In principle, when mutated, this cerebrally expressed ATPase could be the cause of the copper accumulation in the brain. However, Wilson disease patients who are treated with liver transplantation show a marked improvent of both the hepatic and neurological symptoms, unless the nervous tissue is already severely damaged (Eghtesad et al., 1999; Schilsky et al., 1994). This implies that while the cerebral WND might play a part in the development of the neurological symptoms, it is not the primary cause for the degeneration of the nervous tissue. It has been suggested that liver damage leads to the leakage of copper to the circulation and somehow this copper accumulates in

the brain (Cox & Moore, 2002). The details of this process are largely unknown. Apolipoprotein E genotype ε3/ε3 has been observed to be connected to a late-onset age of Wilson disease, indicating that also other genes in addition to *Atp7B* itself can affect the outcome of the disease (Schiefermeier et al., 2000).

Cellular location of WND and MNK

Considering the tasks of MNK and WND in the export of copper from the cell, one would expect to find the ATPases at the plasma membrane. Surprisingly, immunomicroscopy has revealed that both proteins are intracellular and localize in the trans-Golgi network (TGN) (Yamaguchi et al., 1996; Dierick et al., 1997; Hung et al., 1997). The Golgi retention signal has been proposed to be associated in the third TM-helix, as the alternatively spliced MNK missing TM-helices three and four fails to localize in TGN and a plasmamembrane localizing protein CD8 fused with the TM3 is found in the TGN (Francis et al., 1998).

This location is linked to the function of the ATPases in the delivery of copper for the synthesis of Cu-enzymes in the secretory route. One such enzyme is lysyl oxidase, which cannot function properly when copper transfer to the Golgi lumen is impaired in Menkes disease (Rucker et al., 1998). Another example is ceruloplasmin, the most prominent copper protein in plasma. This multicopper oxidase is synthesized in the liver, where copper needed for its biosynthesis is provided by WND (Murata et al., 1995). Ceruloplasmin is a multifunctional protein involved in copper transfer and antioxidation, but its main function seems to be mobilization of the intracellular iron. Aceruloplasminemia is a rare hereditary condition characterized as an iron accumulation disorder due to the absence of ceruloplasmin (Yoshida et al., 1995).

Analogously, a copper ATPase in *S. cerevisiae*, Ccc2, is found to transport copper into the Golgi lumen, where it is incorporated into Fet3 oxidase (Yuan et al., 1995; Yuan et al., 1997). Fet3 is a ceruloplasmin-like multicopper enzyme, which is a critical component of the high-affinity iron uptake system. Both MNK and WND can replace Ccc2 in a ΔCcc2 strain (Hung et al., 1997), suggesting that the universal task of eukaryotic copper ATPases is the intracellular copper transport.

The yeast system has been used widely as an *in vivo* copper transport activity assay (Forbes & Cox, 1998; Forbes et al., 1999; Payne & Gitlin, 1998; Iida et al., 1998; Sambongi et al., 1997; Borjigin et al., 1999). This has been conducted by replacing Ccc2 with other Cu-ATPases and measuring the growth of this yeast strain in iron-deficient environment.

Copper-dependent trafficking

WND and MNK do not function only in the metalloprotein biogenesis, but they are also involved in the copper homeostasis of the cell and the whole organism (Linder & Hazegh-Azam, 1996). Therefore, it was a surprise to find them to be intracellular proteins. The scheme started to make sense, when both MNK and WND were found to undergo copper-dependent trafficking. At elevated copper concentrations MNK moves from the Golgi complex to the plasma membrane (Petris et al., 1996), whereas WND is transferred to a vesicular compartment (Hung et al., 1997). WND has also been reported to exist at the plasma membrane, but these results are controversial (Schaeffer et al., 1999; Roelofsen et al., 2000). The trafficking is linked to a reversible phosphorylation event distinct from the transient phosphorylation taking place during the catalytic cycle (Vanderwerf et al., 2001; Voskoboinik et al., 2003b). In contrast to the catalytic acylphosphate intermediate, this regulatory phosphorylation is not sensitive to hydroxylamine. When the copper concentrations decreases, the ATPase is dephosphorylated and subsequently returns to the TGN.

The expression of WND has been shown to be modulated by copper, although it is constitutively expressed (Oh et al., 2002; Schilsky et al., 1998). The significance of this regulation is not clear.

Copper-dependent trafficking is a way to regulate the copper flow. It can be directed either to the Golgi lumen to be incorporated into luminal metalloproteins, or to the extracellular space to support copper delivery to the other cells and eliminate excess copper.

4.5 Genotype/phenotype correlation in Wilson disease

The world-wide prevalence of Wilson disease is ~ 30 per million which means that the carrier frequency is 1 per 90 (Figus et al., 1995; Petrukhin et al., 1993). So far over a hundred disease-causing missense mutations have been reported (Cox, 2002). In addition, also deletions, insertions and non-sense mutations have been reported. As most of the patients are compound heterozygotes (Thomas et al., 1995; Riordan & Williams, 2001), a considerable amount of different genotypes exists. Consequently, there is a large variety of disease phenotypes and no single diagnostic test can confirm Wilson disease with 100% certainty (Ferenci et al., 2003). This can be achieved by using genetic testing, but it is very laborious owing to the large size (~ 80 kb) of the *ATP7B* gene (Waldenström et al., 1996).

The complexity of genotypes and phenotypes makes it difficult to assign any correlations between them (Thomas et al., 1995). For the most common mutations, patients exist in significant numbers allowing comparisons, but the phenotypes display large variation even among the subjects sharing exactly the same *ATP7B* genotype. One can still draw some conclusions, which are discussed below.

Mutation H1069Q

Among European and North American population H1069Q is the most common mutation (Riordan & Williams, 2001; Loudianos et al., 2000). Homozygous patients carrying this mutation have a mean onset age of about 20 years (17 years in all Wilson disease patients) (Shah et al., 1997; Houwen et al., 1995). In one study, the proportion of patients displaying mainly hepatic or neurological manifestations is roughly equal (Shah et al., 1997), whereas in an other study most patients had neurological symptoms (Czlonkowska et al., 1997). Hepatic copper accumulation varies from normal to six-fold and ceruloplasmin levels from normal to zero (Shah et al., 1997).

The histidine-1069 is strictly conserved among heavy-metal-transporting ATPases and has a complex role in the catalytic cycle (see chapter 5.3). It can be concluded that H1069Q is a relatively mild mutation, because of its tendency to result in a late onset of the disease.

The biochemical findings are discussed in the chapter 2.3 in the results section.

Mutation R778L

In Asia, the mutation R778L is the most prevalent one. It is associated with an early onset of the disease (mean onset at 14 years of age) and with the prevalence of hepatic symptoms (in one study only 3 of 18 patients displayed neurological symptoms) (Wu et al., 2001; Okada et al., 2000).

The arginine-778 is not completely conserved and no function has been assigned to it so far. In contrast to H1069Q mutation, R778L seems to have a strong inhibitory effect on WND. This conclusion is supported by the observation that MNK carrying the R778L mutation is a poor substitute of Ccc2 in ΔCcc2 yeast strain (Forbes & Cox, 1998).

4.6 Molecular basis of the Wilson disease – a trafficking defect?

Soon after the Wilson disease gene was found, it was reported that the mutation H1069Q causes a trafficking defect (Payne et al., 1998). Instead of residing at the TGN, immunomicroscopy revealed that the mutant protein was retained at the endoplasmic reticulum (ER). At a lower temperature WND could reach the TGN, but it was still unable to undergo copper-dependent trafficking. These findings started a discussion about the possibility that Wilson disease might develop not because of an impaired function of the ATPase, but due to its mislocalization. In support of this hypothesis, several other Wilson disease mutations were also reported to cause a trafficking defect (Forbes & Cox, 2000; Forbes & Cox, 1998).

A failure to leave ER implies that the folding of the protein is abnormal. It is a general observation that misfolded proteins are arrested in the ER because they are recognized by the quality-checking machinery (Seng et al., 1990; Deen et al., 1995; Kopito, 1997). At lower temperatures the mutated proteins might fold correctly and be able to escape to the Golgi (Denning et al., 1992). In contrast to this type of general structural defect, which leads to mislocalization of the protein, the impaired copper-dependent trafficking of the proteins that are able to get to the TGN suggests that the mutations have also a more specific effect on the enzyme. It is possible that they affect regions which are responsible for ATPase trafficking.

Is the trafficking defect a primary effect of the mutations?

The recent evidence however implies that the activity and location of the ATPase are not completely independent properties. First of all, destroying the catalytic site by replacing the key aspartate abolishes trafficking completely (Petris et al., 2002). On the other hand, The Menkes disease mutation L873R (Ogawa et al., 1999), or replacement of the TGE motif of WND with the AAA sequence (Petris et al., 2002), both of which impaire dephosphorylation step (Clarke et al., 1990; Portillo & Serrano, 1988), result in a protein that is constitutively located in the vesicular compartment. These results demonstrate that trafficking is connected to the formation of the catalytic phosphointermediate. In the chapter 4.4 it was mentioned that trafficking is linked to a phosphorylation event distinct from the catalytic phosphorylation. However, in the light of the findings discussed above, it seems that this additional phosphorylation alone does not determine the location of the

ATPase, but the catalytic phosphorylation also affects it. Secondly, mutations that impaire the localization or trafficking of WND and MNK are not concentrated on any particular site in the protein. They are found in the N-terminal metal-binding sites, (Goodyear et al., 1999; Strausak et al., 1999), at, or near the intramembraneous metal binding site, (the CPx motif) (Tümer et al., 1999; Petris et al., 2002; Kim et al., 2002), in the nucleotide-binding domain, (the HP motif) (Payne et al., 1998), as well as from the C-terminus (mutation A1364V in the 7th TM-helix) (Ambrosini & Mercer, 1999) of WND, or MNK.

Copper-dependent trafficking plays undoubtedly a significant role in the development of Wilson disease. However, so far there is little, if any, evidence of a specific mechanism which would explain how the mutations would affect trafficking itself. In several cases the failure in trafficking seems to be connected to the impaired activity of a mutated ATPase.

5 Functional sites of P_{1B}-ATPases

5.1 Common mechanism of function

Even though the sequence similarity is generally low among P-type ATPases, the structural motifs forming the catalytic center of phosphorylation and dephosphorylation activities are well conserved throughout the protein family (Møller et al., 1996; Solioz et Vulpe, 1996; Lutsenko & Kaplan, 1995; Axelsen & Palmgren, 1998; Palmgren & Axelsen, 1998). Hence, all P-type ATPases are supposed to function by the same catalytic mechanism despite the differences of the direction, form and stoichiometry of the transported substances. The characteristic features of the individual subfamilies are seen in the other parts of the enzyme. Several sequence motifs have been recognized, which are unique for the P_{1B}-ATPases (Solioz & Vulpe, 1996; Lutsenko & Kaplan, 1995). These include two motifs, the HP and the GxGxxG/A, which are found in the N domain, the CxxC in the N-terminus and the CPx (x is Cys, His, or Ser) located in the putative sixth TM-helix (see Figure 6). The two cysteine motifs form metal-binding sites. These motifs are discussed in the following chapters.

5.2 Metal-binding sites and substrate specificity

N-terminal metal-binding domains

Principally, two forms of N-terminal metal-binding motifs exist. The most commonly encountered is the CxxC motif. These are parts of metal-binding domains (MBD), that are present in one or two copies in prokaryotes, whereas eukaryotic ATPases may have up to six copies, like in WND and MNK (Argüello, 2003). Some ATPases have N-terminal sequences rich in histidines (Odermatt et al., 1993; Argüello, 2003). These histidine-rich sequences exist either alone or together with MBDs (Argüello, 2003).

The structure of an MBD of several ATPases has been determined (Banci et al., 2002; Banci et al., 2001; Gitschier et al., 1998). It resembles closely the bacterial mercury-binding protein MerP (Steele & Opella, 1997) and the copper chaperone Atx1 of yeast (Arnesano et al., 2001), both of which carry a similar cysteine motif. The data from the crystal structures (Wernimont et al., 2000) together with spectroscopic experiments (Ralle et al., 2003) demonstrate that the CxxC motif forms a novel metal-binding site where the metal ion is linearly coordinated between the cysteines. The presence of only two metal ligands instead of three or four normally seen in metalloproteins means that the metal ion is not only bound less tightly, but it is also more accessible to other ligands (Ralle et al., 2003; Pufahl et al., 1997). These properties make the site suitable for transient metal binding, that is, the ion could be easily exchanged with other metal-binding sites in soluble metal ion carriers and with the translocation site, the CPx motif.

The role of MBDs has proved to be complex. WND and MNK both have six MBDs, and these are not interchangeable (see below). The first four domains have been demonstrated to interact with the Atox1 metallochaperone. The metal ion can be exchanged between these four MBDs and Atox1 by a simple equilibrium reaction (Huffman & O'Halloran, 2000; Hamza et al., 1999; Larin et al., 1999). The fifth and sixth domains, on the other hand, do not interact with Atox1 (Larin et al., 1999). Instead, they seem to be important for copper-dependent trafficking. Trafficking is lost if they are deleted and even if they are replaced by any of the first four MBDs (Mercer et al., 2003). At least one of the MBDs has to be intact for the ATPase to be functional (Mercer et al., 2003; Forbes et al., 1999). These results suggest that MBDs are an integral part of the ion-translocation pathway. However, low activity have been observed from MNK with all MBDs mutated (Voskoboinik et al., 2001; Voskoboinik et al., 1999). This is in agreement with reports from studies with

prokaryotic ATPases, in which a deletion or mutagenesis of the N-terminus does not affect severely the function of the enzyme (Mitra & Sharma, 2001; Bal et al., 2001; Fan, et al., 2001; Mandal & Argüello, 2003). Moreover, several P_{1B}-ATPases are known, which do not have MBDs at all (Rutherford et al., 1999; Borjigin et al., 1999). It seems that there must be an alternative way to provide the translocation site with metal ions.

The N-terminus of WND has been shown to interact in a copper-dependent manner with the catalytic loop carrying the N and the P domain (Tsivkovskii et al., 2001). In the presence of copper ions the binding is weaker, whereas in the absence of copper, the N-terminus hinders the binding of the nucleotide to its binding site. This suggest that MBDs could also have a regulatory role by slowing down the residual ATPase activity when copper is not available.

The most recently solved MBD structure is that of ZntA (Banci et al., 2002). In this structure an additional aspartate residue acts as a third ligand for the metal ion bound to the CxxC motif. This aspartate is supposed to be responsible for rendering the site to favour Zn^{2+}, Cd^{2+} and Pb^{2+}, which are the biological substrates of ZntA. The basis of the substrate specificity of the P_{1B}-ATPases is not known. In principle it could be possible that it is determined by the N-terminal metal-binding site. However, a chimeric protein with the N-terminus from WND fused to the C-terminal part of ZntA does not show any alterations in its substrate specificity compared to the wild-type ZntA (Hou et al., 2001). This implies that the metal specificity originates from an other site.

CPx motif and the basis of the metal selectivity

As the N-terminal metal-binding sites do not affect the metal specificity of heavy-metal-transporting ATPases, it must be involved with the intramembraneous metal-binding site. Known as the CPx motif (Solioz & Vulpe, 1996), this site exists in forms of CPC, CPH, CPS, SPC and TPC (two proteins are known to carry an APC motif) (Argüello, 2003). Several studies have been reported in which one or both of the residues flanking the proline have been mutated, and the result has invariably been an inactive ATPase (Forbes & Cox, 1998; Bissig et al., 2001; Yoshimizu et al., 1998). Clearly, this site has to be intact for an ATPase to be functional, consistent with the idea that it is the metal translocation site.

Interestingly, an ATPase with the SPC motif has been shown to be a Co^{2+} pump (Rutherford et al., 1999), while a CPH motif has been found in a Cu^{2+} specific ATPase. Neither of these cations is a good substrate of an ATPase with the CPC motif. However, the CPC variant itself is not associated with a specific metal selectivity, as the group of proteins

carrying this motif includes both Cu^+-ATPases, like WND and MNK, and Zn^{2+}-ATPases, like ZntA (see Table 1). Thus, the CPx motif does not determine the substrate specificity alone.

Table 1. Variants of the metal-binding motif in the 6th TM-helix and its relation to the metal specificity

Motif	Substrate cations	Remarks
CPC	Cu^+, Ag^+ Zn^{2+}, Cd^{2+}, Pb^{2+}	Most common. Carried by both Cu^+- and Zn^{2+}-ATPases
CPH	Cu^{2+}, Cu^+, Ag^+	Primarily Cu^{2+}-ATPases
CPS	Not known	rare
SPC	Co^{2+}	
TPC	Not known	
APC	Not known	rare

A general factor that could play a role in ion selectivity is the helix packing (Mandal et al., 2003). Heavy metal ions differ significantly in their size as well as in their requirements for the geometry of the coordination sphere. While the helix packing may be one factor, the size of the ion does not seem to play any role in the selectivity. Cu^+-ATPases have been shown to transport Ag^+ ions in addition to Cu^+ ions with ionic radii of 126 and 96 pm respectively (Weast, 1979). Similarly ZntA has been demonstrated to transport Zn^{2+}, Cd^{2+} and Pb^{2+} ions with ionic radii of 74, 97 and 120 pm respectively (Weast, 1979). Both types of ATPases are not only able to transport ions that vary widely in size, but also the ionic radii overlap significantly between the two groups of the substrate cations. Several residues have been recently identified in the seventh and eighth TM-helices, conservation of which seems to be connected to the metal specificity (see Table 2) (Argüello et al., 2003).

Interestingly there is an aspartate in the eight TM helix, conserved only among Zn^{2+}-ATPases. In case of the N-terminal metal-binding site, an additional aspartate changed the selectivity of the site in favor of Zn^{2+} (Banci et al., 2002). It is plausible that these residues could affect ion selectivity by functioning as additional ligands for the metal ion at the CPC site, but this idea remains to be experimentally tested.

Table 2. Conserved residues of the 7th and 8th TM-helices in Cu^+- and Zn^{2+}-ATPases. The numbers refer to WND in Cu^+-ATPases and to ZntA in Zn^{2+}-ATPases respectively.

ATPase type	7th TM-helix	8th TM-helix
Cu^+-ATPases	$N^{1331}Y$	$M^{1359}xxSS$
Zn^{2+}-ATPases	K^{693}	$D^{714}xG$

5.3 Nucleotide-binding site – the glycine and HP motifs

The residues forming the nucleotide-binding site in Ca^{2+}- and Na^+/K^+-ATPases are conserved in most P-type ATPases, but none of them are found in P_{1B}-ATPases (**III**). Instead, there are two sequence motifs characteristic only to members of this subfamily. Both of these are located in the N domain. The HP motif is present 34-43 residues from the phosphorylatable aspartate (Lutsenko & Kaplan, 1995; Solioz & Vulpe, 1996) and a protein kinase-like GxGxxG/A motif is found downstream in the same domain (**III**).

The HP motif has aroused much interest, as the histidine is the residue most often mutated among the Western population of Wilson disease patients (Riordan & Williams, 2001; Loudianos et al., 2000). The role of the histidine is ambiguous. *In vivo*, the H1069Q mutation has been shown to reduce the half-life of the protein and prevent trafficking (Payne et al., 1998). The mutant has been reported to retain significant ATPase activity *in vitro* and it is also able to complement partially ΔCcc2 yeast strain (Iida et al., 1998, Payne & Gitlin, 1998). Recent studies indicate that mutations of the residue affect ATP binding (Tsivkovskii et al., 2003; Voskoboinik et al., 2003a, **III**). However, the mutants have their

P_i phosphorylation also impaired, which suggests that the residue might participate in steps of the catalytic cycle other than ATP binding (**I**; Tsivkovskii et al., 2003) (see also chapter 2.3 in the results section).

The GxGxxG motif has been demonstrated to interact with ATP in the nucleotide-binding pocket of protein kinases (Zheng et al., 1993). Two first glycines in this motif are invariant, whereas the last residue is always small; Gly, Ala, or Ser in protein kinases and Gly, Ala, Ser, or Cys in P_{1B}-ATPases (Hanks et al., 1988; **III**). The possibility that this motif would also be functionally similar, and participate in nucleotide binding in P_{1B}-ATPases, has been studied in this thesis (**III**) (see chapters 1 and 2.4 in the results section).

Aims of the study

I) Chracterization of *E. coli*'s zinc-translocating P-type ATPase ZntA. This includes determination of the metal specificity of the ATPase activity and phosphorylation reactions.

II) To investigate whether the ZntA overexpression system could be used for study the effects of Wilson disease mutations.

III) To identify the ATP-binding residues in P_{1B}-ATPases as a part of a major question of how ATP drives the catalytic cycle.

Materials and methods

1 Cloning and mutagenesis

ZntA was cloned into pTrcHis vector as described in **I**. Mutations were introduced by PCR method (Cormack, 1995). When possible, silent mutations were also introduced to screen rapidly the colonies carrying the desired mutation. Finally, the region of the expression plasmid corresponding to the PCR fragment was sequenced to verify the proper genotype.

2 Expression

N-terminally his-tagged ZntA constructs turned out to be unstable; cultures stored on plates often had deletions in the plasmid, resulting in poor expression of the ATPase. Therefore bacterial cultures harboring the expression plasmid were always started from frozen glycerol stocks. The detailed expression protocol is described in **I**.

3 Preparation of membranes

The preparation of bacterial membranes was carried out as described in **I**. ZntA was observed to be susceptible to proteolysis, and PMSF was used in every step to inhibit proteases. SDS-PAGE was used routinely to estimate the expression levels of the mutants. In some early experiments the membranes were prepared with buffers at pH 8.0, but in later experiments pH 7.5 was used, because it preserves the activity better.

4 ATPase activity measurement

ATPase activity was determined directly on the membranes of ZntA-expressing strain using the phosphate analysis method (Lutter et al., 1993) with some modifications (**I**). To create a Cu^{+} species, 5 mM DTT was added to reaction mixture containing $CuSO_4$.

5 Labeling by [^{33}P]ATP and [^{33}P]P_i

ATP phosphorylation

Phosphorylation of the membrane fraction by [γ-^{33}P] ATP (Amersham Pharmacia) was carried out on ice in pH 6.0 as described in **I**. The reaction was started by adding a solution containing ATP and 8 mM $MgCl_2$. The reaction was stopped after 30 s by addition of ice-cold 10% TCA. The membrane pellets were washed once with ice cold water and once with ice-cold 50 mM H_3PO_4, pH 2.4. The acidic conditions are necessary for the stability of the phosphointermediate (Makinose, 1969). In the results section all the data presented is corrected for the dilution factor.

P_i phosphorylation

Phosphorylation by [^{33}P]P_i was carried out at room temperature. The reaction mixture was pipetted as above, but the reaction buffer was 100 mM MES, pH 6.0, 25-40% DMSO when metal ions were included; when the heavy metal ions were not present, the reaction mixture contained also 0.5 mM EDTA. The reaction was started by adding 40 μCi [^{33}P]P_i and 8 mM $MgCl_2$ giving a final concentration of P_i of 100 nM. The reaction time was 10-12 min.

Analysis of the phosphointermediates

The analysis of phosphointermediates by acidic SDS-PAGE was carried out essentially as described by Fairbanks and Avruch, 1972, at pH 2.4. The bands were analyzed in the phosphoimager.

6 Dephosphorylation

The rate of dephosphorylation of the phosphoenzyme intermediate was determined in the absence of ADP (dephosphorylation via the E_2P intermediate) and in the presence of ADP (dephosphorylation directly from the E_1P form). The membrane fractions were first phosphorylated with [γ-^{33}P]ATP as in the phosphorylation assay above. Phosphorylation was allowed to proceed for 30 s after which the reaction was stopped with 5 mM EDTA with 250 μM ADP or with 5 mM EDTA alone. The protocol is described more in detail in **II**.

7 Modelling

Sequence alignment. The alignment in Figure 9 was constructed using ClustalX (Thompson et al., 1997). In order to create gap penalties for the program, the known secondary structure of sarcoplasmic Ca^{2+}-ATPase and the predicted secondary structure of ZntA (see below) were used. The P-type ATPase sequences used are listed in **III**.

Secondary structure predictions. The secondary structure of ZntA was predicted using the PHD program (http://www.embl-heidelberg.de/predictprotein/) (Rost, 1996). The input consisted of all the heavy metal ATPase sequences listed in **III**. To test the reliability of the prediction program, the secondary structure of Ca^{2+}-ATPase was also analysed using the sequences of Na^+, K^+-ATPases and Ca^{2+}-ATPases (the plasma membrane Ca^{2+}-ATPases were not included) as the input. In general, the secondary structure prediction of Ca^{2+}-ATPase, carried out without information about the three-dimensional structure, agreed well with the secondary structure elements observed in the crystal structure. In particular, all the secondary structure elements (see Figure 1) which we proposed to constitute the core of the N domain of P-type ATPases were predicted correctly when using only the Ca^{2+}- and Na^+, K^+-ATPase sequences as the input.

Modelling. The coordinates of sarcoplasmic Ca^{2+}-ATPase (PDB entry 1IWO), describing the Ca^{2+}-ATPase structure in the E_2 state at a 3.1 Å resolution (Toyoshima & Nomura, 2002), were obtained from the Protein Data Bank (PDB). The correspondence between Ca^{2+}-ATPase and ZntA was established using secondary structure prediction and sequence alignment (Figure 1). The loop ranging from G^{503} to V^{510} in ZntA was positioned similarly with the Ca^{2+}-ATPase loop between residues L^{485} and S^{495}. This loop comprises residues $F^{487,}$ R^{489} and K^{492}, suggested to interact with ATP in Ca^{2+}-ATPase. The conformation of the segment G^{503}SGIEAQV of ZntA was then modelled using the structure of the glycine loop (G^{50}TGSFGRV) of cAMP-dependent kinase (cAPK, PDB entry 1ATP) as the template. The conformations of other loops connecting the conserved secondary structure elements were taken from PDB using Insight II loop search utility.

Results

1 Modelling the N domain of ZntA

1.1 Sequence alignment of P-type ATPases

The crystal structures of Ca^{2+}-ATPase (Toyoshima et al., 2000; Toyoshima & Nomura, 2000) provided a possibility to use homology modelling to support the mutagenesis studies. P-type ATPases in general share a low sequence similarity, which is typically in a range of 15-25%. The homology is mainly seen in the conserved sequence motifs, which form the functionally important sites. These sites can be used to align different P-type ATPase sequences. The M and N domains, however, do not contain any sequence motifs common to all P-type ATPases. The latter domain in P_{1B}-ATPases contains several residues not conserved in other P-type ATPases. Mutations in many of these P_{1B}-ATPase-specific residues result in Wilson disease.

The N domain of Ca^{2+}-ATPase comprises the residues N^{359} – P^{602}, whereas in ZntA the domain is significantly smaller, ranging from G^{444} to T^{560} (Figure 9). The identity between the sequences is about 13%. The alignment was made using the secondary structure information of the two proteins (**III**, Figure 9). A comparison of the Ca^{2+}-ATPase secondary structure and the predicted secondary structure of ZntA suggested that the elements forming the core of the N domain in Ca^{2+}-ATPase were preserved also in ZntA. The parts missing from ZntA were largely loops which folded on the surface of the domain in Ca^{2+}-ATPase. The core was defined on the basis of the temperature factors of the E_1 structure (see Figure 9). The alignment with a number of different P-type ATPases demonstrates that the core is conserved throughout the protein family although many insertions and deletions are seen in this area in individual subfamilies.

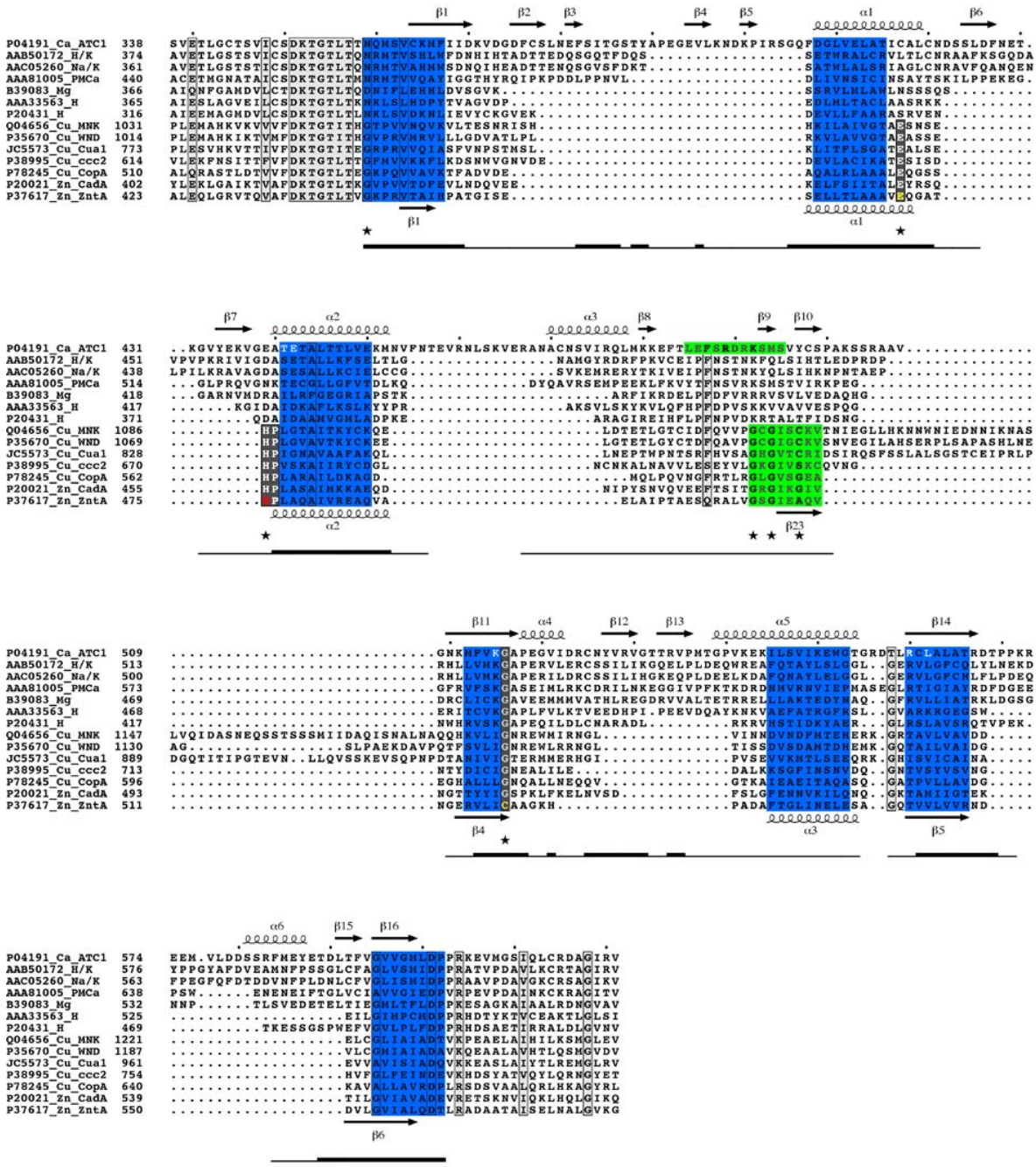

Figure 9. An alignment of N-domain sequences of P_1-, P_2- and P_3-type ATPases. The accession number of each sequence is on the left. The sequences are: P04191 (rabbit sarcoplasmic Ca^{2+}-ATPase), AAB50172 (human H^+,K^+-ATPase), AAC05260 (pig Na^+,K^+-ATPase), AAA81005 (rat plasma membrane Ca^{2+}-ATPase), B39083 (*Salmonella typhimurium* Mg^{2+}-ATPase), AAA33563 (*Neurospora crassa* H^+-ATPase), P20431 (*Arabidopsis thaliana* H^+-ATPase), Q04656 (Menkes disease protein, human Cu^+-ATPase), P35670 (Wilson disease protein, human Cu^+-ATPase), JC5573 (*Caenorhabditis elegans* Cu^+-ATPase), P38995 (*Saccharomyces cerevisiae* Cu^+-ATPase), P78245 (*Escherichia coli* Cu^+-ATPase), P20021(*Staphylococcus aureus* Zn^{2+}-ATPase), P37617 (ZntA, *Escherichia coli* Zn^{2+}-ATPase). The secondary structure of the rabbit sarcoplasmic Ca^{2+}-ATPase, based on the crystal structure 1IWO, is indicated with arrows and helix symbols above the

sequences. The predicted secondary structure of ZntA is shown beneath the sequences. The residues in the Ca^{2+}-ATPase sequence shown in white have been proposed to interact with bound ATP. The bottom line indicates the magnitude of the temperature factor for each amino acid residue in the Ca^{2+}-ATPase crystal structure 1EUL [1]: thick line, B < 35 $Å^2$; thin line 35 $Å^2$ < B < 55 $Å^2$; no line, B > 55 $Å^2$. The segments forming the core secondary structure elements are highlighted with dark grey. The well-conserved residues are in light grey. The ATP-binding loop of Ca^{2+}-ATPase is marked by a black box, which is used to indicate the HP and glycine motifs in the P_{1B}-ATPases. ZntA mutants studied are marked with asterisks. The alignment is modified from **III**.

1.2 The molecular model of the N domain of ZntA

The N domain has a novel fold (Stokes & Green, 2003), preventing the usage of proteins other than P-type ATPases in the modelling. As already mentioned, the ATP-binding residues of the P_2-ATPases are not conserved in the P_{1B}-ATPases. On the other hand, proteins of this subfamily possess two sequence motifs, the HP and GxGxxG/A, which are missing in other P-type ATPases. The major question in the modelling was, whether these two sites could be modelled as part of the putative nucleotide-binding site.

The model of the N domain of ZntA (**III**) and the structure of the N domain of Ca^{2+}-ATPase are compared in figure 10. In general, the N domain of ZntA is composed of a β-sheet surrounded by three α-helices. In Ca^{2+}-ATPase the ATP-binding cleft is formed mainly by the helix α2, strand β11 and a loop containing residues L^{485}-S^{495}. In the sequence alignment the first two elements are conserved in ZntA (helix α2 and strand β4), but there is no clear counterpart for the loop L^{485}-S^{495}. However, the GxGxxG/A motif is found in this region and to preserve the overall form of the ATP-binding site, the GxGxxG/A was modelled in place of the loop in Ca^{2+}-ATPase.

According to the model, the HP dipeptide is a part of the loop V^{469}EQGATH^{475}P, which connects the N domain helices α1 and α2. H^{475} is predicted to be at the N-terminus of the helix α2. In the alignment this residue corresponds to E^{439} in Ca^{2+}-ATPase and D^{443} in Na^+/K^+-ATPase, the latter of which is suggested to be involved in ATP binding (Patchornik et al., 2000; Goldshleger & Karlish, 1999). In Ca^{2+}-ATPase two residues nearby, T^{441} and E^{442}, are likely to play role in ATP binding (Clausen et al., 2003; Hua et al., 2002b). It is also interesting that the in the E_2 structure E^{439} is seen to be very close to the A domain: it is roughly in the distance of 4 Å from S^{186}, or 3 Å from R^{174}. Hence, it is possible that H^{475} in ZntA interacts with the A domain in the E_2 state (see the discussion).

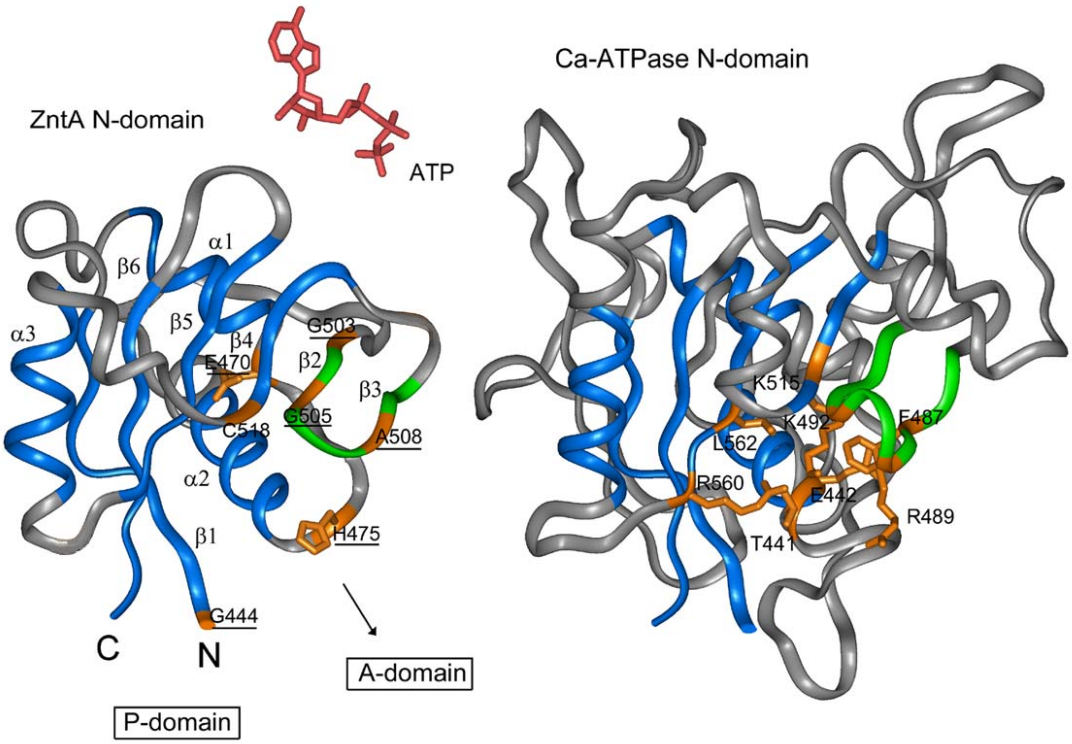

Figure 10. Comparison of the molecular model of the N domain of ZntA and the structure of the Ca^{2+}-ATPase N domain (PDB entry 1IWO). The blue colour indicates the areas constituting the conserved core of the domain. The amino acid residues we have mutated in this work are displayed with orange colour, which is also used to indicate the residues involved in ATP binding in Ca^{2+}-ATPase. The Wilson disease mutation analogues are underlined. The G^{503} loop in ZntA, modelled using the glycine loop of cAPK as a template, and the Ca^{2+}-ATPase loop carrying three ATP-binding residues (F^{487}, R^{489} and K^{492}) are displayed in green.
An ATP molecule coloured red, taken from the crystal structure of cAPK (PDB entry 1ATP), is shown to provide a molecular scale. The approximate locations of the P and A domains are indicated. The figure is modified from **III**.

The GxGxxG/A motif is found in a long stretch of residues between the helix α2 and the strand β4 (β11 in Ca^{2+}-ATPase). Virtually no sequence homology is found between ZntA and Ca^{2+}-ATPase in this region. In Ca^{2+}-ATPase, a part of this sequence folds into a loop that carries the ATP-contacting residues F^{487}, R^{489} and K^{492}. The glycine motif of ZntA, (G^{503}SGIEAQV^{510}) resembles the ATP-binding loop of cAPK (G^{50}TGSFGRV^{57}). Assuming that the overall shape of the ATP-binding site of the P_{1B}-ATPases resembles that

of other P-type ATPases, the glycine loop might replace the ATP-binding loop of the Ca^{2+}-ATPase. Hence, the glycine loop of ZntA was modelled using the cAPK glycine loop structure (Zheng et al., 1993) as a template and it was placed in an analogous orientation to that of Ca^{2+}-ATPase loop L^{485}-S^{495}. In silico, this substitution can be implemented without affecting the core structure of the domain. However, the direction of the peptide chain is reversed in the ZntA model compared to the L^{485}-S^{495} loop in Ca^{2+}-ATPase structure. In conclusion, a model for ZntA N domain can be constructed, in which the HP and GxGxxG/A motifs are placed in the putative ATP-binding site, while preserving the core structure of the domain.

The model predicts two residues, C^{518} and E^{470}, which do not belong to the two motifs, to be also found in the nucleotide binding site. The former is situated on the edge of the nucleotide-binding cleft, whereas the latter is found at the bottom of the binding site. Two Wilson disease mutations, E470A and E470K, have been found to affect E^{470} (Shah et al., 1997; Figus et al., 1995). The mutants C518P and E470A have been reported in publications **I** and **III** (see Table 3). Both mutations result in a significant ATP-binding defect, namely impaired phosphorylation by ATP and resistance to ATP-driven E_2-E_1 state conversion (**III**). These results are consistent with the idea that the residues are close to the ATP-binding site.

Table 3. Mutants C518P and E470A.

Mutant	Expression (%)	ATPase activity (%)	ATP phosphorylation (%)		P_i Phosphorylation (%)		
			60 nM	58 μM	P_i	P_i+ATP	P_i+Zn
WT	100	100	14	100	100	12	16
E470A	184	17	0.1	5.2	86	79	17
C518P	115	88	1.2	67	65	32	12

2 Introducing Wilson disease mutations into ZntA

2.1 ZntA as a model for WND

Wilson disease mutations are found in all regions of the WND sequence, but many of them affect residues conserved among P_{1B}-ATPases. This allows using ZntA to study the function of the residues mutated in Wilson disease. ZntA is an ideal protein for studying the function of an P_{1B}-ATPase, as it does not contain multiple metal-binding domains, additional phosphorylation sites, or sugar residues that would complicate the experiments and interpretation of the results. While the bacterial system cannot be used to study trafficking, it does have some advantages in comparison to the yeast system. Unlike in eukaryotes, in which the ATPase localizes to the TGN membranes, in bacteria it is found at the plasma membrane, being readily accessible for the experimentation. Overexpression of ZntA allows direct measurements of ATPase activities and phosphorylation of mutant proteins in the membranes.

2.2 Conformational mutants G444V and P634L

One functionally interesting class of mutants is composed of those affecting the conformational stability of the ATPase. In this work two mutants were found, displaying characteristical features of a conformational mutant: G444V (**III**) and P634L (**II**), corresponding to Wilson disease mutations G1035V and P1274L reported in Nanji et al., 1997 and in Loudianos et al., 1996. G^{444} is located at the strain connecting the N and P domains. Comparison of the E_1 and E_2 structures reveals that this sequence stretch undergoes structural changes during the state conversion. P^{634} is situated in the GDGxNDxP motif at the P domain. This motif was originally thought to function as a hinge (MacLennan et al., 1985; Taylor & Green 1989). However, when the crystal structures of Ca^{2+}-ATPase were reported, it turned out that the motif remains immobile in respect to the rest of the P domain, when the domain itself moves during the catalytic cycle. However, in the E_2 state the A domain packs together with the P domain and P^{709} (corresponding to P^{634} in ZntA) is at the interface of the two domains.

Expression and ATPase activity

Both G444V and P634L displayed a wt-like expression (Table 4). The G444V mutant retained a moderate ATPase activity of 32%, whereas the mutation P634L resulted in a severe reduction of activity, preserving only 7% of the wt activity.

Table 4. Expression and ATPase activity of mutants of putative communication pathways. The numbers refer to the percentage compared to the wt activity. The ATP concentration used was 4 mM.

Mutant	Expression (%)	ATPase activity (%)
G444V	92	32
P634L	105	7

ATP and P_i phosphorylation

The mutant G444V was able to autophosphorylate to a level roughly corresponding to its ATPase activity level (Figure 11a). Surprisingly, the mutant P634L displayed normal ATP phosphorylation practically indistinguishable from the wt.

In the P_i phosphorylation assay the mutants G444V and P634L behaved exactly in the opposite way in respect to the ATP phosphorylation. G444V was hyperphosphorylated to a level three times as high as the wt phosphorylation (Figure 11b). In contrast, the phosphorylation of the mutant P634L was barely visible.

The nature of the P_i phosphorylation of mutant G444V was investigated further by measuring the phosphorylation level in the presence of ATP and zinc. Both of these substances stabilize the E_1 state and therefore reduce the P_i phosphorylation. Interestingly, the mutant retained normal zinc sensitivity of the P_i phosphorylation, whereas a clearly reduced ATP sensitivity was observed (Figure 11c).

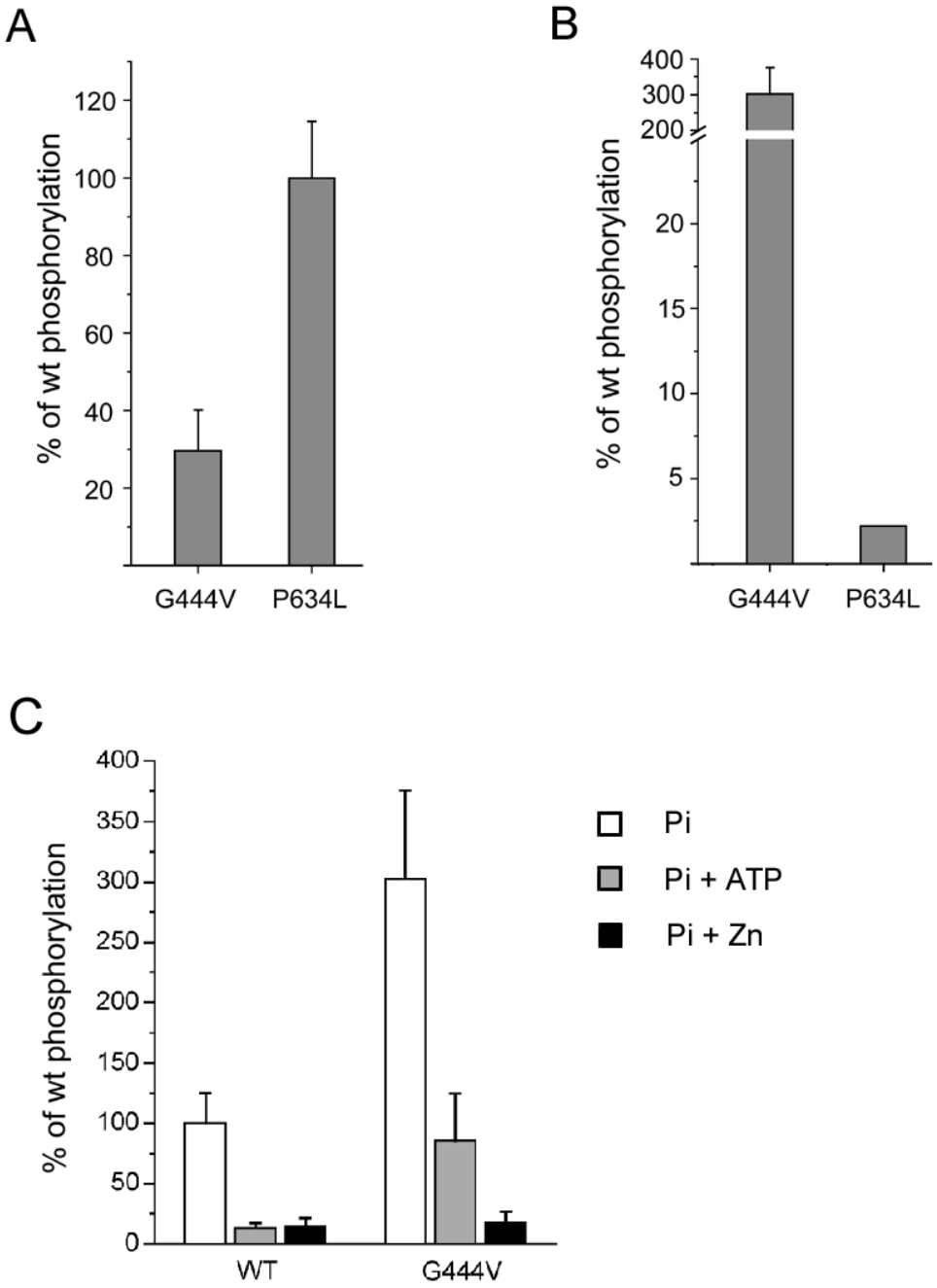

Figure 11. Phosphorylation of the mutants by ATP **(A)** and P_i **(B)**. The ATP concentration was 2.5 μM with P634L mutant, whereas a 5 μM ATP was used with G444V. **C)** P_i phosphorylation of the wt and mutant G444V in the absence and presence of 1 mM ATP or 100 μM Zn^{2+}.

Dephosphorylation

Both mutants displayed abnormal dephosphorylation kinetics (Figure 12). In overall, the mutants G444V and P634L dephosphorylated at a similar rates, but G444V seems to have biphasic kinetics with a slow phase during the first five seconds, while the P634L mutant shows a wt-like dephosphorylation with only one phase.

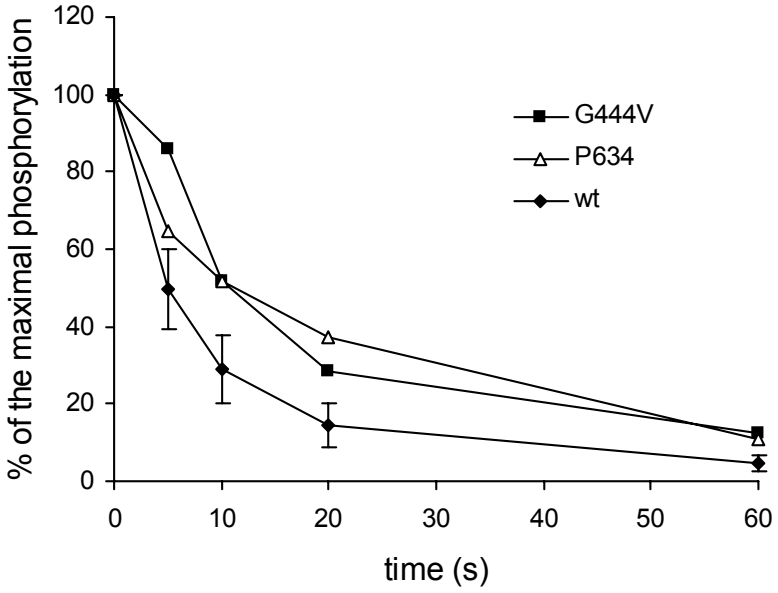

Figure 12. Dephosphorylation of the mutants.

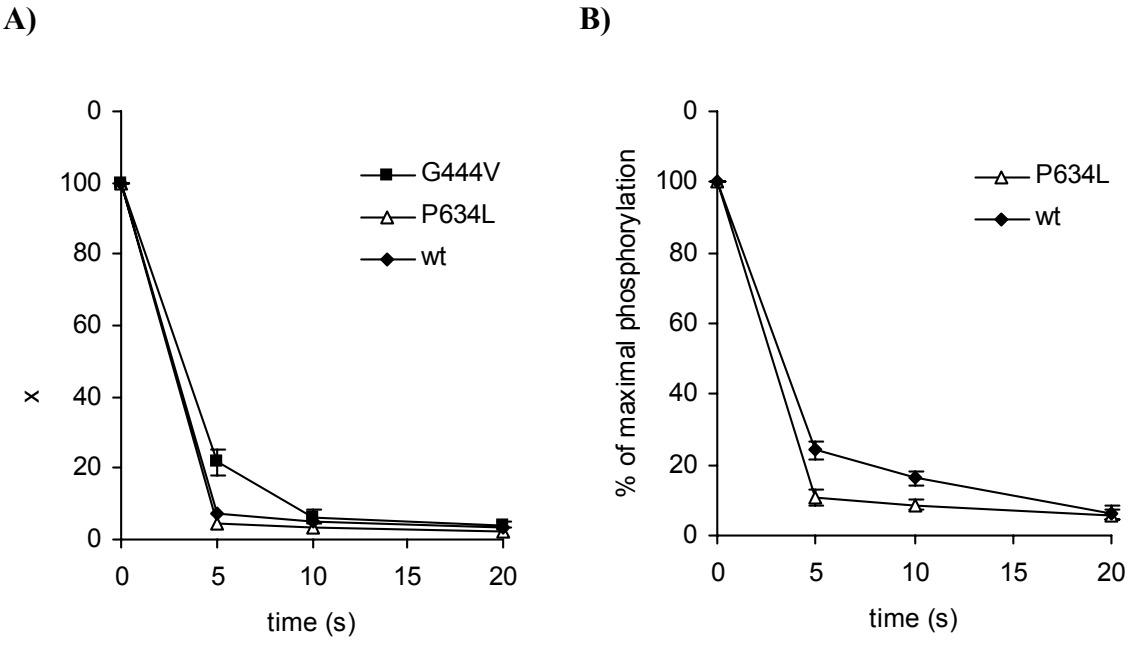

Figure 13. Dephosphorylation of the mutants in the presence of 250 μM ADP (A). Dephosphorylation of the wt and P634L in the presence of 25 μM ADP (B).

In the presence of ADP, dephosphorylation occurs from the E_1~P to the E_1 state. Dephosphorylation rate of mutant G444V is slowed down also in this assay (Figure 13A). In contrast, P634L has a very fast dephosphorylation rate, which could be verified to be faster than that of the wt by using a lower ADP concentration (Figure 13B).

2.3 H475Q – a unique multirole residue

The HP motif is found 34-43 residues from the DKTG aspartate in P_{1B}-ATPases. The histidine-475 is the most common Wilson disease mutation site in the Western population (Riordan & Williams, 2001; Loudianos et al., 2000). The WND mutant H1069Q displays abnormal trafficking and reduced ATP affinity (Payne et al., 1998; Tsivkovskii et al., 2003; Voskoboinik et al., 2003a). In this work the motif was studied by characterizing mutants carrying the analogous mutation H475Q (**I**; **II**; **III**) as well as substitutions H475A, H475L, H475S and H475D (**III**).

Table 5. Expression and ATPase activity of H^{475} mutants. The activity was assayed at 4 mM ATP. The numbers refer to the percentage of the wt activity.

Mutant	Expression (%)	ATPase activity (%)	
		4 mM	0.45 mM
WT	100	100	69
H475Q	106	43	6
H475A	115	8	
H475L	110	5	
H475S	139	16	
H475D	168	1	

Expression and ATPase activity of the H475 mutants

All mutants are expressed at a little higher level than the wt (Table 5). Artificially expressed ATPase is likely to be toxic to the cell and probably for this reason mutants with lower ATPase activity are tolerated better.

At a 4 mM ATP concentration, which corresponds to cellular conditions, the H475Q mutant has substantial ATPase activity of ~ 40% of the wt level. Other substitutions result in a more severe reduction of activity. Aspartate is an especially unfavorable replacement leading to an almost complete loss of activity.

The activity of the H475Q mutant depends strongly on the ATP concentration. Reducing the concentration to 0.45 mM, results in the ATPase activity of the H475Q mutant to drop 7-fold, whereas the wt enzyme was observed to slow down only by 30%.

ATP phosphorylation of the H475 mutants

A range of ATP concentrations from 60 nM to 58 μM was used in the ATP phosphorylation assay (Figure 14). At submicromolar concentrations the histidine mutants are phosphorylated to a level of less than 5% of that of the wt. All mutants show improved phosphorylation at a 58 μM ATP concentration. The phosphorylation of H475Q indicates that the K_m for ATP of the mutant is two orders of magnitude higher than that of the wt. This result agrees with the previous findings with corresponding MNK mutant 1086Q showing similarly roughly a hundred fold increase of K_m for ATP (Voskoboinik et al., 2003a).

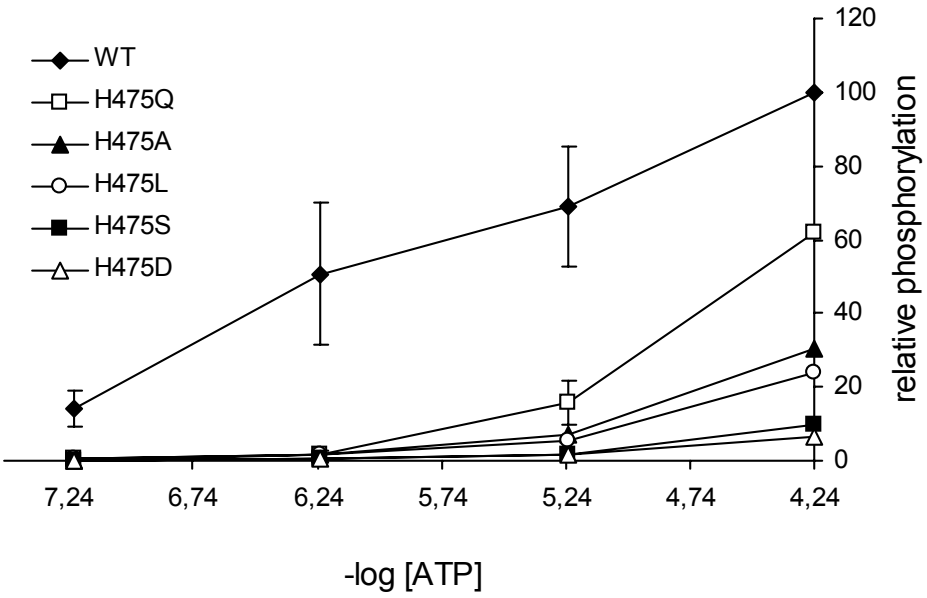

Figure 14. ATP phosphorylation of H^{475} mutants.

P_i phoshorylation of the H475 mutants

Keeping in mind that the N domain does not participate in P_i phosphorylation, one would expect that the mutations of H^{475} do not affect this event. Surprisingly, none of the mutants display normal P_i phosphorylation (Figure 15). Moreover, the level of phosphorylation does not reflect the ATPase activity or the ATP phosphorylation of the mutants. Unlike in the previous assays, in this experiment the H475Q substitution is not the most favorable one (**III**). The highest phosphorylation levels are shown by the mutants having the smallest sidechains: H475A and H475S. There seems to be a correlation between P_i phosphorylation and the size of the side chain. The only exception is the mutant H475D, which has the weakest phosphorylation despite its small size. A likely explanation is that the aspartate is the only substituent carrying a charge. It might be that charged residues are not tolerated in this position, or alternatively, that the negatively charged residue is an especially unfavorable substitution, because the histidine might carry an opposite charge.

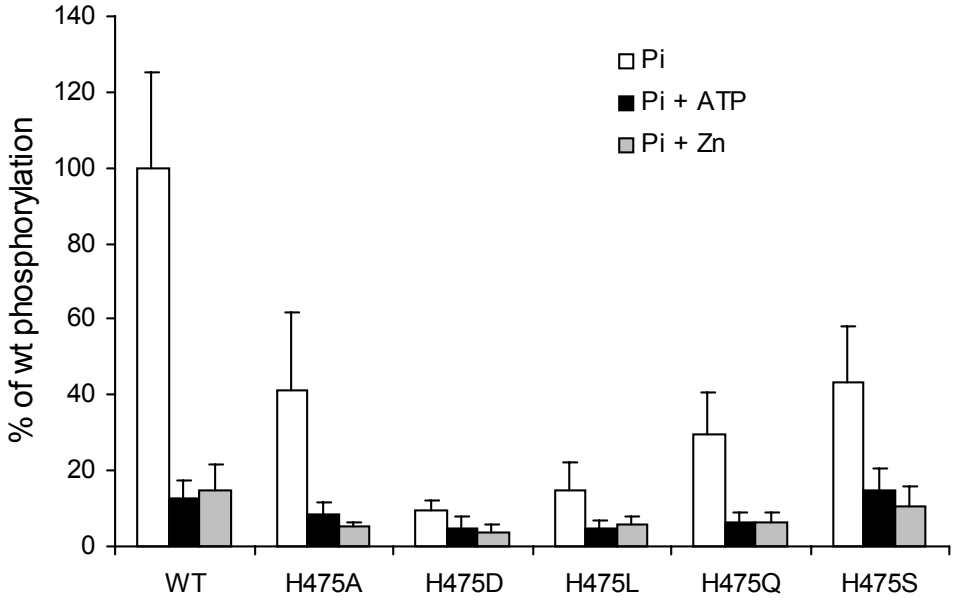

Figure 15. P_i phosphorylation of the H^{475} mutants. The phosphorylation was also assayed in the presence of 1 mM ATP (black bars) and 100 μM Zn^{2+} (grey bars).

P_i phosphorylation is sensitive both to the presence of substrate cations and to the presence of ATP. However, the mutants are less sensitive to these substances than the wt, especially

mutant H475S. In every H^{475} mutant, ATP and Zn^{2+} have a roughly equal effect on P_i phosphorylation, regardless of how sensitive the particular mutant is to these substances. Hence, unlike in the previous assays, no purely ATP-dependent mutational phenomena are observed in this experiment.

2.4 Mutants G503S, G505R and A508F in the putative ATP-binding loop

The N domain of P_{1B}-ATPases carries a protein kinase-like GxGxxG/A motif, which in the case of ZntA is G^{503}xxGxA, whereas a G^{1099}xxGxC sequence is found in WND. Several Wilson disease mutations target the conserved residues of the motif: G1099S, G1101R and C1104F (Loudianos et al., 1999; Loudianos et al., 2000). Here, the analogous ZntA mutants G503S, G505R and A508F, were characterized (**III**). Glycine motifs tend to be found at nucleotide-binding sites (Saraste et al., 1990; Bossemeyer, 1994; Kinoshita et al., 1999; Vetter & Wittinghofer, 1999). However, they vary not only in their exact primary structure, but also in the way they interact with the nucleotide (Bossemeyer, 1994; Vetter & Wittinghofer, 1999). In the modelling section (see chapter 1.2) the motif was shown in principle to be able to reach the putative nucleotide binding site. The biochemical evidence is discussed here.

Expression and ATPase activities of the glycine loop mutants

The expression of the mutants was slightly increased compared to the wt, excluding G505R, which was expressed at a little lower level. All three mutants showed reduced ATPase activities (Table 6).

Surprisingly, at 4 mM ATP the mutation G505R has a considerable activity (60% of the wt level), despite the fact that the small glycine was replaced with a very large arginine, which also introduces a charge. However, a clearly impaired ATPase activity was observed when the ATP concentration was lowered to 0.45 mM. When the residue is substituted by glutamate, i.e., when the opposite charge is introduced, a severe drop in ATPase activity is evident even at 4 mM ATP.

Table 6. Expression and activity of the glycine motif mutants. The numbers refer to the percentage compared to the wt activity.

Mutant	Expression (%)	ATPase activity (%)	
		4 mM	0.45 mM
G503S	133	22	
G505R	90	60	13
A508F	116	11	
G503D	136	22	
G505E	159	11	

ATP phosphorylation of the glycine loop mutants

The overall ATPase activities of the mutants reflect their abilities to undergo ATP-dependent phosphorylation (Figure 16). However, at 58 μM ATP, which was the highest concentration used in the measurement, the phosphorylation defect of the G^{503} and G^{505} mutants becomes much less severe than would be expected on the basis of their overall activities. This implies that ATP phosphorylation is not alone causing impaired activity. The mutant A508F remains poorly phosphorylated in the concentration range used.

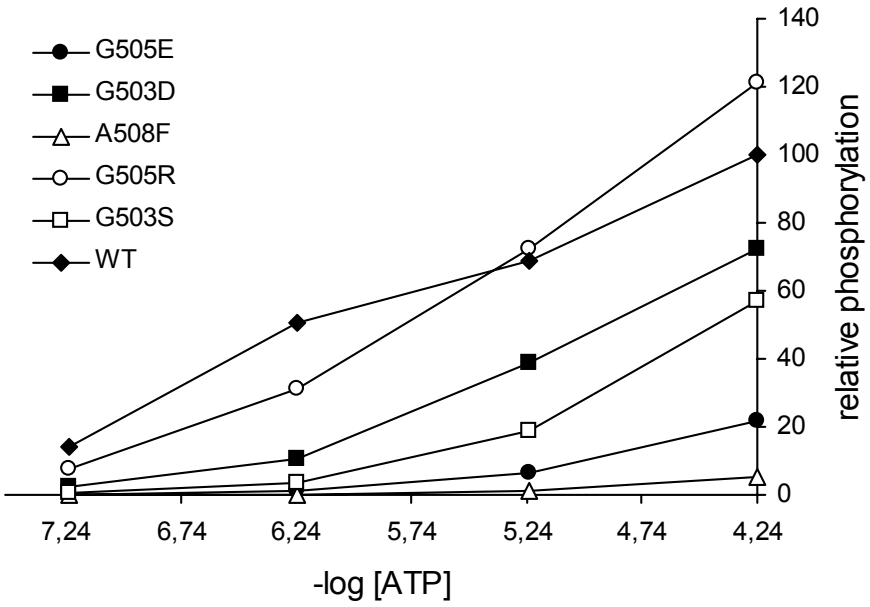

Figure 16. ATP phoshorylation of the mutants of the glycine motif.

P_i phosphorylation of the G-loop mutants

The mutations G503D, G505E, and G505R do not affect the P_i phosphorylation reaction (Figure 17). Instead, the mutant G503S is hyperphosphorylated, whereas mutant A508F is hypophosphorylated in this assay (**III**). It seems that the G503S mutant favors the E_2 state. The mutant A508F seems to have an overall phosphorylation defect, because it remains poorly phosphorylated regardless of the phosphate donor used.

When P_i phosphorylation is carried out in the presence of 1 mM ATP, none of the mutants display a wt-like behaviour. All of them phosphorylate better than the wt when ATP is present. In contrast, they respond normally to the presence of zinc. The only exception is the mutant G503S, which is hyperphosphorylated in all conditions tested. However, while the phosphorylation level was approximately 1.5 and 2 times higher in the absence and presence of zinc, respectively, more than a six-fold increase was observed in the presence of ATP. This indicates that ATP binding is affected also in the G503S mutant.

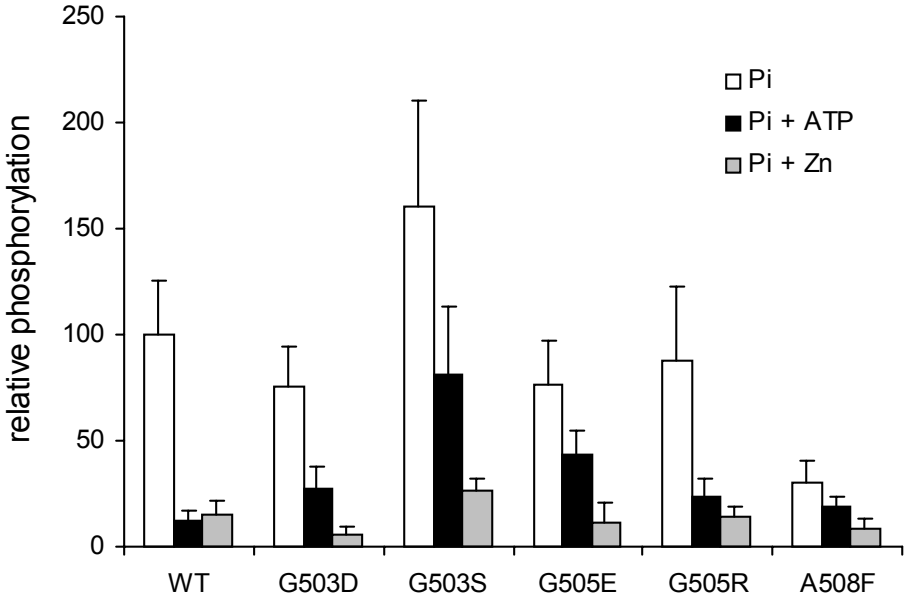

Figure 17. P_i phosphorylation of the mutants of the glycine motif. The phosphorylation was also assayed in the presence of 1 mM ATP (black bars) and 100 μM Zn^{2+} (grey bars).

3 Characterization of the metal-binding sites of ZntA

3.1 Metal specificity of ZntA

Metal specificity of the ATPase activity

Initially, ZntA was found in a mutant strain that was reported to be sensitive to Zn^{2+}, Cd^{2+} and Co^{2+} salts (Beard et al., 1997). ZntA-mediated $^{65}Zn^{2+}$ and $^{109}Cd^{2+}$ transport was demonstrated in the second study, but the ZntA knock-out strain did not show any changes in the rate of growth in Co^{2+} containing media (Rensing et al., 1997). In the third study, a strain with a disrupted ZntA gene was observed to be sensitive also to Pb^{2+} salts. In addition, Pb^{2+} was shown to activate ZntA. The actual ZntA-mediated transport of Pb^{2+} was not demonstrated (Rensing et al., 1998).

In this work, the metal specificity of ZntA was studied by measuring the ATPase activity of *E. coli* membranes in the presence and absence of several heavy metals (**I**). The ATPase can also be purified and reconstituted, but it retains activity only if a substrate metal is present during the purification, complicating the characterization of the metal selectivity of the purified protein (results not shown).

Initial measurements failed to detect any significant induction of ATPase activity in the membranes incubated with Ni^{2+}, Mn^{2+}, Co^{2+}, Hg^{2+} and Cu^{2+}. Clearly enhanced ATPase activities were observed in the presence of Zn^{2+}, Cd^{2+}, Pb^{2+} and Ag^{+} (**I**, Figure 6A). The Ag^{+}-dependent activity turned out to be an artefact caused by the precipitation of Ag^{+} (results not shown).

Metal specificity of the [^{33}P]-ATP phosphorylation

Metal specificity was tested also with the ATP phosphorylation assay (**I**). The experiment confirmed the results of the ATPase activity assay, namely that ZntA is active in the presence of Zn^{2+}, Cd^{2+} and Pb^{2+} (**I**, Figure 6B). Interestingly, the phosphorylation levels in the presence of these three metals did not correspond to ATPase activity. Cd^{2+} is the weakest inducer of ATPase activity, but it is able to induce the highest level of ATP phosphorylation.

Surprisingly, also Cu^{2+} stimulated significant ATP phosphorylation, despite the fact that it could not induce measurable ATPase activity. When the metal was reduced to Cu^{+} by adding 5 mM DTT to the solution, phosphorylation disappeared. Weak phosphorylation was induced also by Ni^{2+}. These results have been reproduced by Hou and Mitra, 2003. In

addition they discovered that also Co^{2+} induced weak ATP phosphorylation, roughly at the same level than Ni^{2+}. Currently there is no evidence of the Cu^{2+}, Ni^{2+} and Co^{2+} ions to be actually translocated by ZntA.

3.2 Mutations of the N-terminal metal-binding domain

Role of the N-terminal metal-binding domain

The function of the N-terminal metal-binding domain remains unclear. Human ATPases seem to possess them to capture the substrate metal from the chaperone as well as to regulate copper-dependent trafficking. There is no trafficking in bacteria and so far no chaperones for Zn^{2+} have been found. Moreover, ZntA remains functional both *in vivo* and *in vitro* if the N-terminus is deleted (Mitra & Sharma, 2001).

In this work the function of the N-terminal metal-binding site was studied by characterizing the properties of the two mutants, in which the C^{59}AAC site was disrupted by mutating it to S^{59}AAS (named SAAS) and A^{59}AAA (named AAAA). The latter mutant was produced to ensure that the metal-binding site is non-functional (see chapter 3.3). These results have not been previously published.

Expression and ATPase activity of SAAS and AAAA mutants

Both mutant proteins were markedly overexpressed, being roughly 2-3 times as abundant as the wt (Table 7). The ATPase activity assay showed that the mutations reduce the V_{max} of the enzyme approximately by 50%. No change in K_m was observed (Figure 20). These results agree with those reported in Mandal & Argüello, 2003.

Table 7. Expression and activity of the mutants of the N-terminal metal-binding site. The numbers refer to the percentage compared to the wt activity.

Mutant	Expression (%)	ATPase activity (%)
SAAS	327	42
AAAA	259	50

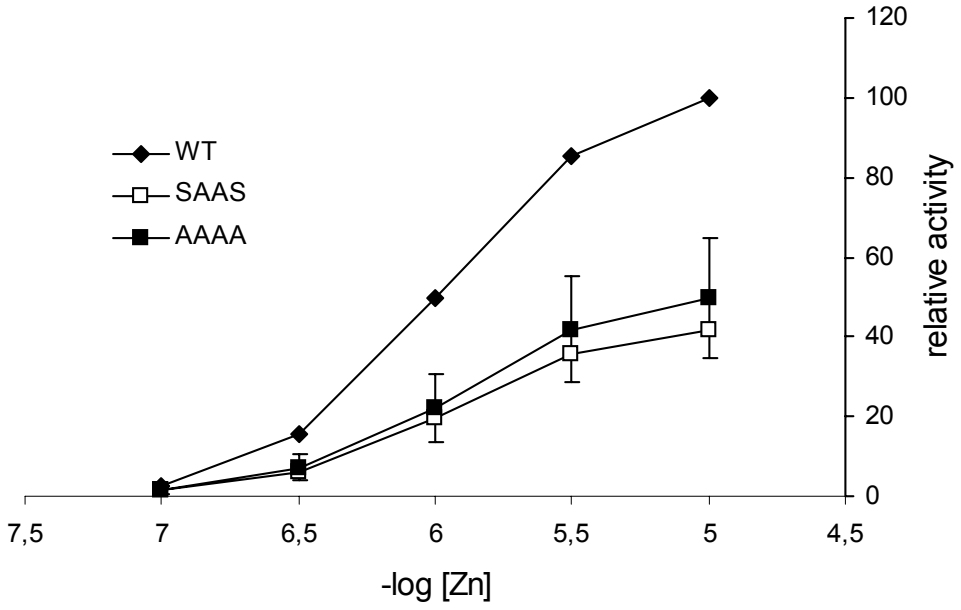

Figure 20. Zinc-dependence of the ATPase activity.

ATP and P_i phosphorylation

The mutants were phosphorylated almost normally by ATP in the range of 0.1-10 μM Zn^{2+} (Figure 21). This excludes the proposed role of MBDs as enhancers of the ATPase activity at low metal concentrations (Voskoboinik et al., 2001).

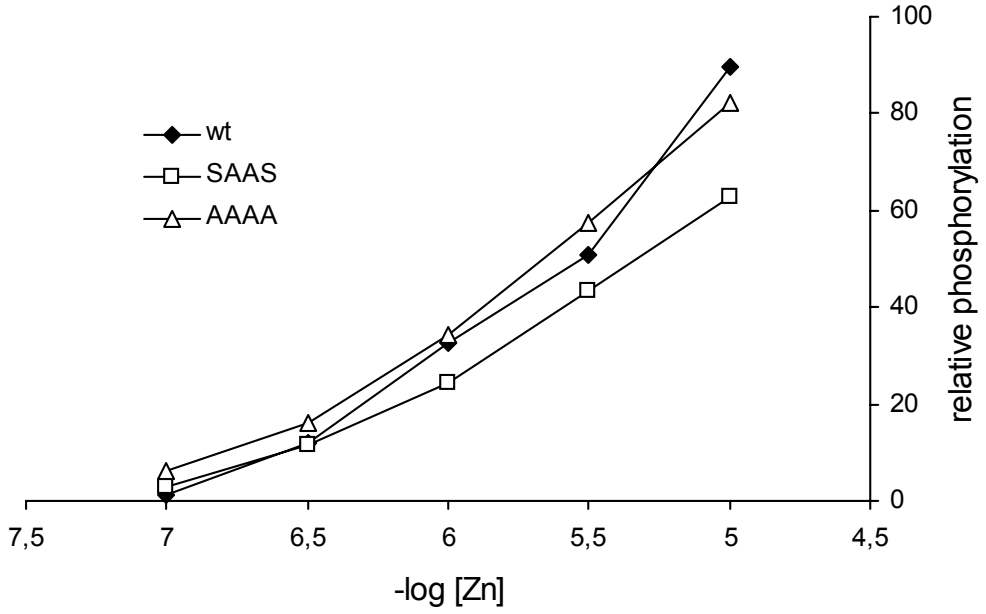

Figure 21. ATP phosphorylation of mutants of N-terminal metal-binding site.

In the presence of P_i, the mutants SAAS and AAAA were phosphorylated to the level of 40% and 60% of the wt level respectively (Figure 22A). This corresponds roughly to their ATPase activities. In the presence of Zn^{2+} the mutants behave peculiarly (Figure 22B). The P_i phosphorylation of both mutants show increased sensitivity to zinc at 2 μM concentration in comparison to the wt. Between 2 and 200 μM phosphorylation of the mutants remains relatively unchanged. In contrast, the P_i phosphorylation of the wt drops roughly by 75%. At millimolar zinc concentrations there is no significant difference between the mutants and the wt.

A)

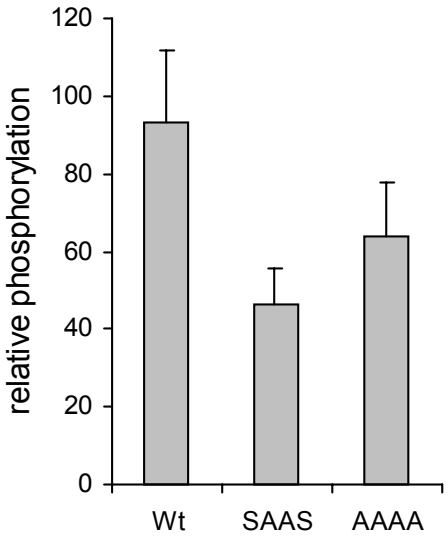

B)

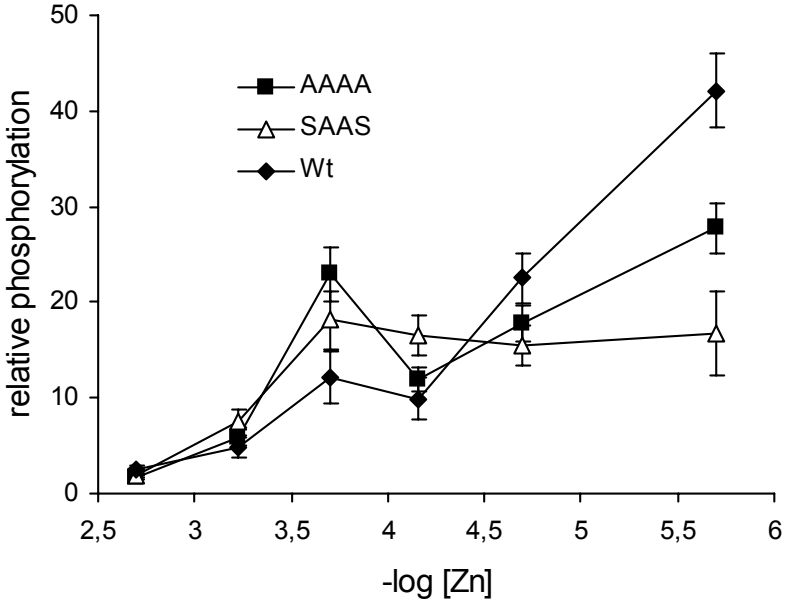

Figure 22. A) P_i phosphorylation of mutants of N-terminal metal-binding site. **B)** Zinc sensitivity of P_i phosphorylation.

3.3 Translocation site – mutant SPS

Disease mutations have been found to affect the CPx motif both in Wilson disease (C985Y, Haas et al., 1999) and in Menkes disease (C1000R, Tümer et al., 1999). Consistently, several studies have demonstrated that it is essential for the ATPase function that the site is intact (Forbes & Cox, 1998; Bissig et al., 2001; Yoshimizu et al., 1998). ZntA carries a $C^{392}PC$ sequence, which is also found in WND. Despite having identical motifs in their translocation sites, the two ATPases have different substrate specificities. In this work the function of the site was studied by mutating the cysteines to create an $S^{392}PS$ motif (named as SPS mutant). These results have not been previously published.

Expression and activity

The mutant was clearly overexpressed being approximately twice (230% of the wt expression) as abundant as the wt in the membranes. A very low level of activity of 2% was measured for the SPS mutant, but this value is close to the detection limit of the colorimetric method and the standard error of the measurement was 3%.

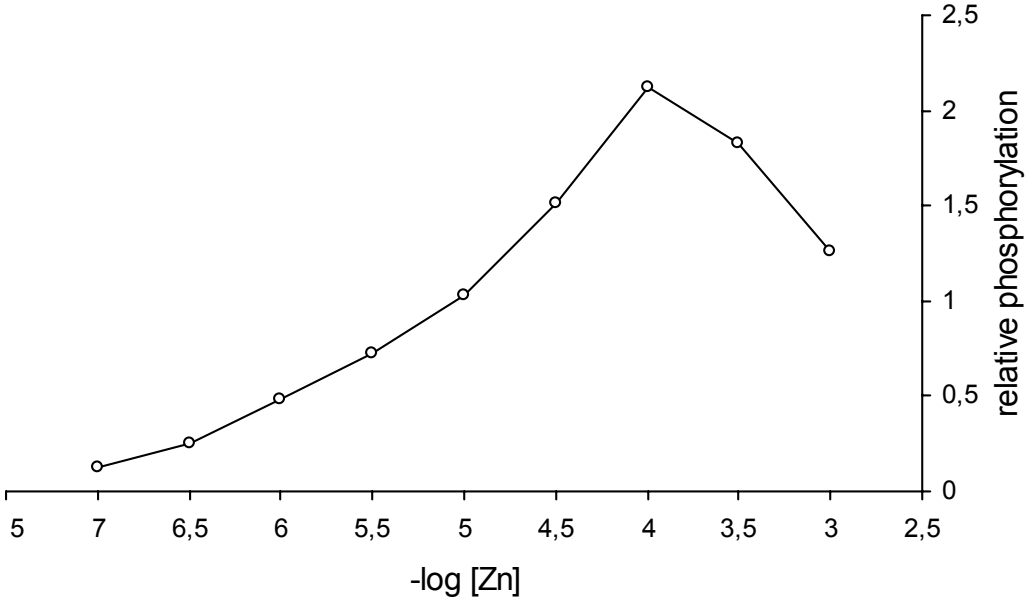

Figure 23. ATP phosphorylation of the SPS mutant. Phosphorylation level of the wt is 100 at 10 μM Zn^{2+}.

Phosphorylation by ATP and P_i

Consistently with possible ATPase activity, the SPS mutant displays Zn^{2+}-dependent ATP phosphorylation (Figure 23). This phosphorylation is much weaker than that of the wt, but it can be detected in a zinc concentration as low as 0.1 μM. The maximum is reached at 100 μM Zn^{2+}. If the CPC site is mutated to APA, phosphorylation is completely abolished (results not shown).

In contrast to the Ca^{2+}-ATPase mutants with substitutions in Ca^{2+}-binding residues (Clarke et al., 1989), the SPS mutant was extremely poorly phosphorylated by P_i. Even more surprising is that, unlike the wt, the SPS mutant is maximally phosphorylated in the presence of a micromolar concentration of Zn^{2+}, and not in the absence of Zn^{2+}. This phenotype has not been observed in any other ZntA mutant studied. Normally, zinc reduces P_i phosphorylation because it stabilizes the E_1 state.

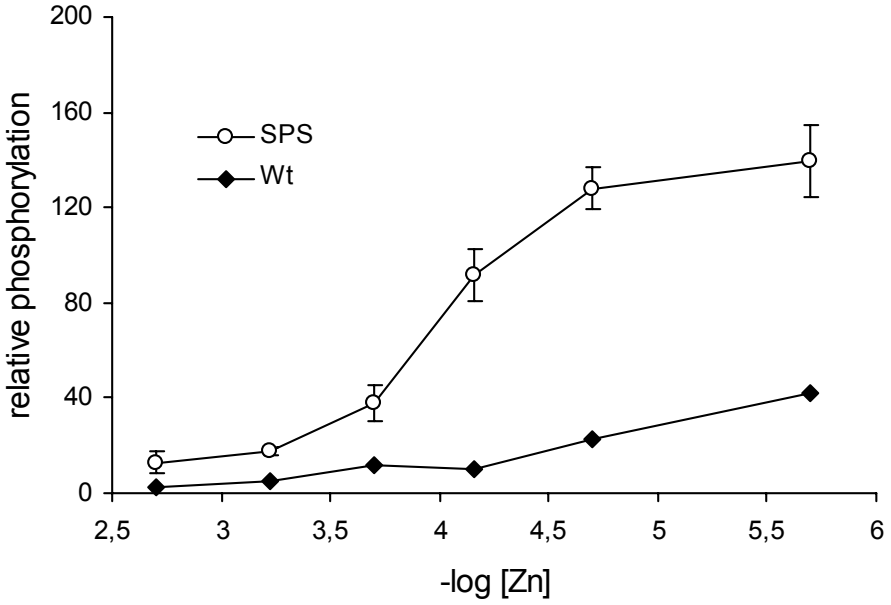

Figure 24. The zinc sensitivity of the relative P_i phosphorylation of the wt and SPS. The value 100 refers to the P_i phosphorylation of a strain in the absence of zinc.

Discussion

1 Modelling of the N domain of ZntA

The modelling of ZntA was carried out assuming that the N domain has a common core structure, which is conserved in all P-type ATPases. In general the N domains of ZntA and Ca^{2+}-ATPase share an identity of 13%, but in the region, which contains the glycine motif there is practically no sequence similarity at all. The glycine motif resembles that found in protein kinases, which is why the cAPK structure (Zheng et al., 1993) was used as a template instead of Ca^{2+}-ATPase to model this particular region. As the glycine-rich loops are likely to be evolved by convergent evolution (Via et al., 2000), the two motifs found in ZntA and cAPK are not necessarily identical structurally, but the secondary structure predictions for the two proteins are very similar in this region (results not shown). Moreover, nothing is known about the location and orientation of the glycine motif loop in the N domain. However, the modelling demonstrates that it is possible to construct the model in a way that brings the HP and G^{503}xGxxG/A motifs close to the putative ATP-binding site together with E^{470} and C^{518} (see Table 3), all of which are experimentally shown to be likely participating in forming the ATP-binding site, without breaking the common core structure of the N domain.

The N domain of WND has been modelled by Efremov et al., 2004. While the alignment made in this work differs partly from the one in Figure 9, the region containing the residue E^{470} is aligned similarly. This model was tested by docking an ATP molecule in the putative binding site. While in their model the corresponding residue E^{1064} points away from the nucleotide, it can adopt a conformation where it can interact with the NH_2 group of the nucleotide (Efremov et al., 2004). Replacing the glutamate with alanine renders the ATPase almost insensitive to ATP, when phosphorylated by P_i. This implies that E^{470} has a strong contribution in nucleotide binding, which is consistent with both models.

2 Conformational mutants G444V and P634L

The mutants G444V and P634L are classified as conformational mutants on the basis of their phosphorylation properties. The mutant G444V prefers the E_2 state, observed as

increased P_i phosphorylation. In accordance with this observation, ATP is less capable of facilitating the enzyme to adopt the E_1 state. However, in the presence of zinc the enzyme behaves similarly to the wt showing only a low level of P_i phosphorylation. While the mutation shifts the conformational balance towards the E_2 state, it does not prevent the E_2-E_1 transition *per se*, but seems specifically to hinder the ATP-driven state conversion.

The mutant P634L is also a conformational mutant, but unlike G444V, it favors the E_1 state. The mutant displays a very low ATPase activity despite the normal ATP phosphorylation. On the other hand, P_i phosphorylation is severely affected. Previous studies with the Ca^{2+}-ATPase mutant P709A did not reveal any major changes in the function (Vilsen et al., 1991). However, the E_2 structure reveals that the residue is situated on the surface that contacts the A domain in this conformation. Hence, it is likely that the different results are due to the difference in size between the two side chains. The most probable interpretation is that the mutation P634L hinders the interaction of the A and P domains impairing the formation of the E_2 state. Interestingly, the N domain is able to associate normally with the P domain, judged by the unaffected ATP phosphorylation.

3 Histidine (H^{475}) mutants of the HP motif

The histidine-475 is strictly conserved among P_{1B}-ATPases and mutations of this residue result in multiple effects. First of all, they have a significant negative impact on ATP phosphorylation. The defect is partially compensated for by higher ATP concentrations suggesting that the mutations influence ATP binding. Consistently, ATPase activity shows also a strong dependence on ATP concentration.

Glutamine is able to adopt a conformation where the amide nitrogen is in a similar position in comparison to the histidine ε2 nitrogen. The fact that glutamine is a relatively good substitute for the histidine compared with the other amino acids tested suggests that the side chain nitrogen might play a functional role. On the basis of the sequence alignment, the HP motif is located at the N-terminus of the N domain helix α2. This area has been shown to be close to the Mg^{2+} ion at the E_2 state of the cycle (Hua et al., 2002b; Patchornik et al., 2000; Goldshleger et Karlish 1999). The residues D^{443} and T^{441}, in the Na^+/K^+- and Ca^{2+}-ATPases respectively, have been suggested to be coordinating the Mg^{2+} ion. A His is rarely encountered as a Mg^{2+} ligand, but a few examples are known. MurD ligase from *E. coli* has been crystallized with an ADP molecule and Mg^{2+} (PDB entry 2AUG; Bertrand et al.,

1999). Mg^{2+} is seen to be coordinated by H^{183}. Fitting a γ-phosphate to the bound ADP would bring the phosphate close to the Mg^{2+} ion (Bertrand et al., 1999). At this point it can be only speculated how H^{475} interacts with an ATP molecule, but having an analogous role to H^{183} of MurD in Mg^{2+} binding seems to be a possibility.

In addition to ATP phosphorylation, P_i phosphorylation is also severely impaired, which cannot be explained by an ATP binding defect. The WND mutant H1069C has been reported to display reduced ATP sensitivity in the P_i phosphorylation assay (Tsivkovskii et al., 2003). Similar behaviour was observed with some H^{475} mutants, especially with H475S. This was considered as evidence for a nucleotide binding defect. However, this conclusion is complicated by the fact that P_i phosphorylation of the mutants H1069C and H475S is also clearly less sensitive to substrate cations. As a conclusion, no clear nucleotide related effects are seen in the P_i phosphorylation assay. The observation that the P_i phosphorylation defect is related to the size of a side chain suggests that sterical factors are likely to play a role here. Indeed, according to the molecular model of the N domain H^{475} is an equivalent of E^{439} in Ca^{2+}-ATPase, which is located at the interface of N and A domains in the E_2 structure (Toyoshima et Nomura, 2002).

ATP phosphorylation takes place when the enzyme is in the E_1 state, whereas P_i phosphorylation occurs only when the enzyme resides in the E_2 conformation. The data suggest that H^{475} participates in ATP binding during the phosphorylation step, while there is little support for H^{475} to have a significant role in the nucleotide binding during the E_2-E_1 state transition.

4 Glycine motif mutants

All mutants of the glycine motif display non-wt behaviour in the experiments in which ATP is used. The mutants G505R, G503D and G505E have completely normal P_i phosphorylation in the absence and the presence of substrate cations. Still, all of them display diminished ATPase activity and ATP phosphorylation. Their P_i phosphorylation is less affected by 1 mM ATP compared to the wt. The mutants G503S and A508F display not only impaired ATPase activity and ATP phosphorylation, but also abnormal P_i phosphorylation. This suggests that they have other defects in addition to ATP binding. The mutation G503S is likely to affect the conformational equilibrium favoring the E_2 state, whereas A508F might hinder the enzyme to adopt the E_2 conformation.

The mutation G505R results in a surprisingly mild phenotype. At 4 mM ATP there is only a small reduction of ATPase activity, while ATP phosphorylation is normal. However, its P_i phosphorylation in the presence of 1 mM ATP is higher than that of the wt, suggesting an ATP-binding defect. Consistently, ATPase activity is much more severely affected at a lower ATP concentration. In conclusion, all mutations in the glycine motif studied interfere with ATP binding.

5 Metal-binding sites of ZntA

5.1 Metal specificity of ZntA

The metal specificity of ZntA was determined by measuring the ATPase activity and ATP phosphorylation on the membranes of ZntA-expressing strain in the presence of different metal salts. The ATPase activity assay confirmed the earlier findings that ZntA is active in the presence of Zn^{2+}, Cd^{2+} and Pb^{2+}. In the ATP phosphorylation assay also Cu^{2+} induced a marked phosphorylation of the protein, whereas Ni^{2+} had a small effect. These findings have been confirmed by Hou et Mitra, 2003. However, the current evidence does not tell, whether these two cations are really transported by ZntA. Clearly, an actual transport activity assay is needed to answer this question.

5.2 N-terminal metal-binding site CxxC

Mutations in the N-terminal metal-binding site have little effect on ATP phosphorylation. Instead, P_i phosphorylation is clearly affected. In the presence of zinc the mutants reveal their complex phenotype that is difficult to explain fully at this stage. It can be concluded that the mutations affect specifically the E_2 state. The N-terminus has been previously reported to interact with the loop containing N and P domains (Tsivkovskii et al., 2001). Also, mutations at the metal-binding site have been reported to affect the dephosphorylation step, which occurs in the E_2 state (Mandal & Argüello, 2003). One possibility is that the N-terminus interacts with the P domain in a way that prevents the function of the A domain. The binding of a metal ion to the N-terminus would break down the interaction, thus enhancing the rate of ZntA. The results do not support the N-terminus to enhance the activity in low metal concentrations as suggested in Voskoboinik et al.,

2001. Instead, it seems that the N-terminus functions to inhibit ATPase activity at low metal concentrations.

5.3 CPx motif – The translocation site

The SPS mutant undergoes phosphorylation in the presence of ATP and $P_{i,}$ suggesting that it might have low residual ATPase activity. Also, it reacts with zinc at submicromolar concentrations, in spite of the fact that both metal liganding cysteines have been replaced with serines. Phosphorylation is completely abolished if the CPC sequence is replaced with APA. These results imply that there are other liganding residues in the intramembraneous metal-binding site. The N-terminal metal-binding site of ZntA has been shown to consist of an aspartate residue in addition to two cysteines (Banci et al., 2002). An aspartate is also found in the seventh TM-helix that is conserved only among Zn^{2+}-ATPases (Argüello, 2003). The role of the aspartate remains to be characterized, but these results provide the first experimental evidence for the idea that the intramembraneous metal-binding site is not formed solely by the CPx motif.

Conclusions

The important general finding of this study is that all Wilson disease mutation analogs characterized resulted in a clear biochemical effect on the bacterial counterpart, ZntA. This suggests that the P_{1B}-ATPases share a common functional mechanism despite the structural differences.

The modelling of N domain suggests that the core is conserved throughout the members of the P-type ATPase superfamily. It is demonstrated, that a model can be constructed bringing all the putative ATP-binding-site-forming residues ($H^{475}P$ and G^{503}xGxxG/A motif, C^{518} and E^{470}) together without disturbing the common core structure of the N domain.

Two new conformational mutants were discovered in this work. G444V and P634L are both Wilson disease mutant analogs. On the basis of their ATP and P_i phosphorylation characteristics, they favor E_2 and E_1 states respectively. G444V results in a phenotype, that responds normally to the binding of substrate cations by converting from the E_2 to E_1 state, but fails to do so in the presence of ATP. The mutation P634L leads to the accumulation of the E_1~P state, which dephosphorylates slowly in normal conditions, but very fast in the presence of excess ADP.

The experimental evidence from molecular modelling and mutagenesis suggests the two conserved sequence motifs found in the N domain of P_{1B}-ATPases, the $H^{475}P$ and the G^{503}xGxxA to participate in the ATP binding. Mutations in these motifs dramatically reduce ATP phosphorylation, which is relieved at higher ATP concentrations, suggesting an ATP-binding defect. Mutations in the glycine motif also partially impaire the ATP-dependent E_2-E_1 state transition, while no such effect is observed in H^{475} mutants.
Instead, mutations of the His^{475} result in a general P_i phosphorylation defect, which can be explained if the residue makes contact with the A domain. This is supported by the molecular model of the N domain of ZntA.

Mutations in the N-terminal metal-binding site C^{59}xxC do not change the metal affinity of the ATPase. Hence, the domain is not taking part in metal translocation. Instead, mutational

effects are seen in P_i phosphorylation, indicating a regulatory role for the CxxC metal-binding site. It is suggested to be inhibitory in nature, preventing the futile ATPase activity in the absence of substrate cations.

Replacing the intramembraneous $C^{392}PC$ site with APA results in an inactive ATPase, whereas substituting it with SPS retains a residual activity. This finding supports the recent suggestion that the intramembraneous metal-binding site is not formed solely by the CPx motif, but also other metal ligands exist.

Acknowledgements

The Laboratory work of this study was carried out at the Department of Biochemistry, Institute of Biomedicine, University of Helsinki. There is a number of colleagues and friends for whom I am sincerely grateful for the direct and indirect help they have provided during this process. However, in this context I would like to thank especially the following persons:

My supervisor Tuomas Haltia for sharing his extensive knowledge with me and giving all the recources at my disposal.

The coauthors of the publications, Eija Bencomo, Marja Pietilä and Liisa Laakkonen for their contribution to this scientific achievement.

Teija Inkinen, Katja Sissi and Lea Armassalo for their invaluable technical assistance.

Kimmo Mattila for 1) the expert advice, 2) for the nice company.

Kari Keinänen and Mauno Vihinen for reviewing the manuscript and giving their valuable comments.

Carl Gahmberg and Mauno Vihinen for their contribution to this work as the members of the Viikki Graduate School follow-up group.

The members of Helsinki Bioenergetics Group, for the excellent discussions at the group meetings (and elsewhere too).

My wife Eija for lots of things, but for checking the spelling and grammar of the manuscript to name one.

The Association of Finnish Chemical societies, and Sigrid Juselius, Magnus Ehrnrooth and Oskar Öflund foundations for the financial support.

References

Abu-Abed, M., Mal, T.K., Kainosho, M., MacLennan, D.H., and Ikura, M. (2002) Characterization of the ATP-binding domain of the sarco(endo)plasmic reticulum Ca^{2+}-ATPase: probing nucleotide binding by multidimensional NMR. Biochemistry 41: 1156-1164

Albers, R.W. (1967) Biochemical aspects of active transport. Ann. Rev. Biochem. 36: 727-756

Ambrosini, L., and Mercer, J.F.B. (1999) Defective copper-induced trafficking and localization of the Menkes protein in patients with mild and copper-treated classical Menkes disease. Hum. Mol. Genet. 8: 1547-1555

Andersen, J.P., Clausen, J.D., Einholm, A.P., and Vilsen, B. (2003) Mutagenesis of residues involved in control of the Ca^{2+} entry pathway and conformational changes associated with Ca^{2+} binding in the SR Ca^{2+}-ATPase. Ann. NY Acad. Sci. 986: 72-81

Aravind, L. (1998) The catalytic domain of the P-type ATPase has the haloacid dehalogenase fold. Trends. Biochem. Sci. 23: 127-129

Argüello, J.M. (2003) Identification of ion-selectivity determinants in heavy-metal transport P_{1B}-type ATPases. J. Membr. Biol. 195: 93-108

Arnesano, F., Banci, L., Bertini, I., Huffman, D., and O'Halloran, T.V. (2001) Solution structure of the Cu(I) and apo forms of the yeast metallochaperone Atx1. Biochemistry 40: 1528-1539

Auer, M., Scarborough, G.A., and Kühlbrandt, W. (1998) Three-dimensional map of the plasma membrane H^+-ATPase in the open conformation. Nature 392: 840-843

Auland, M.E., Roufogalis, B.D., Devaux, P.F., Zachowski, A. (1994) Reconstitution of ATP-dependent aminophospholipid translocation in proteoliposomes. Proc. Natl. Acad. Sci. 91: 10938-10942

Axelsen, K.B., and Palmgren, M.G. (1998) Evolution of substrate specificities in the P-type ATPase superfamily. J. Mol. Evol. 46: 84-101

Bal., N., Mintz, E., Guillain, F., and Catty, P. (2001) A possible regulatory role for the metal-binding domain of CadA, the Listeria monocytogenes Cd^{2+}-ATPase. FEBS Lett. 506: 249-252

Banci, L., Bertini, I., Ciofi-Baffoni, S., Del Conte, R., and Gonnelli, L. (2003) Understanding copper trafficking in bacteria: interaction between the copper transport protein CopZ and the N-terminal domain of the copper ATPase CopA from *Bacillus subtilis*. Biochemistry 42: 1939-1949

Banci, L., Bertini, I., Ciofi-Baffoni, S., Finney, L.A., Outten, C.E., and O'Halloran, T.V. (2002) A new zinc-protein coordination site in intracellular metal trafficking: solution structure of the Apo and Zn(II) forms of ZntA(46-118). J. Mol. Biol. 323: 883-897

Banci, L., Bertini, I., Ciofi-Baffoni, S., Huffman, D., and O'Halloran, T.V. (2001) Solution structure of the yeast copper transporter domain Ccc2a in the apo and Cu(I)-loaded states. J. Biol. Chem. 276: 8415-8426

Bayle, D., Wängler, S., Weitzenegger, T., Steinhilber, W., Volz, J., Przybylski, M., Schäfer, K.P., Sachs, G., and Melchers, K. (1998) Properties of the P-type ATPases by the *copAP* operons of *Helicobacter pylori* and *Helicobacter felis*. J. Bacteriol. 180: 317-329

Beard, S. J., Hashim, R., Wu, G., Binet, M. R. B., Hughes, M. N., and Poole, R. K. (2000) Evidence for the transport of zinc(II) ions via the Pit inorganic phosphate transport system in Escherichia coli. FEMS Microbiol. Lett. 184: 231-235

Beard, S.J., Hashim, R., Membrillo-Hernandez, J., Hughes, M.N., and Poole, R.K. (1997) Zinc(II) tolerance in *Escherichia coli* K-12: evidence that the zntA gene (o732) encodes a cation transport ATPase. Mol. Microbiol. 25: 883-891

Bertrand, J.A., Auger, G., Martin, L., Fanchon, E., Blanot, D., Le Beller, D., van Heijenoort, J., and Dideberg, O. (1999) Determination of the MurD mechanism through crystallographic analysis of enzyme complexes. J. Mol. Biol. 289: 579-590

Bissig, K.-D., Wunderli-Ye, H., Duda, P.W., and Solioz, M. (2001) Structure-function analysis of purified *Enterococcus hirae* CopB copper ATPase: Effect of Menkes/Wilson disease mutation homologs. Biochem. J. 357: 217-223

Borjigin, J. Payne, A.S., Deng, J., Li, X., Wang, M.M., Ovodenko, B., Gitlin, J.D., and Snyder, S.H. (1999) A novel pineal night-specific ATPase encoded by the Wilson disease gene. J. Neurosci. 19: 1018-1026

Bossemeyer, D. (1994) The glycine-rich sequence of protein kinases: a multifunctional element. Trends Biochem. Sci. 19: 201-205

Brocklehurst, K.R., Hobman, J.L., Lawley, B., Blank, L., Marshall, S.J., Brown, N.L., and Morby, A.P. (1999) ZntR is a Zn(II)-responsive MerR-like transcriptional regulator of ZntA in *Escherichia coli*. Mol. Microbiol. 31: 893-902

Brouwer, M., and Brouwer-Hoexum, T. (1992) Glutathione-mediated transfer of copper(I) into american lobster apohemocyanin. Biochemistry 31: 4096-4102

Bull, P.C., Thomas, G.R., Rommens, J.M., Forbes, J.R., and Cox, D.W. (1993) The Wilson disease gene is a putative copper transporting P-type ATPase similar to the Menkes disease gene. Nat. Genet. 5: 327-337

Carvalho, M.G.C., de Souza, D.G., and de Meis, L. (1976) On a possible mechanism of energy conservation in sarcoplasmic reticulum membrane. J. Biol. Chem. 251: 3629-3636

Changela, A., Chen, K., Xue, Y., Holschen, J., Outten, C.E., O'Halloran, T.V., and Mondragon, A. (2003) Molecular basis of metal-ion selectivity and zeptomolar sensitivity by CueR. Science 301: 1383-1387

Chelly, J. Tümer, Z., Tønnesen, T., Petterson, A., Ishikawa-Brush, Y., Tommerup, N., Horn, N., and Monaco, A.P. (1993) Isolation of a candidate gene for Menkes disease that encodes a potential heavy metal binding protein. Nat. Genet. 3: 14-19

Ciriolo, M., Desideri, A., Paci, M., and Rotilio, G. (1990) Reconstitution of Cu,Zn-superoxide dismutase by the Cu(I) glutathione complex. J. Biol. Chem. 265: 11030-11034

Clarke, D.M., Loo, T.W., and MacLennan, D.H. (1990) Functional consequences of mutations of conserved amino acids in the β-strand domain of the Ca^{2+}-ATPase of sarcoplasmic reticulum. J. Biol. Chem. 265: 14088-14092

Clarke, D.M., Loo, T.W., Inesi, G., and MacLennan, D.H. (1989) Location of high affinity Ca^{2+}-binding sites within the predicted transmembrane domain of the sarcoplasmic reticulum Ca^{2+}-ATPase. Nature 339: 476-478

Clausen, J.D., McIntosh, D.B., Vilsen, B., Woolley, D.G., and Andersen, J.P. (2003) Importance of conserved N domain residues Thr^{441}, Glu^{442}, Lys^{515}, Arg^{560}, and Leu^{562} of sarcoplasmic reticulum Ca^{2+}-ATPase for MgATP binding and subsequent catalytic steps: plasticity of the nucleotide binding site. J. Biol. Chem. 278: 20245-20258

Clausen, J.D., McIntosh, D.B., Woolley, D.G., and Andersen, J.P. (2001) Importance of Thr-353 of the conserved phosphorylation loop of the sarcoplasmic reticulum Ca^{2+}-ATPase in MgATP binding and catalytic activity. J. Biol. Chem. 276: 35741-35750

Cobine, P., Wickramasinghe, W.A., Harrison, M.D., Weber, T., Solioz, M., Dameron, C.T. (1999) The Enterococcus hirae copper chaperone CopZ delivers copper(I) to the CopY repressor. FEBS Lett. 445: 27-30

Cormack, B (1995) In Short protocols of molecular biology (Ausubel, F, Brent, R., Kongston, R.E., Moore, D.D., Seidman, J.G., Smith, J.A., and Struhl, K. Eds.) Third ed., Chapter 8, p. 22, Wiley, New York

Cornelius, F., and Skou, J. (1987) The sided action of Na^+ and of K^+ on reconstituted shark (Na^+ + K^+)-ATPase engaged in Na^+-Na^+ exchange accompanied by ATP hydrolysis. I. The ATP activation curve. Biochem. Biophys. Acta 904: 353-364

Cox, D.W. (2002) Wilson disease mutation database. http://www.uofa-medical-genetics.org/wilson/index.php

Cox, D.W., and Moore, S.D.P. (2002) Copper transporting P-type ATPases and human disease. J. Bioenerg. Biomembr. 34: 333-338

Cumings, J.N. (1948) The copper and iron content of brain and liver in the normal and in hepato-lenticular degeneration. Brain 71: 410-415

Czlonkowska, A., Rodo, M., Gajda, J., Ploos van Amstel, H.K., Juyn, J., and Houwen, R.H.J. (1997) Very high frequency of the His1069Gln mutation in Polish Wilson disease patients. J. Neurol. 244: 591-599

da Costa Ferreira, A. M., Ciriolo, M. R., Marcocci, L., and Rotilio, G. (1993) Copper(I) transfer into metallothionein mediated by glutathione. Biochem. J. 292: 673-676

Danks, D.M., Campbell, P.E., Stevens, B.J., Mayne, V., and Cartwright, E. (1972) Menkes's kinky hair syndrome: an inherited defect in copper absorption with widespread effects. Pediatrics 50: 188-201

de Meis, L., and Vianna, A. L. (1979) Energy interconversion by the Ca^{2+}-dependent ATPase of the sarcoplasmic reticulum. Annu. Rev. Biochem. 48: 275-292

de Pont, J.J.H.H.M., Swarts, H.G.P., Willems, P.H.G.M., and Koenderink, J.B. (2003) The E1/E2 preference of gastric H,K-ATPase mutants. Ann. NY Acad. Sci. 986: 175-182

Deen, P.M.T., Croes, H., van Aubel, R.A.M.H., Ginsel, L.A., and van Os, C.H. (1995) Water channels encoded by mutant aquaporin-2 genes in nephrogenic diabetes insipidus are impaired in their cellular routing. J. Clin. Invest. 95: 2291-2296

Denning, G. M., Anderson, M.P., Amara, J.F., Marshall, J., Smith, A.E., and Welsh, M.J. (1992) Processing of mutant cystic fibrosis transmembrane conductance regulator is temperature-sensitive. Nature 358: 761-764

Dierick, H.A., Adam, A.N., Escara-Wilke, J.F., and Glover, T.W. (1997) Immunocytochemical localization of the Menkes copper transport protein (ATP7A) to the *trans*-Golgi network. Hum. Mol. Genet. 6: 409-416

Dupont, Y. (1982) Low-temperature studies of the sarcoplasmic reticulum pump mechanism of calcium binding. Biochim. Biophys. Acta 688: 75-87

Dupont, Y. (1980) Occlusion of divalent cations in the phosphorylated calcium pump of sarcoplasmic reticulum. Eur. J. Biochem. 109: 231-238

Efremov, R.G., Kosinsky, Y.A., Nolde, D.E., Tsivkovskii, R., Arseniev, A.S., and Lutsenko, S. (2004) Molecular modeling of the nucleotide-binding domain of the Wilson' disease protein: location of the ATP-binding site, domain dynamics, and potential effects of the major disease mutations. Biochem. J. (In press)

Eghtesad, B., Nezakatgoo, N., Geraci, L., Jabbour, N., Irish, W.D., Marsh, W., Fung, J.J., and Rakela, J. (1999) Liver transplantation for Wilson's disease: a single-center experience. Liver Transpl. Surg. 5: 467-474

Ettrich, R., Melichercik, M., Teisinger, J., Ettrichova, O., Krumscheid, R., Hofbauerova, K., Kvasnicka, P., Schoner, W., and Amler, E. (2001) Three-dimensional structure of the large cytoplasmic H4-H5 loop of Na^+/K^+-ATPase deduced by restraint-based comparative modeling shows only one ATP binding site. J. Mol. Model. 7: 184-192

Fairbanks, G., and Avruch, J. (1972) Four gel systems for electrophoretic fractionation of membrane proteins using ionic detergents. J. Supramol. Struct. 1: 66-75

Fan, B., Grass, G., Rensing, C., and Rosen, B. (2001) *Escherichia coli* CopA N-terminal $Cys(X)_2Cys$ motifs are not required for copper resistance or transport. Biochem. Biophys. Res. Commun. 286: 414-418

Ferenci, P., Caca, K., Loudianos, G., Mieli-Vergani, G., Tanner, S., Sternlieb, I., Schilsky, M., Cox, D., and Berr, F. (2003) Diagnosis and phenotypic classification of Wilson disease. Liver Int. 23: 139-142

Field, L. S., Luk, E., and Culotta, V. C. (2002) Copper chaperones: personal escorts for metal ions. J. Bioenerg. Biomembr. 34: 373-379

Figus, A., Angius, A., Loudianos, G., Bertini, C., Dessi,V., Loi, A., Deiana, M., Lovicu, M., Olla, N., Sole, G., De Virgilis, S., Lilliu, F., Farci, A.M.G., Nurchi, A., Giacchino, R., Barabino, A., Marazzi, M., Zancan, L., Greggio, N.A., Marcellini, M., Solinas, A., Deplano, A., Barbera, C., Devoto, M., Ozsoylu, S., Kocak, N., Akar, N., Karayalcin, S., Mokini, V., Cullufi, P., Balestrieri, A., Cao, A., and Pirastu, M. (1995) Molecular pathology and haplotype analysis of Wilson disease in Mediterranean populations. Am. J. Hum. Genet. 57: 1318-1324

Finney, L. A., and O'Halloran, T. V. (2003) Transition metal speciation in the cell: insights from the chemistry of metal ion receptors. Science 300: 931-936

Forbes, J.R., and Cox, D.W. (2000) Copper-dependent trafficking of Wilson disease mutant ATP7B protein. Hum. Mol. Genet. 9: 1927-1935

Forbes, J.R., His, G., and Cox, D.W. (1999) Role of the copper-binding domain in the copper transport function of ATP7B, the P-type ATPase defective in Wilson disease. J. Biol. Chem. 274: 12408-12413

Forbes, J.R. and Cox, D.W. (1998) Functional characterization of missense mutations in ATP7B: Wilson disease mutation or normal variant. Am. J. Hum. Genet. 63: 1663-1674

Francis, M.J., Jones, E.E., Levy, E.R., Ponnambalam, S., Chelly, J., and Monaco, A.P. (1998) A Golgi localization signal identified in the Menkes recombinant protein. Hum. Mol. Genet. 7: 1245-1252

Francis, M.S., and Thomas, C.J. (1997) Mutants in the CtpA copper transporting P-type ATPase reduce virulence of *Listeria monocytogenes*. Microb. Pathog. 22: 67-78

Freedman, J. H., Ciriolo, M. R., and Peisach, J. (1989) The role of glutathione in copper metabolism and toxicity. J. Biol. Chem. 264: 5598-5605

Fridovich, I. (1997) superoxide anion radical (O_2^-), superoxide dismutases, and related matters. J. Biol. Chem. 272: 18515-18517

Fukushima, Y., and Post, R.L. (1978) Binding of divalent cation to phosphoenzyme of sodium- and potassium-transport adenosine triphosphate. J. Biol. Chem. 253: 6853-6872

Garrick, M.D., Dolan, K.G., Horbinski, C., Ghio, A.J., Higgins, D., Porubcin, M., Moore, E.G., Hainsworth, L.N., Umbreit, J.N., Conrad, M.E., Feng, L., Lis, A., Roth, J.A., Singleton, S., and Garrick, L.M. (2003) DMT1: A mammalian transporter for multiple metals. BioMetals 16: 41-54

Gazaryan, I.G., Krasnikov, B.F., Ashby, G.A., Thorneley, R.N.F., Kristal, B.S., and Brown, A.M. (2002) Zinc is a potent inhibitor of thiol oxidoreductase activity and stimulates reactive oxygen species production by lipoamide dehydrogenase. J. Biol. Chem. 277: 10064-10072

Gitschier, J., Moffat, B., Reilly, D., Wood, W.I., and Fairbrother, W.J. (1998) Solution structure of the fourth metal-binding domain from the Menkes copper-transporting ATPase. Nat. Struct. Biol. 5: 47-54

Glerum, D.M., Shtanko, A., and Tzagoloff. A. (1996) Characterization of Cox17, a yeast gene involved in copper metabolism and assembly of cytochrome oxidase. J. Biol. Chem. 271: 14504-14509

Glynn, I.M., and Karlish, S.J.D. (1975) The sodium pump. Annu. Rev. Physiol. 37: 13-55

Goldshleger, R., and Karlish, S.J.D. (1999) The energy transduction mechanism of Na,K-ATPase studied with iron-catalyzed oxidative cleavage. J. Biol. Chem. 274: 16213-16221

Goldshleger, R., and Karlish, S.J.D. (1997) Fe-catalyzed cleavage of the α-subunit of Na/K-ATPase: Evidence for conformation sensitive interactions between cytoplasmic domains. Proc. Natl. Acad. Sci. USA 94: 9596-9601

Goodyear, I.D., Jones, E.E., Monaco, A.P., and Francis, M.J. (1999) Characterization of the Menkes protein copper-binding domains and their role in copper-induced protein relocation. Hum. Mol. Genet. 8: 1473-1478

Gunshin, H., Mackenzie, B., Berger, U.V., Gunshin, Y., Romero, M.F., Boron, W.F., Nussberger, S., Gollan, J.L., and Hediger, M.A. (1997) Cloning and characterization of a mammalian proton-coupled metal-ion transporter. Nature 388: 482-488

Haas, R., Gutierrez-Rivero, B., Knoche, J., Böker, K., Manns, M.P., and Schmidt, H.H.-J. (1999) Mutation analysis in patients with Wilson disease: identification of 4 novel mutations. Hum. Mutat. 14: 88-95

Hamer, D.H., Thiele, D.J., and Lemontt, J.E. (1985) Function and autoregulation of yeast copperthionein. Science 228: 685-690

Hamza, I., Schaefer, M., Klomp, L. W. J., and Gitlin, J. (1999) Interaction of the copper chaperone HAH1 with the Wilson disease protein is essential for copper homeostasis. Proc. Natl. Acad.Sci. USA 96: 13363-13368

Hanks, S.K., Quinn, A.M., and Hunter, T. (1988) The protein kinase family: Conserved features and deduced phylogeny of the catalytic domains. Science 241: 42-52

Hasselbach, W., and Makinose, M. (1961) Die calciumpumpe der erschlaffungsgrane des muskels und ihre abhängigkeit von der ATP – spaltung. Biochem. Z. 333: 518-528

Hilge, M., Siegal, G., Vuister, G.W., Güntert, P., Gloor, S.M., and Abrahams, J.P. (2003) ATP-induced conformational changes of the nucleotide-binding domain of Na,K-ATPase. Nat. Struct. Biol. 10: 468-474

Homen, E.A. (1892) Eine eigenthumliche bei drei geschwinstern auftrende typische krankheit unter der form einer progressiven dementia in verbindung mit ausgedehnten gefässveränderungen (wohl Lues hereditaria tarda). Archiv fur Psychiatrie und Nervenkrankheiten 24: 1-38

Homen, E.A. (1890a) Eine eigenthumlige familienkrankheit, unter der form einer progressiven dementia, mit besonderem anatomischen befund. Neurologisches Centralblatt 17: 1-6

Homen, E.A. (1890b) En sägeren familjesjukdom under form af progressiv dementia, I samband med utbredda kärlförändringar. Patologisk-anatomiska institutionens festkrift pp. 1-12. Helsingfors centraltryckeri, Helsingfors 1890

Hou, Z., and Mitra, B. (2003) The metal specificity and selectivity of ZntA from *Escherichia coli* using the acylphosphate intermediate. J. Biol. Chem. 278: 28455-28461

Hou, Z.J., Narindrasorasak, S., Bhushan, B., Sarkar, B., and Mitra, B. (2001) Functional analysis of chimeric proteins of the Wilson Cu(I)-ATPase (ATP7B) and ZntA, a Pb(II)/Zn(II)/Cd(II)-ATPase from *Escherichia coli*. J. Biol. Chem. 276: 40858-40863

Houwen, R.H.J., Juyn, J., Hoogenraad, T.U., Ploos van Amstel, J.K., Berger, R. (1995) H714Q mutation in Wilson disease is associated with late, neurological presentation. J. Med. Genet. 32: 480-482

Hsi, G., and Cox, D.W. (2004) A comparison of the mutation spectra of Menkes disease and Wilson disease. Hum. Genet. 114: 165-172

Hua, S., Ma, H., Lewis, D., Inesi, G., and Toyoshima, C. (2002a) Functional role of "N" (nucleotide) and "P" (phosphorylation) domain interactions in the sarcoplasmic reticulum (Serca) ATPase. Biochemistry 41: 2264-2272

Hua, S., Inesi, G., Nomura, H., and Toyoshima, C. (2002b) Fe^{2+}-catalyzed oxidation and cleavage of sarcoplasmic reticulum ATPase reveals Mg^{2+} and Mg^{2+}–ATP sites. Biochemistry 41: 11405-11410

Huffman, D.L., O'Halloran, T.V. (2000) Energetics of copper trafficking between theAtx1 metallochaperone and the intracellular copper transporter, ccc2. J. Biol. Chem. 275: 18611-18614

Hung, I., Suzuki, M., Yamaguchi, Y., Yuan, D.S., Klausner, R.D., and Gitlin, J.D. (1997) Biochemical characterization of the Wilson disease protein and functional expression in the yeast *Saccharomyces cerevisiae*. J. Biol. Chem. 272: 21461-21466

Iida, M., Terada, K., Sambongi, Y., Wakabayashi, T., Miura, N., Koyama, K., Futai, M., and Sugiyama, T. (1998) Analysis of functional domains of Wilson disease protein (ATP7B) in *Saccharomyces cerevisiae*. FEBS Lett. 428: 281-285

Ikemoto, N. (1976) Behaviour of the Ca^{2+} transport sites linked with the phosphorylation reaction of ATPase purified from the sarcoplasmic reticulum. J. Biol. Chem. 251: 7275-7277

Ikemoto, N. (1975) Transport and inhibitory Ca^{2+} binding sites on the ATPase enzyme isolated from the sarcoplasmic reticulum. J. Biol. Chem. 250: 7219-7224

Inesi, G. (1987) Sequential mechanism of calcium binding and translocation in sarcoplasmic reticulum adenosine triphosphatase. J. Biol. Chem. 262: 16338-16342

Inesi, G., Goodman, J.J., and Watanabe, S. (1967) Effect of diethyl ether on the Adenosine triphosphatase activity and the calcium uptake of fragmented sarcoplasmic reticulum of rabbit skeletal muscle. J. Biol. Chem. 242: 4637-4643

Jacobsen, M.D., Pedersen, P.A., and Jørgensen, P.L. (2002) Importance of Na,K-ATPase residue α1-Arg^{544} in segment Arg^{544}–Asp^{567} for high-affinity binding of ATP, ADP, or MgATP. Biochemistry 41: 1451-1456

Jardetzky, O. (1966) Simple allosteric model for membrane pumps. Nature 211: 969-970

Jensen, L.T., Ajua-Alemanji, M., and Culotta, V.C. (2003) The *saccharomyces cerevisiae* high affinity phosphate transporter encoded by *PHO84* also functions in manganese homeostasis. J. Biol. Chem 278: 42036-42040

Jørgensen, P.L. (2003) Transmission of E_1-E_2 structural changes in response to Na^+ or K^+ binding in Na,K-ATPase. Ann. NY Acad. Sci. 986: 22-30

Jørgensen, P.L. (1977) Purification and charcterization of (Na^+, K^+)-ATPase. VI. Differential tryptic modification of catalytic functions of the purified enzyme in presence of NaCl and KCl. Biochim. Biophys. Acta 466: 97-108

Jørgensen, P.L. (1975) Purification and charcterization of (Na^+, K^+)-ATPase. V. Conformational changes in the enzyme. Transitions between the Na-form and the K-form studied with tryptic digestion as a tool. Biochim. Biophys. Acta 401: 399-415

Kaler, S.G., Gallo, L.K., Proud, V.K., Percy, A.K., Mark, Y., Segal, N.A., Goldstein, D.S., Holmes, C.S., and Gahl, W.A. (1994) Occipital horn syndrome and a mild Menkes phenotype associated with splice site mutations at the MNK locus. Nature Genet. 8: 195-202

Kanazawa, T., Yamada, A., Yamamoto, T., and Tonomura, Y. (1971) Reaction mechanism of the Ca^{2+}-dependent ATPase of sarcoplasmic reticulum from skeletal muscle. V. Vectorial requirements for calcium and magnesium ions of three partial reactions of ATPase: formation and decomposition of a phosphorylated intermediate and ATP-formation from ADP and the intermediate. J. Biochem. 70:95-123

Kaplan, J.H. (2002) Biochemistry of Na,K-ATPase. Annu. Rev. Biochem. 71: 511-535

Kato, S., Kamidochi, M., Daiho, T., Yamasaki, K., Gouli, W., and Suzuki, H. (2003) Val^{200} residue in Lys^{189}-Lys^{205} outermost loop on the A domain of sarcoplasmic reticulum Ca^{2+}-ATPase is critical for rapid processing of phosphoenzyme intermediate after loss of ADP sensitivity. J. Biol. Chem. 278: 9624-9629

Kim, B.-E., Smith, K., Meagher, C.K., and Petris, M.J. (2002) A conditional mutation affecting localization of the Menkes disease copper ATPase. J. Biol. Chem. 277: 44079-44084

Kinoshita, K., Sadanami, K., Kidera, A., and Go, N. (1999) Structural motif of phosphate-binding site common to various protein superfamilies: all-against-all structural comparison of protein-mononucleotide complexes. Prot. Eng. 12: 11-14

Kopito, R.R. (1997) ER quality control: The cytoplasmic connection. Cell 88: 427-430

Kubala, M., Teisinger, J., Ettrich, R., Hofbauerova, K., Kopecky, V.Jr., Baumruk, V., Krumscheid, R., Plasek, J., Schoner, W., and Amler, E. (2003) Eight amino acids form the ATP recognition site of Na^+/K^+-ATPase. Biochemistry 42: 6446-6452

Kubala, M., Hofbauerova, K., Ettrich, R., Kopecky, V.Jr., Krumscheid, R., Plasek, J., Teisinger, J., Schoner, W., and Amler, E. (2002) Phe^{475} and Glu^{446} but not Ser^{445} participate in ATP-binding to the α-subunit of Na^+/K^+-ATPase. Biochem. Biophys. Res. Commun. 297: 154-159

Kühlbrandt, W., Zeelen, J., and Dietrich, J. (2002) Structure, mechanism and regulation of the *Neurospora* plasma membrane H^+-ATPase. Science 297: 1692-1696

La Fontaine, S., Firth, S.D., Camakaris, J., Englezou, A., Theophilos, M.B., Petris, M.J., Howie, M., Lockhart, P.J., Greenough, M., Brooks, H., Reddel, R.R., and Mercer, J.F.B. (1998) Correction of the copper transport defect of Menkes patient fibroblasts by expression of the Menkes and Wilson ATPases. J. Biol. Chem. 273: 31375-31380

Larin, D., Mekios, C., Das, K., Ross, B., Yang, A.-S., and Gilliam, C. (1999) Characterization of the interaction between the Wilson and Menkes disease proteins and the cytoplasmic copper chaperone, HAH1p. J. Biol. Chem. 274: 28497-28504

Levy, D., Seigneuret, M., Bluzat, A., and Rigaud, J.-L. (1990) Evidence for proton countertransport by the sarcoplasmic reticulum Ca^{2+}-ATPase during calcium transport in reconstituted proteoliposomes with low ionic permeability. J. Biol. Chem. 265: 19524-19534

Lin, S.-J., Pufahl, R. A., Dancis, A., O'Halloran, T. V., and Culotta, V. C. (1997) A role for the *Saccharomyces cerevisiae* ATX1 gene in copper trafficking and iron transport J. Biol. Chem. 272: 9215-9220

Linder, M. C., and Hazegh-Azam, M. (1996) Copper biochemistry and molecular biology. Am. J. Clin. Nutr. 63: 797S-811S

Loudianos, G., Lovicu, M., Solinas, P., Kanavakis, E., Tzetis, M., Manolaki, N., Panatiotakaki, E., Karpathios, T., and Cao, A. (2000) Delineation of the spectrum of Wilson disease mutations in the Greek population and the identification of six novel mutations. Genet. Test. 4: 399-402

Loudianos, G., Dessi, V., Lovicu, M., Angius, A., Altuntas, B., Giacchino, R., Marazzi, M., Marcellini, M., Sartorelli, M.R., Sturniolo, G.C., Kocak, N., Yuce, A., Akar, N., Pirastu, M., and Cao, A. (1999) Mutation analysis in patients of Mediterranean descent with Wilson disease: identification of 19 novel mutations. J. Med. Genet. 36: 833-836

Loudianos, G., Dessi, V., Angius, A., Lovicu, M., Loi, A., Deiana, M., Akar, N., Vajro, P., Figus, A., Cao, A., and Pirastu, M. (1996) Wilson disease mutations associated with uncommon haplotypes in Mediterranian patients. Hum. Genet. 98: 640-642

Lu, Z. H., Dameron, C. T., and Solioz, M. (2003) The paradigm of copper homeostasis: copper chaperone turnover, interactions, and transactions. BioMetals 16: 137-143

Lutsenko, S., and Kaplan, J.H. (1995) Organization of P-type ATPases: significance of structural diversity. Biochemistry 34: 15607-15613

Lutter, R., Saraste, M., van Walraven, H.S., Runswick, M.J., Finel, M., Detherage, J.F., and Walker, J.E. (1993) F_1F_0-ATP synthase from bovine heart mitochondria: development of the purification of a monodisperse oligomycin-sensitive ATPase. Biochem. J. 295: 799-806

Ma, H., Inesi, G., and Toyoshima, C. (2003) Substrate-induced conformational fit and headpiece closure in the Ca^{2+}-ATPase (SERCA). J. Biol. Chem. 278: 28938-28943

MacLennan, D.H., Brandl, C.J., Korczak, B., and Green, N.M. (1985) Amino-acid sequence of a Ca^{2+} + Mg^{2+}-dependent ATPase from rabbit muscle sarcoplasmic reticulum, deduced from its complementary DNA sequence. Nature 316: 696-700

Makinose, M. (1973) Possible functional states of the enzyme of the sarcoplasmic calcium pump. FEBS Lett. 37: 140-143

Makinose, M. (1971) Calcium efflux dependent formation of ATP from ADP and orthophosphate by the membranes of the sarcoplasmic vesicles. FEBS Lett. 12: 269-270

Makinose, M., and Hasselbach, W. (1971) ATP synthesis by the reverse of the sarcoplasmic calcium pump. FEBS Lett. 12: 271-272

Makinose, M. (1969) The phosphorylation of the membranal protein of the sarcoplasmic vesicles during active calcium transport. European J. Biochem. 10: 74-82

Mandal, A.K., and Argüello, J.M. (2003) Functional roles of metal binding domains of the *Archaeoglobus fulgidus* Cu^{+}-ATPase CopA. Biochemistry 42: 11040-11047

Mandal, D., Rulli, S.J., and Rao, R. (2003) Packing interactions between transmembrane helices alter ion selectivity of the yeast Golgi Ca^{2+}/Mn^{2+}-ATPase PMR1. J. Biol. Chem. 278: 35292-35298

Maret, W., Jacob, C., Vallee, B.L., and Fischer, E.H. (1999) Inhibitory sites in enzymes: Zinc removal and reactivation by thionein. Proc. Natl. Acad. Sci. USA 96: 1936-1940

Martonosi, A. (1967) The role of phospholipids in the ATP-ase activity of skeletal muscle microsomes. Biochem. Biophys. Res. Commun. 29: 753-757

Masuda, H., and de Meis, L. (1973) Phosphorylation of the sarcoplasmic reticulum membrane by orthophosphate. Inhibition by calcium ions. Biochemistry 12: 4581-4585

McIntosh, D.B., Woolley, D.G., Vilsen, B., and Andersen, J.P. (1996) Mutagenesis of segment ^{487}Phe-Ser-Arg-Asp-Arg-Lys^{492} of sarcoplasmic reticulum Ca^{2+}-ATPase produces pumps defective in ATP binding. J. Biol. Chem. 271: 25778-25789

McIntosh, D.B. (1992) Glutaraldehyde cross-links Lys-492 and Arg-678 at the active site of sarcoplasmic reticulum Ca^{2+}-ATPase. J. Biol. Chem. 267: 22328-22335

Melchers, K.J., Weitzenegger, T., Buhmann, A., Steinhilber, W., Sachs, G., and Schäfer, K.P. (1996) Cloning and membrane topology of a P-type ATPase from *Helicobacter pylori*. Biol. Chem. 271: 446-457

Menkes, J.H., Alter, M., Steigleder, G.K., Weakley, D.R., and Sung, J.H. (1962) A sex-linked recessive disorder with retardation of growth, peculiar hair, and focal cerebral and cerebellar degeneration. Pediatrics 29: 764-779

Mercer, J. F. B., Barnes, N., Stevenson, J., Strausak, D., and Llanos, R. M. (2003) Copper-induced trafficking of the Cu-ATPases: a key mechanism for copper homeostasis. BioMetals 16: 175-184

Mercer, J.F.B., Livingston, J., Hall, B., Paynter, J.A., Begy, C., Chandrasekharappa, S., Lockhart, P., Grimes, A., Bhave, M., Siemieniak, D., and Glover, T.W. (1993) Isolation of a partial candidate gene for Menkes disease by positional cloning. Nat. Genet. 3: 20-25

Mitchinson, C., Wilderspin., A.F., Trinnaman, B.J., and Green, N.M. (1982) Identification of a labelled peptide after stoichiometric reaction of fluorescein isothiocyanate with the Ca^{2+}-dependent adenosine triphosphate of sarcoplasmic reticulum. FEBS Lett. 146: 87-92

Mitra, B., and Sharma, R. (2001) The cysteine-rich amino-terminal domain of ZntA, a Pb(II)/Zn(II)/Cd(II)-translocating ATPase from *Escherichia coli*, is not essential for its function. Biochemistry 40: 7694-7699

Multhaup, G., Strausak, D., Bissig, K.D., Solioz, M. (2001) Interaction of the CopZ copper chaperone with the CopA copper ATPase of Enterococcus hirae assessed by surface plasmon resonance. Biochem. Biophys. Res. Commun. 288: 172-177

Munson, K., Vagin, O., Sachs, G., and Karlish, S. (2003) Molecular modeling of SCH28080 binding to the gastric H,K-ATPase and MgATP interactions with SERCA- and Na,K-ATPases. Ann. NY Acad. Sci. 986: 106-110

Murata, Y., Yamakawa, E., Iizuka, T., Kodama, H., Abe, T., Seki, Y., and Kodama, M. (1995) Failure of copper incorporation into ceruloplasmin in the Golgi apparatus of Lec rat hepatocytes. Biochem. Biophys. Res. Commun. 209: 349-355

Musci, G., Di Marco, S., Bellenchi, G. C., and Calabrese, L. (1996) Reconstitution of ceruloplasmin by the Cu(I)-glutathione complex. Evidence for a role of Mg^{2+} and ATP. J. Biol. Chem. 271: 1972-1978

Møller, L.B., Tümer, Z., Lund, C., Petersen, C., Cole, T., Hanuch, R., Seidel, J., Jensen, L.R., and Horn, N. (2000) Similar splice-site mutations of the *ATP7A* gene lead to different phenotypes: classical Menkes disease or occipital horn syndrome. Am. J. Hum. Genet. 66: 1211-1220

Møller, J.V., Juul, B., and Le Maire, M. (1996) Structural organization, ion transport, and energy transduction of P-type ATPases. Biocem. Biophys. Acta 1286: 1-51

Nanji, M.S., Nguyen, V.T.T., Kawasoe, J.H., Inui, K., Endo, F., Nakajima, T., Anezaki, T., and Cox, D.W. (1997) Haplotype and mutation analysis in Japanese patients with Wilson disease. Am. J. Hum. Genet. 60: 1423-1429

Nies, D.H. (2003) Efflux-mediated heavy metal resistance in prokaryotes. FEMS Microbiol. Rev. 27: 313-339

Odermatt, A., Suter, H., Krapf, R., and Solioz, M. (1993) Primary structure of two P-type ATPases involved in copper homeostasis in *Enterococcus hirae*. J. Biol. Chem. 268:12775-12779

Ogawa, A., Yamamoto, S., Takayanagi, M., Kogo, T., Kanazawa, M., and Kohno, Y. (1999) Identification of three novel mutations in the MNK gene in three unrelated Japanese patients with classical Menkes disease. J. Hum. Genet. 44: 206-209

Oh, W.J., Kim, E.K., Ko, J.H., Yoo, S.H., Hahn, S.H., and Yoo, O.-J. (2002) Nuclear proteins that bind to metal response element a (MREa) in the Wilson disease gene promoter are Ku autoantigens and the Ku-80 subunit is necessary for basal transcription of the WD gene. Eur. J. Biochem. 269: 2151-2161

Okada, T., Shiono, Y., Hayashi, H., Satoh, H., Sawada, T., Suzuki, A., Takeda, Y., Yano, M., Michitaka, K., Onji, M., and Mabuchi, H. (2000) Mutational analysis of *ATP7B* and genotype-phenotype correlation in Japanese with Wilson's disease. Hum. Mut. 15: 454-462

Outten, C. E., and O'Halloran, T. V. (2001) Femtomolar sensitivity of metalloregulatory proteins controlling zinc homeostasis. Science 292: 2488-2492

Palmgren, M.G., Axelsen, K.B. (1998) Evolution of P-type ATPases. Biochim. Biophys. Acta 1365: 37-45

Patchornik, G., Munson, K., Goldshleger, R., Shainskaya, A., Sachs, G., and Karlish, S.J.D. (2002) The ATP-Mg^{2+} binding site and cytoplasmic domain interactions of Na^+,K^+-ATPase investigated with Fe^{2+}-catalyzed oxidative cleavage and molecular modeling. Biochemistry 41: 11740-11749

Patchornik, G., Goldshleger, R., and Karlish, S.J.D. (2000) The complex ATP-Fe^{2+} serves as a specific affinity cleavage reagent in ATP-Mg^{2+} sites of Na,K-ATPase: Altered ligation of Fe^{2+} (Mg^{2+}) ions accompanies the $E_1P \rightarrow E_2P$ conformational change. Proc. Natl. Acad. Sci. USA 97: 11954-11959

Patzer**,** S.I., and Hantke, K. (1998) The ZnuABC high-affinity zinc uptake system and its regulator Zur in *Escherichia coli*. Mol. Microbiol. 28:1199-210

Payne, A.S., and Gitlin, J.D. (1998) Functional expression of the Menkes disease protein reveals common biochemical mechanisms among the copper-transporting P-type ATPases. J. Biol. Chem. 273: 3765-3770

Payne, A.S., Kelly, E.J., and Gitlin, J. (1998) Functional expression of the Wilson disease protein reveals mislocalization and impaired copper-dependent trafficking of the common H1069Q mutation. Proc. Natl. Acad. Sci. 95: 10854-10859

Pedersen, P.A., Jørgensen, J.R., and Jørgensen, P.L. (2000) Importance of conserved α-subunit segment ^{709}GDGVND for Mg^{2+} binding, phosphorylation, and energy transduction in Na,K-ATPase. J. Biol. Chem. 275: 37588-37595

Petersen, C., and Møller, L.B. (2000) Control of copper homeostasis in Escherichia coli by a P-type ATPase, CopA, and a MerR-like transcriptional activator, CopR. Gene 261: 289-298

Petris, M.J., Voskoboinik, I., Cater, M., Smith, K., Kim. B.-E., Llanos, R.M., Strausak, D., Camakaris, J., and Mercer, J.F.B. (2002) Copper-regulated trafficking of the Menkes disease copper ATPase is associated with formation of a phosphorylated catalytic intermediate. J. Biol. Chem. 277: 46736-46742

Petris, M.J., Mercer, J.F.B., Culvenor, J.G., Lockhart, P., Gleeson, P.A., and Camakaris, J. (1996) Ligand-regulated transport of the Menkes copper P-type ATPase efflux pump from the Golgi apparatus to the plasma membrane: a novel mechanism of regulated trafficking. EMBO J. 15: 6084-6095

Petrukhin, K., Fischer, S.G., Pirastu, M., Tanzi, R.E., Chernov, I., Devoto, M., Brzustowicz, L.M., Cayanis, E., Vitale, E., Russo, J.J., Matseoane, D., Boukhgalter, B., Wasco, W., Figus, A.L., Loudianos, J., Cao, A., Sternlieb, I., Evgrafov, O., Parano, E., Pavone, L., Warburton, D., Ott, J., Penchaszadeh, G.K., Scheinberg, I.H., and Gilliam,

T.C. (1993) Mapping, cloning and genetic characterization of the region containing the Wilson disease gene. Nat. Genet. 5: 338-343

Portillo, F., and Serrano, R. (1988) Dissection of functional domains of the yeast proton-pumping ATPase by directed mutagenesis EMBO J. 7: 1793-1798

Post, R.L., Toda, G., and Rogers, F.N. (1975) Phosphorylation by inorganic phosphate of sodium plus potassium ion transport adenosine triphosphate. J. Biol. Chem. 250: 691-701

Post, R.L., Hegyvary, C., and Kume, S. (1972) Activation by adenosine triphosphate in the phosphorylation kinetics of sodium and potassium ion transport adenosine triphosphatase. J. Biol. Chem. 247: 6530-6540

Post, R.L., Amar, K.S., and Rosenthal, A.S. (1965) A phosphorylated intermediate in adenosine triphosphate-dependent sodium and potassium transport across kidney membranes. J. Biol. Chem. 240: 1437-1445

Pufahl, R. A., Singer, C. P., Peariso, K. L., Lin, S.-J., Penner-Hahn, J. E., and O'Halloran, T. O. (1997) Metal ion chaperone function of the soluble Cu(I) receptor Atx1. Science 278: 853-856

Rae, T.D., Schmidt, P.J., Pufahl, R.A., Culotta, V.C., O'Halloran, T.V. (1999) Undetectable intracellular free copper: the requirement of a copper chaperone for superoxide dismutase. Science 284: 805-808

Ralle, M., Lutsenko, S., and Blackburn, N. J. (2003) X-ray absorption spectroscopy of the copper chaperone HAH1 reveals a linear two-coordinate Cu(I) center capable of adduct formation with exogenous thiols and phosphines. J. Biol. Chem. 278: 23163-23170

Reinstein, J., and Jencks, W.P. (1993) The binding of ATP and Mg^{2+} to the calcium adenosinetriphosphatase of sarcoplasmic reticulum follows a random mechanism. Biochemistry 32: 6632-6642

Rensing, C., Sun, Y., Mitra, B., and Rosen, B.P. (1998) Pb(II)-translocating P-type ATPases. J. Biol. Chem. 273: 32614-32617

Rensing, C., Mitra, B., and Rosen, P.B. (1997) The ZntA gene of *Escherichia coli* encodes a Zn(II)-translocating P-type ATPase. Proc. Natl. Acad. Sci. USA 94: 14326-14331

Richter, O.-M., H., and Ludwig, B. (2003) Cytochrome c oxidase—structure, function, and physiology of a redox-driven molecular machine. Rev. Phys. Biochem. Pharmacol. 147: 47-74

Ridder, I.S., and Dijkstra, B.W. (1999) Identification of the Mg^{2+}-binding site in the P-type ATPase and phosphatase members of the HAD (haloacid dehalogenase) superfamily by structural similarity to the response regulator protein CheY. Biochem. J. 339: 223-226

Riordan, S.M., and Williams, R. (2001) The Wilson's disease gene and phenotypic diversity. J. Hepatology 34: 165-171

Robinson, J.D., and Flashner, M.S. (1979) The ($Na^+ + K^+$)-activated ATPase. Enzymatic and transport properties. Biochim. Biophys. Acta 549: 145-176

Roelofsen, H., Wolters, H., Van Luyn, M.J.A., Miura, N., Kuipers, F., and Vonk, R.J. (2000) Copper-induced apical trafficking of ATP7B in polarized hepatoma cells provides a mechanism for biliary copper excretion. Gastroenterology 119: 782-793

Rosen, B. P. (2002) Transport and detoxification systems for transition metals, heavy metals and metalloids in eukaryotic and prokaryotic microbes. Comp. Biochem. Biophys. A133: 689-693

Rost, B. (1996) PHD: predicting one-dimensional protein structure by profile based neural networks. Methods Enzymol. 266: 525-539

Rucker, R.B., Kosonen, T., Clegg, M.S., Mitchell, A.E., Rucker, B.R., Uriu-Hare, J.Y., and Keen, C.L. (1998) Copper, lysyl oxidase, and extracellular matrix protein cross-linking. Am. J. Clin. Nutr. 67: 996S-1002S

Rutherford, J.C., Cavet, J.S., and Robinson, N.J. (1999) Cobalt-dependent transcriptional switching by a dual-effector MerR-like protein regulates a cobalt-exporting variant of CPx-type ATPase. J. Biol. Chem. 274: 25827-25832

Sambongi, Y., Wakabayashi, T., Yoshimizu, T., Omote, H., Oka, T., and Futai, M. (1997) *Caenorhabditis elegans* cDNA for Menkes/Wilson disease gene homologue and its function in a yeast CCC2 gene deletion mutant. J. Biochem. 121: 1169-1175

Saraste, M., Sibbald, P.R., and Wittinghofer, A. (1990) The P-loop – a common motif in ATP- and GTP-binding proteins. Trends Biochem. Sci. 15: 430-434

Sarkar, B. (1999) Treatment of Wilson and Menkes diseases. Chem. Rev. 99: 2535-2544

Schaeffer, M., Roelofsen, H., Wolters, H., Hofmann, W.J., Müller, M., Kuipers, F., Stremmel, W., and Vonk, R.J. (1999) Localization of the Wilson's disease protein in human liver. Gastroenterology 117: 1380-1385

Schiefermeier, M., Kollegger, H., Madl, C., Polli, C., Oder, W., Kühn, H.-J., Berr, F., and Ferenci, P. (2000) The impact of apolipoprotein E genotypes on age at onset of symptoms and phenotypic expression in Wilson's disease. Brain 123: 585-590

Schilsky, M. L., Stockert, R. J., Kesner, A., Gorla, G. R., Gagliardi, G. S., Terada, K., Miura, N., and Czaja, M. J. (1998) Copper resistant human hepatoblastoma mutant cell lines without metallothionein induction overexpress ATP7B. Hepatology 28: 1347-1356

Schilsky, M.L., Scheinberg, I.H., and Sternlieb, I. (1994) Liver transplantation for Wilson's disease: indications and outcome. Hepatology 19: 583-587

Seng, H., Gregory, R.J., Marshall, J., Paul, S., Souza, D.W., White, G.A., O'Riordan, C.R., and Smith, A.E. (1990) Defective intracellular transport and processing of CFTR is the molecular basis of most cystic fibrosis. Cell 63: 827-834

Shah, A.B., Chernov, I., Zhang, H.T., Ross, B.M., Das, K., Lutsenko, S., Parano, E., Pavone, L., Evgrafov, O., Ivanova-Smolenskaya, I.A., Anneren, G., Westermark, K., Urrutia, F.H., Penchaszadeh, G.K., Sternlieb, I., Scheinberg, I.H., Gilliam, T.C., and Petrukhin, K. (1997) Identification and analysis of mutations in the Wilson disease gene (ATP7B): population frequencies, genotype-phenotype correlation, and functional analyses. Am. J. Hum. Genet. 61: 317-328

Sharma, R., Rensing, C., Rosen, B.P., and Mitra, B. (2000) The ATP hydrolytic activity of purified ZntA, a Pb(II)/Cd(II)/Zn(II)-translocating ATPase from *Escherichia coli*. J. Biol. Chem. 275: 3873-3878

Shigekawa, M., and Dougherty, J.P. (1978) Reaction mechanism of Ca^{2+}-dependent ATP hydrolysis by skeletal muscle sarcoplasmic reticulum in the absence of added alkali metal salts. J. Biol. Chem. 253: 1458-1464

Shim, H., and Harris, Z.L. (2003) Genetic defects in copper metabolism. J. Nutr. 133: 1527-1531

Shull, G.E., Okunade, G., Liu, L.H., Kozel, P., Periasamy, M., Lorenz, J.N., and Prasad, V. (2003) Physiological functions of plasma membrane and intracellular Ca^{2+} pumps revealed by analysis of null mutants. Ann. N.Y. Acad. Sci. 986: 453-460

Silke, P., and Hantke, K. (1998) The ZnuABC high-affinity zinc uptake system and its regulator Zur in *Escherichia coli*. Mol. Microbiol. 28: 1199-1210

Skou, J.C., and Esmann, M. (1983) The effects of Na^+ and K^+ on the conformational transitions of (Na^+ + K^+)-ATPase. Biochim. Biophys. Acta 746: 101-113

Skou, J. C. (1979) Effects of ATP on the intermediary steps of the reaction of the (Na^+ + K^+)-ATPase. IV. Effects of ATP on $K_{0.5}$ for Na^+ and on hydrolysis at different pH and temperature. Biochim. Biophys. Acta 567: 421-435

Skou, J.C. (1957) The influence of some cations on an adenosine triphosphatase from peripheral nerves. Biochim. Biophys. Acta 23: 394-401

Sofia, H.J., Burland, V., Daniels, D.L., Plunkett III, G., and Blattner, F.R. (1994) Analysis of the Escherichia coli genome. V. DNA sequence of the region from 76.0 to 81.5 minutes. Nucleic Acids Res. 22: 2576-2586

Solioz, M., and Vulpe, C. (1996) CPx-type ATPases: a class of P-type ATPases that pump heavy metals. Trends Biochem. Sci. 21: 237-241

Solioz M, and Odermatt A. (1995) Copper and silver transport by CopB-ATPase in membrane vesicles of *Enterococcus hirae*. J. Biol. Chem. 270: 9217-9221

Steele, R., and Opella, S.J. (1997) Structures of the reduced and mercury-bound forms of the MerP, the periplasmic protein of the bacterial mercury detoxification system. Biochemistry 36: 6885-6895

Stokes, D.L., and Green, N.M. (2003) Structure and functions of the calcium pump. Annu. Rev. Biophys. Biomol. Struct. 32: 445-468

Strausak, D., La Fontaine, S., Hill, J., Firth, S.D., Lockhart, P.J., and Mercer, J.F.B. (1999) The role of GMXCXXC metal binding sites in the copper-induced redistribution of the Menkes protein. J. Biol. Chem. 274: 11170-11177

Subramanian, I., Vanek, Z.F., and Bronstein, J.M. (2002) Diagnosis and treatment of Wilson's disease. Curr. Neurol. Neurosci. Rep. 2: 317-323

Sumida, M., and Tonomura, Y. (1974) Reaction mechanism of the Ca^{2+}-dependent ATPase of sarcoplasmic reticulum from skeletal muscle X. Direct evidence for Ca^{2+} translocation coupled with formation of a phosphorylated intermediate. J. Biochem. 75: 283-297

Tang, X., Halleck, M.S., Schlegel, R.A., Williamson, P. (1996) A subfamily of P-type ATPases with aminophospholipid transporting activity. Science 272: 1495-1497

Tanzi, R.E., Petrukhin, K., Chernov, I., Pellequer, J.L., Wasco, W., Ross, B., Romano, D.M., Parano, E., Pavone, L., Brzustowicz, L.M., Devoto, M., Peppercorn, J., Bush, A.I., Sternlieb, I., Pirastu, M., Gusella, J.F., Evgrafov, O., Penchaszadeh, G.K., Honig, B., Edelman, I.S., Soares, M.B., Scheinberg, I.H., and Gilliam, T.C. (1993) The Wilson disease gene is a copper transporting ATPase with homology to the Menkes disease gene. Nature Genet. 5, 344-348

Taylor, W.R., and Green, N.M. (1989) The predicted secondary structures of the nucleotide-binding sites of six cation-transporting ATPases lead to a propable tertiary fold. Eur. J. Biochem. 179: 241-248

Teramachi, S., Imagawa, T., Kaya, S., and Taniguchi, K. (2002) Replacement of several single amino acid side chains exposed to the inside of the ATP-binding pocket induces different extents of affinity change in the high and low affinity ATP-binding sites of rat Na/K-ATPase. J. Biol. Chem. 277: 37394-37400

Thiele, D.J., Walling, M.J., and Hamer, D.H. (1986) Mammalian metallothionein is functional in yeast. Science 231: 854-856

Thomas, G.R., Forbes, J.R., Roberts, E.A., Walshe, J.M., and Cox, D.W. (1995) The Wilson disease gene: spectrum of mutations and their consequences. Nat. Genet. 9: 210-217

Thompson, J.D., Gibson, T.J., Plewniak, F., Jeanmougin, F., and Higgins, D.G. (1997) The CLUSTAL_X windows interface: flexible strategies for multiple sequence alignment aided by quality analysis tools. Nucleic Acids Res. 24: 4876-4882

Toustrup-Jensen, M., and Vilsen, B. (2003) Importance of T^{214} in domain A of the Na^+,K^+-ATPase for stabilization of the phosphoryl transition state complex in E_2P dephosphorylation. J. Biol. Chem. 278: 11402-11410

Toyoshima, C., Nomura, H., and Sugita, Y. (2003) Structural basis of ion pumping by Ca^{2+}-ATPase of sarcoplasmic reticulum. FEBS Lett. 555: 106-110

Toyoshima, C., and Nomura, H. (2002) Structural changes in the calcium pump accompanying the dissociation of calcium. Nature 418: 605-611

Toyoshima, C., Nakasako, M., Nomura, H., and Ogawa, H. (2000) Crystal structure of the calcium pump of sarcoplasmic reticulum at 2.6 Å resolution. Nature 405: 647-655

Tsai, K.-J., Lin, Y.-F., Wong, M.D., Yang, H.H.-C., Fu, H.-L., and Rosen, B.P. (2002) Membrane topology of the p1258 CadA Cd(II)/Pb(II)/Zn(II)-translocating P-type ATPase. J. Bioenerg. Biomembr. 34: 147-156

Tsivkovskii, R., Efremov, R.G., and Lutsenko, S. (2003) The role of the invariant His-1069 in folding and function of the Wilson's disease protein, the human copper-transporting ATPase ATP7B. J. Biol. Chem. 278: 13302-13308

Tsivkovskii, R., MacArthur, B.C., and Lutsenko, S. (2001) The Lys1010-Lys1325 fragment of the Wilson's disease protein binds nucleotides and interacts with the N-terminal domain of this protein in a copper-dependent manner. J. Biol. Chem. 276: 2234-2242

Tümer, Z., Møller, L.B., and Horn, N. (1999) Mutation spectrum of *ATP7A*, the gene defective in Menkes disease. Adv. Exp. Med. Biol. 448: 83-95

Van Veen, H.W., Abee, T., Korstee, G.J.J., Konings, W.N., and Zehnder, A.J.B. (1994) Translocation of metal phosphate via the phosphate inorganic transport system of *Escherichia coli*. Biochemistry 33: 1766-1770

Vanderwerf, S.M., Cooper, M.J., Stetsenko, I.V., and Lutsenko, S. (2001) Copper specifically regulates intracellular phosphorylation of the Wilson's disease protein, a human copper-transporting ATPase. J. Biol. Chem. 276: 36289-36294

Vetter, I.R., and Wittinghofer, A. (1999) Nucleoside triphosphate-binding proteins: different scaffolds to achieve phosphoryl transfer. Quart. Rev. Biophys. 32: 1-56

Via, A., Ferre, F., Brannetti, B., Valencia, A., and Helmer-Citterich, M. (2000) Three-dimensional view of the surface motif associated with the P-loop structure: *Cis* and *trans* cases of convergent evolution. J. Mol. Biol. 303: 455-465

Videla, L. A., Fernandez, V., Tapia, G., and Varela, P. (2003) Oxidative stress-mediated hepatotoxicity of iron and copper: role of Kupffer cells. BioMetals 16: 103-111

Vilsen, B., Andersen, J.P., and MacLennan, D.H. (1991) Functional consequences of alterations to amino acids located in the hinge domain of the Ca^{2+}-ATPase of sarcoplasmic reticulum. J. Biol. Chem. 266:16157-16164

Voskoboinik, I., Mar, J., and Camakaris, J. (2003a) Mutational analysis of the Menkes copper ATPase (ATP7A) Biochem. Biophys. Res. Commun. 301: 488-494

Voskoboinik, I., Fernando, R., Veldhuis, N., Hannan, K.M., Marmy-Conus, N., Pearson, R.B., and Camakaris, J. (2003b) Protein kinase-dependent phosphorylation of the Menkes copper P-type ATPase. Biochem. Biophys. Res. Commun. 303: 337-342

Voskoboinik, I., Mar, J., Strausak, D., and Camakaris, J. (2001) The regulation of catalytic activity of the Menkes copper-translocating P-type ATPase. J. Biol. Chem. 276: 28620-28627

Voskoboinik, I., Strausak, D., Greenough, M., Brooks, H., Petris, M., Smith, S., Mercer, J.F., and Camakaris, J. (1999) Functional analysis of the N-terminal CXXC metal-binding motifs in the human Menkes copper-transporting P-type ATPase expressed in cultured mammalian cells. J. Biol. Chem. 274: 22008-22012

Vulpe, C., Levinson, B., Whitney, S., Packman, S., and Gitschier, J. (1993) Isolation of a candidate gene for Menkes disease and evidence that it encodes a copper-transporting ATPase. Nat. Genet. 3: 7-13

Waldenström, E., Lagerkvist, A., Dahlman, T., Westermark, K., and Landegren, U. (1996) Efficient detection of mutations in Wilson disease by manifold sequencing. Genomics 37: 303-309

Watanabe, T., and Inesi, G. (1982) The use of 2',3'-O-(2,4,6-trinitrophenyl) adenosine 5'-triphosphate for studies of nucleotide interaction with sarcoplasmic reticulum vesicles. J. Biol. Chem. 257: 11510-11516

Weast, R.C. (1979) CRC hadbook of chemistry and physics, 59th edition, 1978-1979. Weast, R.C., and Astle, M., eds., CRC Press, Boca Raton, p. F-213

Wernimont, A.K., Huffman, D.L., Lamb, A.L., O'Halloran, T.V., and Rosenzweig, A.C. (2000) Structural basis for copper transfer by the metallochaperone for the Menkes/Wilson disease proteins. Nat. Struct. Biol. 7: 766-771

Wilson, S.A.K. (1912) Progressive lenticular degeneration: a familial nervous disease associated with cirrhosis of the liver. Brain 34: 295-509

Wu, Z.-Y., Wang, N., Lin, M.-T., Fang, L., Murong, S.-X., and Yu, L. (2001) Mutation analysis and the correlation between genotype and phenotype of Arg778Leu mutation in Chinese patients with Wilson disease. Arch. Neurol. 58: 971-976

Xu, C., Rice, W.J., Wanzhong, H., and Stokes, D.L. (2002) A structural model for the catalytic cycle of Ca^{2+}-ATPase. J. Mol. Biol. 316: 201-211

Yamaguchi, Y., Heiny, M.E., Suzuki, M., and Gitlin, J.D. (1996) Biochemical characterization and intracellular localization of the Menkes disease protein. Proc. Natl. Acad. Sci. USA 93: 14030-14035

Yamaguchi, Y., Heiny, M.E., and Gitlin, J.D. (1993) Isolation and characterization of a human liver cDNA as a candidate gene for Wilson disease. Biochem. Biophys. Res. Commun. 197: 271-277

Yamamoto, T., and Tonomura, Y. (1968) Reaction mechanism of the Ca++-dependent ATPase of sarcoplasmic reticulum from skeletal muscle. II. Intermediate formation of phosphoryl protein J. Biochem. 62: 137-145

Yamamoto, T., and Tonomura, Y. (1967) Reaction mechanism of the Ca++-dependent ATPase of sarcoplasmic reticulum from skeletal muscle. I. Kinetic studies. J. Biochem. 62: 558-575

Yoshida, K., Furihata, K., Takeda, S., Nakamura, A., Yamamoto, K., Morita, H., Hiyamuta, S., Ikeda, S.-I., Shimizu, N., and Yanagisawa, N. (1995) A mutation in the ceruloplasmin gene is associated with systemic hemosiderosis in humans. Nat. Genet. 9: 267-272

Yoshimizu, T. Omote, H., Wakabayashi, T. Sambongi, Y., and Futai, M. (1998) Essential Cys-Pro-Cys motif of *Caenorhabditis elegans* copper transport ATPase. Biosci. Biotechnol. Biochem. 62: 1258-1260

Yu, X., Carroll, S., Rigaud, J.-L., and Inesi, G. (1993) H^+ countertransport and electrogenicity of the sarcoplasmic reticulum Ca^{2+} pump in reconstituted proteoliposomes. Biophys. J. 64: 1232-1242

Yuan, D.S., Dancis, A., and Klausner, R.D. (1997) Restriction of copper export in *Saccharomyces cerevisiae* to a late Golgi and Post-Golgi compartment in the secretory pathway. J. Biol. Chem. 272: 25787-25793

Yuan, D.S., Stearman, R., Dancis, A., Dunn, T., Beeler, T., and Klausner, R.D. (1995) The Menkes/Wilson disease gene homologue in yeast provides copper to a ceruloplasmin-like oxidase required for iron uptake. Proc. Natl. Acad. Sci. USA 92: 2632-2636

Zheng, J., Knighton, D.R., Ten Eyck, L.F., Karlsson, R., Xuong, N., Taylor, S.S., and Sowadski, J.M. (1993) Crystal structure of the catalytic subunit of cAMP-dependent protein kinase complexed with MgATP and peptide inhibitor. Biochemistry 32: 2154-2161